ROTATIONAL COOLING, NUCLEAR ORIENTATION AND RELAXATION

J. LUBBERS

ROTATIONAL COOLING, NUCLEAR ORIENTATION AND RELAXATION

ROTATIONAL COOLING, NUCLEAR ORIENTATION AND RELAXATION

PROEFSCHRIFT

TER VERKRIJGING VAN DE GRAAD VAN DOCTOR IN DE WISKUNDE EN NATUURWETENSCHAPPEN AAN DE RIJKSUNIVERSITEIT TE LEIDEN, OP GEZAG VAN DE RECTOR MAGNIFICUS DR K. A. H. HIDDING, HOOGLERAAR IN DE FACULTEIT DER GODGELEERDHEID, TEN OVERSTAAN VAN EEN COMMISSIE UIT DE SENAAT TE VERDEDIGEN OP WOENSDAG 18 JANUARI 1967 TE 15 UUR

DOOR

JACOB LUBBERS

GEBOREN TE LEIDEN IN 1937

KONINKLIJKE DRUKKERIJ VAN DE GARDE N.V. - ZALTBOMMEL

Promotor: Prof. Dr C. J. GORTER

Dit proefschrift is bewerkt onder toezicht van

Dr W. J. HUISKAMP

STELLINGEN

I

Het lijkt mogelijk een preparaat van sterk gepolariseerde kernen te vervaardigen, dat tevens dun is. Het is van belang de β-straling, uitgezonden door een dergelijk preparaat, te onderzoeken.

Zie ook dit proefschrift, hoofdstuk IV.

II

Voor Ce in $La_2Zn_3(NO_3)_{12} \cdot 24H_2O$ is de g-waarde in de richting van de kristallografische c-as $g_{//} = 0{,}072 = \pm 0{,}005$. Deze waarde is belangrijk hoger dan de corresponderende waarde in het Mg-zout. Zowel uit theoretisch oogpunt, als voor toepassing voor draaikoeling is het interessant de g-waarden van Ce, opgenomen in andere dubbelnitraten, te meten.

M. J. Leask, R. Orbach, M. J. D. Powell, W. P. Wolff, Proc. Roy. Soc. A **272** (1963) 371.
Zie ook dit proefschrift, blz. 86.

III

Bij onderzoek van kernorientatie in $Ce_2Mg_3(NO_3)_{12}.24H_2O$ kristallen wordt dikwijls een magneetveld in de richting van de c-as aangebracht, waarin de g-waarde klein is, terwijl de temperatuur bepaald wordt uit de differentiële susceptibiliteit in de richting loodrecht daarop. De gecombineerde invloed van demagnetiserende factor, paramagnetische verzadiging en misorientatie van het kristal t.o.v. het magneetveld op deze temperatuurbepaling kan veel groter zijn dan ieder van deze factoren afzonderlijk zou doen vermoeden.

W. J. Huiskamp, A. N. Diddens, J. C. Severiens, A. R. Miedema en M. J. Steenland, Physica **23** (1957) 605.

IV

In $Ce_2Mg_3(NO_3)_{12}.24H_2O$ kristallen wordt het warmtecontact tussen Ce en het rooster beperkt door een zgn. "fonon-bottleneck".

Na opname van een geringe hoeveelheid Cu^{++}-ionen in het kristal is de begrenzing van de warmtestroom door de fonon-bottleneck niet meer van practisch belang.

H. R. Hart jr., J. C. Wheatley, Bull. Inst. Intern. Froid Annexe Suppl. 1958–1, 311.
O. E. Vilches en J. C. Wheatley, Rev. Sci. Inst. **37** (1966) 819.

V

De bewering van Mage ,dat de mengwarmte van gassen bij druk nul ongelijk aan nul zou kunnen zijn, is onjuist.

D. T. Mage, proefschrift University of Michigan, 1964, p. 14–17.

VI

Het is mogelijk de meetmethode voor relaxaties, zoals deze beschreven is door De Vries, uit te breiden tot een frequentiegebied van 10 Hz tot 100 MHz.

A. J. de Vries, Academisch proefschrift, Leiden 1965.

VII

Een geschikte maat om de koelcapaciteit van een koelzout bij de temperatuur T te beoordelen is de "magnetische enthalpie" ${}_0^T\int c_H \mathrm{d}T$, genomen per volume-eenheid (c_H is de soortelijke warmte in een magneetveld H). Het is van belang voor de gebruikelijke koelzouten over diagrammen te beschikken, waarin de magnetische enthalpie tegen de temperatuur is uitgezet en waarin lijnen zowel voor constante enthalpie als voor constant magneetveld zijn getekend.

VIII

Proeven over het Curiepunt van gadoliniummetaal zijn met eenvoudige middelen uit te voeren. Het meten van de soortelijke warmte en de verzadigingsmagnetisatie als functie van de temperatuur heeft instructieve waarde voor 2e jaars studenten in de natuurkunde.

IX

De warmteontwikkeling in een stookoog, zoals dit o.a. door Van Kempen gebruikt wordt, wordt mede bepaald door de zelfinductie van het oog.

H. van Kempen, Academisch proefschrift, Leiden 1965, blz. 17.

X

Het is wenselijk door een uitgebreider oecologisch en ethologisch onderzoek de hypothese van Lindroth, dat de verdeling van macroptere en brachyptere vormen van loopkevers over Scandinavië samenvalt met respectievelijk jonge en oude populaties, nader te toetsen.

P. J. den Boer, Vakblad voor biologen, **42** (1962) 110.
C. H. Lindroth, Die Fennoskandischen Carabidae III Göteborgs Kungl. Vetesk. Handl. **4** (1949) 3.

XI

Voor het afvoeren van warmte bij lage temperaturen heeft een koudereservoir verkregen door adiabatische expansie van ^{3}He in superfluide ^{4}He, voordelen boven een koudereservoir, dat verkregen is door adiabatische demagnetisatie van een paramagnetisch zout.

Voor temperaturen $0{,}03 \lesssim T < 0{,}4$°K ligt dit voordeel voornamelijk in de mogelijkheid met He een continu koelproces te verwezenlijken, terwijl voor lagere temperaturen de mogelijkheid van een groot contactoppervlak tussen He en een metaal de voornaamste factor is.

K. W. Taconis en R. de Bruyn Ouboter, Progr. Low Temp. Phys. IV, p. 81. Ed. C. J. Gorter, North Holland Publ. Comp. (1964) Amsterdam.
O. E. Vilches en J. C. Wheatley, Rev. Sci. Inst. **37** (1966) 819.

XII

Het is wenselijk dat een roeivereniging, door welke regelmatig roeitochten worden gehouden, over één zespersoons wherry beschikt.

Stellingen behorende bij het proefschrift van J. Lubbers.

aan mijn ouders
aan Aaltje

Het in dit proefschrift beschreven onderzoek werd uitgevoerd als onderdeel van het programma van de werkgroep K IV van de stichting voor Fundamenteel Onderzoek der Materie met financiële steun van de Nederlandse Organisatie voor Zuiver Wetenschappelijk Onderzoek.

Teneinde te voldoen aan het verzoek van de Faculteit der Wiskunde en Natuurwetenschappen volgt hieronder een overzicht van mijn studie

De grondslag voor mijn studie werd gelegd op het Stedelijk Gymnasium te Leiden, waar ik in 1954 het eindexamen β aflegde. Studie in de natuurkunde aan de Leidse universiteit leidde in 1958 tot het candidaatsexamen a'. Het doctoraal examen in de experimentele natuurkunde legde ik in 1961 af. Voor het doctoraal examen volgde ik de colleges van Prof. Dr S. R. de Groot, Prof. Dr P. Mazur, Dr J. A. M. Cox, Ir J. Snijder, Prof. Dr C. Visser en Prof. Dr J. Kistemaker.

Mijn experimentele opleiding begon in 1958 op de afdeling paramagnetische relaxatie onder leiding van Dr L. C. van der Marel en Dr J. van den Broek. Daarna leidde Dr D. de Klerk mij in de techniek van het opwekken van sterke magneetvelden in. In november 1959 ging ik over naar de afdeling adiabatische demagnetisatie en kernorientatie onder leiding van Dr W. J. Huiskamp. Hier assisteerde ik bij de opbouw van een nieuwe opstelling voor adiabatische demagnetisatie. Na voltooiing van deze opstelling in 1961 werden de metingen begonnen, waarop dit proefschrift gebaseerd is.

Sinds 1959 heb ik op het natuurkundig practicum geassisteerd.

De stichting Fundamenteel Onderzoek der Materie (F.O.M.) verleende mij sinds 1959 een studiebeurs; in 1961 werd ik als wetenschappelijk medewerker bij de F.O.M. aangesteld.

Behalve van Dr W. J. Huiskamp heb ik ook bijzonder veel steun ondervonden van Dr A. R. Miedema, die steeds bereid was mij met suggesties en raad terzijde te staan. Het werk en de adviezen van de heer J. van Weesel hebben veel bijgedragen tot het slagen van de metingen. De glazen apparatuur is vervaardigd door de heer A. R. B. Gerrtise. In de loop der jaren heb ik de hulp gehad van vele medewerkers. Hiervan wil ik noemen de heren P. Bloembergen, J. A. M. Potters, H. F. van der Land, L. Niesen en H. B. Brom. De plezierige en waardevolle medewerking die ik mocht ondervinden van de dames en heren van de wetenschappelijke, technische, administratieve en huishoudelijke staf van het Kamerlingh Onnes Laboratorium is door mij zeer op prijs gesteld.

Dr A. S. Edelstein, Dr D. A. Curtis en Dr T. W. Adair corrigeerden de Engelse tekst.

CONTENTS

INTRODUCTION AND SURVEY

Nuclear orientation is said to occur when the spins of an ensemble of nuclei do not point equally in all directions in space. This situation can also be described with the aid of the hyperfine structure energy levels: nuclear orientation occurs when these levels are unequally occupied.

One of the ways to study nuclear orientation is to observe gamma radiation emitted by radioactive nuclei. The directional distribution of gamma rays is in general anisotropic. If the decay characteristics of the nucleus are known, it is possible to deduce from the observed gamma ray anisotropies data on the character and degree of nuclear orientation.

The splitting of energy levels, which is required for nuclear orientation can be brought about in the following ways:

a) the action of an external magnetic field H on the magnetic moment of the nucleus ("brute force method")

b) the action of an electric field gradient, caused by surrounding ions in a crystal on the electric quadrupole moment of a nucleus ("electric hyperfine structure interaction")

c) the interaction between the magnetic moment of a nucleus and the electronic spin of the same atom ("magnetic hyperfine structure interaction").

These methods, as well as several others are extensively discussed in ref. 1, 2, 3.

In order to obtain a considerable degree of nuclear orientation very low temperatures are required. Generally, methods a) and b) require temperatures of the order of 10^{-3}°K, method c) a temperature of the order of 10^{-2}°K. Temperatures in this region have up to now only been reached by the technique of adiabatic demagnetization (cf. ref. 3, 4, 5). For method a) and also for some variants of method c) the presence of a magnetic field is required. Then it is not possible to reach such low temperatures by demagnetization of the sample which contains the radioactive nuclei; but the sample may be cooled by another substance ("cooling salt") which is at some distance out of the magnetic field. We designate this way of cooling as: "indirect cooling". The poor thermal conductivity at very low temperatures of the used materials has prevented for a long time to reach temper-

atures below 0.010°K. Recently progress has been made by the use of He as a contact medium [6]).

An alternative approach to reach at the same time a very low temperature and a strong magnetic field in one sample can be found in the following way. The essential feature of adiabatic demagnetization is cooling caused by reduction of energy level splittings. In this thesis other ways to reduce energy splittings have been investigated and applied. We may distinguish between an increase of the magnetic field and rotational cooling [7]) [8]). In the former case an ion is used which has a crystalline field splitting which can be considerably reduced by a magnetic field (e.g. Ni^{++}, ch. II § 3). Rotational cooling is possible when the ion has anisotropic magnetic properties, which can be described by an anisotropic spin-hamiltonian (see for a definition of spin-hamiltonian ref. 9). When the decrease of the energy splittings is carried out adiabatically, the spin temperature of the ions is reduced accordingly. The spins which are used in this cooling process will further be designated as the "cooling spins". The occurrence of a low temperature is in our experiments detected by the orientation of radioactive nuclei of another kind of ions ("thermometer spins").

In this thesis investigations on several systems of cooling and thermometer spins are described. The goal of this work has been to find ways to orient nuclei in relatively high magnetic fields ($H \gg 1$ kOe) and at low temperatures ($T \ll 1$°K), thus making a considerable degree of nuclear orientation feasible.

In the adiabatic cooling processes proposed above the following steps may be distinguished:

1. While the energy splittings of the cooling spins are large, these spins are cooled in order to reduce the entropy of this system ("precooling").

2. The energy splittings of the cooling spins are reduced adiabatically, so that these spins reach a very low temperature.

3. Thermal contact between cooling and thermometer spins is established; if desired this contact may be broken again when thermal equilibrium is established.

4. The thermometer spins must be isolated sufficiently from their warmer surroundings, in order to guarantee a sufficiently long measuring time at the very low temperature.

Both for steps 1 and 4 it is advantageous to precool the sample and its surroundings as far as possible. Thus, starting at 0.9°K, a two stage cooling is applied. The first stage consists of demagnetizing a CrK-alum cooling salt, which precools the sample containing cooling and thermometer spins to temperatures between 0.03 and 0.06°K.The second cooling stage has been described above; generally a rotation of the magnetic field is used. The mobility of our magnet, which was mounted on a hydraulic lift which could rotate around its piston, has much contributed to the feasibility of our experiments.

Apart from step 2, all steps considered above consist of energy transfer between two different spin systems or between a spin system and the lattice vibrations. It was soon found that a good knowledge of these heat transfer rates is essential in order to design a cooling system. When we started our measurements little experience existed about these processes in the extreme conditions concerned, i.e. for very dilute nuclear thermometer spins and, more importantly, at very high values of H/T, thus at strongly polarized electron spin systems. Hence the relevant rates of heat exchange were studied for several combinations of cooling and thermometer spins. Special attention was given to the influence of numerous cooling spins on the relaxation rates of the few thermometer spins.

In the considerations given above we described the different kinds of spins as forming different thermal systems, each having its own spin temperature. It must be stressed however, that this description has only limited validity, especially for dilute spin systems. More correctly the state of a number of spins is described by saying that these spins have a few energy levels in a magnetic field and that each level has an occupation density. For the case that a species of spins has only two energy levels at a distance ΔE, a temperature for these spins can be defined as

$$T = -\frac{\Delta E}{k} \cdot \ln \frac{N_+}{N_-},$$

in which N_+ and N_- are the occupation numbers of respectively the upper and the lower level. For spins with more than two energy levels the population densities may not fit to a thermal equilibrium, and thus no spin temperature can be defined. It remains then possible to introduce a temperature for any pair of levels in the way it was done above, different pairs of levels having different temperatures. In large magnetic fields it may occur that the electron spin temperature of certain ions (i.e. the temperature derived from levels characterized by different values of the electron spin quantum number S_z) differs from the nuclear spin temperature of the same ions (i.e. the temperature derived from levels characterized by different values of the nuclear spin quantum number I_z). Such different temperatures may persist during long times in dilute spin systems when no ways are open to equalize these temperatures. Similarly different kinds of ions may maintain different spin temperatures for a long time. In this context the principle of conservation of energy plays an important rôle. Only those processes between spins occur in which the total energy is conserved. When the difference between various energy splittings is much larger than the broadening of the energy splittings such processes cannot occur.

In more concentrated samples the same description with energy levels applies. However, by the mutual interactions between the ions the energy levels are strongly broadened. Thus there is more opportunity than in

dilute systems for the various spin systems to exchange energy and to come in thermal equilibrium in a rather short time. However, when the magnetic field is made very strong isolation can occur again (cf. chap. I § 5).

Energy is also present in the form of lattice vibrations (phonons). A spin system and the lattice may exchange energy, i.e. a phonon may be emitted by the spin system. This process is called the direct relaxation process. Other relaxation processes in which more than one phonon take part are unimportant far below 1°K. Spins of the same kind have equal energy splittings, thus they all are "on speaking terms" whith the same phonons. When studying the energy exchange between spins and the lattice vibrations it is sometimes found [10] [11] [12] that the rate at which the phonons on speaking terms can transfer energy to the other phonons is the main bottleneck in the spin-lattice relaxation. The relaxation may then said to be "phonon bottlenecked".

In contrast with electron spin relaxation, the direct relaxation rate for nuclear spins is generally prohibitively slow. Thus, apart from the usually slow quadrupole relaxation, the nuclear spins can only exchange energy with the lattice through processes in which an electron spin takes part. For a more detailed description we refer to ref. 13.

In the temperature region of interest to us the heat capacity c_L of the lattice is extremely small compared to the heat capacities c_S of the spin systems. For instance, for cerium magnesium nitrate is for $T = 0.1°K$ and $H = 1$ kOe, $c_L = 8 \times 10^{-2}$ erg cm^{-3}°K^{-1} and $c_S = 5 \times 10^4$ erg cm^{-3}°K^{-1}. Thus the energy of our samples is, even for high magnetic dilution ($1 : 10^4$) still completely determined by the spin systems. The rôle of the lattice vibrations consists in acting as a medium by which the spin systems have thermal contact with other thermal baths (e.g. the cooling salt).

The investigations which are described in this thesis can be distinguished according to the systems or according to the phenomena studied. As far as the phenomena are concerned three main topics occur: 1°. methods to reduce energy splittings, 2°. energy transfer between the lattice and a nuclear spin system and 3°. energy transfer between two different spin systems.

The systems studied can be distinguished according to the type of thermometer spins, the type of cooling spins and the concentration of the cooling spins. As thermometer spins we used ^{54}Mn, which can be oriented through its rather large and isotropic magnetic hyperfine structure coupling, and ^{137}Cs which was oriented by the electric hyperfine structure coupling method. The cooling spins were Co^{2+} (anisotropic hyperfine structure), Ni^{2+} (crystalline field splitting) and Ce^{3+} (anisotropic g-value). Co^{2+} and Ni^{2+} were merely studied at high concentrations, for Ce^{3+} a range of concentrations was studied.

In chapter I the method of rotational cooling, using ions with an aniso-

tropic h.f.s. coupling is discussed and its practicability demonstrated using Co^{2+} as cooling spins and ^{54}Mn and ^{137}Cs as thermometer spins. An experiment with ^{60}Co (radioactive cooling spin) confirmed roughly the theoretical description given for this cooling method. Intermediate state reorientation of the 2.6 min ^{137}Ba level in the decay of ^{137}Cs was observed and could be influenced by a magnetic field.

In chapter II the spin-lattice relaxation of ^{54}Mn nuclei is studied in concentrated crystals with various types of cooling spins. It is found that the electron spins of the cooling ions provide the thermal contact between the lattice and the ^{54}Mn nuclei. The thermal contact becomes very poor when the electron spins are strongly polarized by a magnetic field.

In chapter III again the spin-lattice relaxation of nuclei is studied, this time for low concentrations of cooling spins (Ce). The relaxation of the Mn nuclei is here predominantly provided by the electron spin of the Mn ion itself, at low temperatures very long relaxation times are found. When the energy splittings of Ce and Mn are made equal in the period that indirect cooling is applied to the sample, strong interactions between both types of ions are observed, which may lead to an anomalous (i.e. non-Boltzmann) type of nuclear orientation.

In chapter IV spin-spin interactions between cooling (Ce) and thermometer (^{54}Mn) spins are described for a dilute system of cooling spins. It is found that, when the energy splittings are made equal, even at Ce concentrations as low as 0.1% the interactions are able to lead to almost complete polarization of the Mn nuclei. The long nuclear spin-lattice relaxation time for the Mn can give an efficient isolation of the nuclear spins from their surroundings.

Both in chapters III and IV it is found that adequate models can be given to calculate the nuclear relaxation times. These models are only applicable for dilute systems of cooling spins. For the concentrated samples considered in chapters I and II only a qualitative discussion of the relaxation rates is presented.

Cooling methods using dilute systems of cooling spins seem the most promising for further applications.

REFERENCES

1) de Groot, S. R., Tolhoek, H. A., Huiskamp, W. J., p. 1199 in Alpha-beta- and gamma-ray spectroscopy, ed. K. Siegbahn. (North-Holland Publ. Co. Amsterdam 1964).
2) Ambler, E., Methods of nuclear orientation in Progress in Cryogenics **2**, Ed. K. Mendelssohn (Temple Press Books Ltd. London 1960).
3) Daniels, J. M., Oriented nuclei, (Academic Press, New York 1965).
4) de Klerk, D., Handbuch der Physik XV (Springer Verlag, Berlin 1956).
5) Little, W. A., Magnetic cooling in Progress in Cryogenics, **4** Ed. K. Mendelssohn, (Temple Press Books Ltd. London 1964).
6) Vilches, O. E., and Wheatley, J. C., Rev. sci. Inst. **37** (1966) 819.
7) Bogle, G. S., Cooke, A. H., and Whitley, S., Proc. Phys. Soc. (G.B.) A**64** (1951) 931.
8) Wheatley, J. C. and Estle, T. L., Phys. Rev. **104** (1956) 264.
9) Abragam, A. and Pryce, M. H. L., Proc. Roy. Soc. London A**205** (1951) 105.
10) van Vleck, J. H., Phys. Rev. **59** (1941) 724.
11) Gorter, C. J., van der Marel, L. C. and Bölger, B., Commun. Kamerlingh Onnes Lab. Leiden suppl. 109*c*; Physica **21** (1955) 103.
12) Scott, P. L. and Jeffries, C. D., Phys. Rev. **127** (1962) 32.
13) Abragam, A., Principles of nuclear magnetism. (Oxford University Press, London 1961).

CHAPTER I

COOLING BY MEANS OF ANISOTROPIC HYPERFINE STRUCTURE COUPLING

Synopsis

A new method is given for obtaining low temperatures in paramagnetic crystals in the presence of a large magnetic field by utilizing anisotropic hyper fine structure coupling. The method consists essentially of reduction of h.f.s. splittings by rotation of a magnetic field under adiabatic conditions.

A discussion of the requirements on the properties of the usable paramagnetic ions is given.

The usefulness of the method was demonstrated with crystals of $CoCs_2(SO_4)_2.6D_2O$ in which ^{54}Mn was incorporated in order to serve as a thermometer. The ratio between initial and final temperature was 4 to 5, resulting in a lowest temperature of 0.006°K, which could be maintained for at least one hour.

In high magnetic fields establishment of thermal equilibrium between the ^{54}Mn and stable ^{59}Co nuclei could not be obtained, indicating extremely long relaxation times in the interaction of nuclear spins of unlike paramagnetic ions. However, for medium field strengths relaxation time measurements could be carried out as a function of field strength, of the direction of the field and of the temperature. It was found that the relaxation time was very strongly dependent on the field strength when the field was in a fixed direction, but was approximately constant for a fixed value of the sum of electronic Zeeman splittings of Mn and Co-ions, when varying both the direction and magnitude of the field.

Gamma ray intensity measurements of ^{54}Mn at a very high degree of nuclear polarization ($> 97\%$) resulted in the establishment of an upper limit to the possible disturbance of the ^{54}Mn nuclear polarization due to K-capture or to its after-effects.

The rotational cooling procedure was further investigated by measurements of anisotropies of ^{60}Co gamma radiations; the main features of the experimental results, obtained for various field directions, were in agreement with theoretical predictions. However, at the lowest temperatures significant deviations were found.

^{137}Cs-nuclei were oriented by electric h.f.s. coupling; peculiar relaxation phenomena were observed which led to the conclusion that ^{137m}Ba has a negative sign for its nuclear electric quadrupole moment. The magnitude of the crystalline electric field gradient was found to be at least a factor of 30 larger than that found by Kiddle et Proctor by means of nuclear quadrupole resonance at room temperature.

The relaxation time for establishment of thermal equilibrium between Cs and

Co-nuclei was found to be a few orders of magnitude shorter than that between Co- and Mn-nuclear spins.

Negative results concerning attempts to orient ^{134}Cs, ^{86}Rb and ^{83}Rb are reported.

1. *Introduction.* Cooling to temperatures of roughly 0.01°K has been possible for a long time exclusively by the technique of adiabatic demagnetization. For instance the widely used crystals of cerium magnesium nitrate (CMN) allow one to obtain a temperature of about 0.003°K. If one tries to cool other samples, such as are required in nuclear orientation experiments, to about the same temperature simply by establishing heat contact with the CMN, serious difficulties arise. At about 0.015°K this procedure, called indirect cooling hereafter, becomes very difficult, because of the poor heat conductivity of all suitable substance at these low temperatures. Still more problems are encountered if one requires, for purposes of nuclear orientation experiments, the presence of a magnetic field at the position of the sample, partly because of a temperature rise of the cooling salt. To circumvent the latter difficulty the technique of rotational cooling may be applied, as has been shown by Wheatley and Estle on CMN[1]). In their experiment the electronic Zeeman splittings were not reduced by decreasing the magnetic field strength but by rotating the magnetic field from a direction of high g-value, $g_\perp$, to a direction of small g-value, $g_{//}$, in the crystal; for CMN they found $g_{//}/g_\perp \leqslant 0.02$.

Considerably lower temperatures, down to about 10^{-5} °K, have been obtained by Hobden and Kurti[2]) by nuclear demagnetization of copper, i.e. the nuclear Zeeman splittings in a large external field (30 kOe) were reduced by a factor 10^4 through removal of the magnetic field. At those temperatures the specific heat of the sample becomes extremely small, making it very difficult to cool other samples efficiently, apart from heat conductivity problems. Their method might of course be modified in the sense that the magnetic field is reduced by a factor, say of 10 to 20, such that temperatures of about 10^{-3} °K would have been obtained and a considerably larger cooling capacity would remain. However, both temperature and cooling capacity would then be sensitively dependent on the field strength.

In the following a cooling procedure will be discussed which makes use both of the rotation of an external magnetic field and of the reduction of *nuclear* Zeeman splittings, for instance of Co-ions. The external magnetic field serves only to polarize the electronic magnetic moments in the direction of the field; if the magnetic field is thereafter slowly rotated with respect to the crystal, the electronic magnetic moments are also rotated. Making use of the anisotropy of the hyperfine structure (h.f.s.) coupling in some crystals, this procedure may result in a considerable reduction of the nuclear Zeeman energy splittings and a concurrent reduction of the temperature. Or ex-

pressed differently: this "rotational cooling" amounts to a simultaneous rotation and decrease of the magnetic field, which the electrons exert on the nucleus.

It is further shown that the magnitude of the external magnetic field has not much influence on the final temperature of the nuclear spin system; since the magnitude of the known h.f.s. energies takes an intermediate position in between the mutual interaction energy of electronic magnetic moments and the interaction energies of nuclear magnetic moments in a metal, it was expected to obtain temperatures and cooling capacities somewhere between those of electronic paramagnetic salts and those of nuclear spin systems in metals.

The cooling method was tested with the aid of nuclear orientation of both ^{60}Co and ^{54}Mn nuclei. The degree of nuclear orientation was derived from the anisotropy in the intensity distribution of the emitted gamma rays

Some of the aspects of the cooling method will be discussed in § 2, in particular with respect to the obtainable temperatures and cooling capacities and as to the choice of suitable substances.

In § 3 details about the apparatus and the experimental procedure will be discussed.

In § 4 a discussion will be given of the theoretical formula for the directional distribution of the M4-radiation of ^{137}Cs and also for the directional distribution of the ^{60}Co-radiations in the particular circumstances involved in this rotational cooling experiment.

In § 5 results of experiments will be shown, in which ^{54}Mn gamma radiation provided the thermometer and where pronounced nuclear relaxation phenomena were found. In § 6 it will be seen that ^{137}Cs nuclei, incorporated into the CoCs-salt, show an anisotropy in the gamma ray intensity after rotational cooling of the sample.

In § 7 results will be given of ^{60}Co gamma ray anisotropy measurements, which will be compared with results of calculations of the directions of the ^{60}Co nuclear spins for various directions of the external magnetic field.

In § 8 some unsuccessful attempts to orient other radioactive Cs- and Rb-nuclei are mentioned.

2. *Theoretical discussion of rotational cooling by means of anisotropic hyperfine structure coupling.* 2.1. *Principle.* A paramagnetic salt, having ions with a strongly anisotropic hyperfine structure coupling, is indirectly cooled to a temperature, T_1, of a few hundredths of a degree. A magnetic field is applied in a direction, z, of the crystal along which the h.f.s. interaction is large. The order of magnitude of the field (10^3 Oe) needs only to be large enough to give practically complete polarization of the electronic magnetic moments (called electron spins hereafter); that is, one requires $g\mu_B H \gg kT$; so that the electron spin entropy is almost entirely removed.

The h.f.s. energy levels will be populated according to a Boltzmann distribution, and if the average energy level distance, ΔE_i, is roughly equal to kT_i, an appreciable part of the nuclear spin entropy is also removed. Thereafter the magnetic field is rotated (in principle rather slowly in order to make the process adiabatic) so that the h.f.s. energy splitting is reduced from ΔE_i to ΔE_f. Under adiabatic conditions a final temperature, T_f, will then be obtained which is related to the initial temperature, T_i, according to $T_i/T_f = \Delta E_i/\Delta E_f$.

2.2. *Calculation of effective h.f.s. coupling.* For purposes of discussion we assume the spin-hamiltonian for the paramagnetic ion to have the form:

$$\mathscr{H} = g_z\mu_B H_z S_z + g_x\mu_B H_x S_x + AS_z I_z + BS_x I_x, \tag{2.1}$$

where the effective spin $S = \frac{1}{2}$ and the h.f.s. coupling constant A is larger than B; the directions x and z are defined with respect to the crystallographic axes and terms in S_y are omitted since they are irrelevant to this discussion, which is restricted to the xz-plane. Suppose the magnetic field, $\boldsymbol{H}$, makes an angle ψ_H with the z-axis, so that $\operatorname{tg} \psi_H = H_x/H_z$; let us further provisionally assume the temperature, T, to be zero. Then the electron spins will be completely polarized, not along the direction of $\boldsymbol{H}$, but at an angle, ψ_S, with the z-axis. It can easily be shown (c.f. § 7.2) that, neglecting the h.f.s. terms,

$$\operatorname{tg} \psi_S = (g_x/g_z) \operatorname{tg} \psi_H. \tag{2.2}$$

Similarly, under the assumption that $g\mu_B H \gg A, B$, one finds that the average direction of the nuclear spins makes an angle ψ_N with the z-axis, for which the relation holds:

$$\operatorname{tg} \psi_N = (B/A) \operatorname{tg} \psi_S = (Bg_x/Ag_z) \operatorname{tg} \psi_H \tag{2.3}$$

If in the expression (2.1) the operators S_x etc. are replaced by their expectation values one obtains the following classical expression for the total h.f.s. energy

$$E = KSI, \text{ where } K = \pm \sqrt{\frac{g_z^2 A^2 \cos^2 \psi_H + g_x^2 B^2 \sin^2 \psi_H}{g_z^2 \cos^2 \psi_H + g_x^2 \sin^2 \psi_H}}. \tag{2.4}$$

If $\boldsymbol{H}$ is rotated from the z-direction to the x-axis K changes by the factor A/B.

Dropping the assumption $T = 0$ and assuming the nuclear spin entropy to remain constant when rotating $\boldsymbol{H}$ (since the electron spin entropy was supposed to be practically zero), one expects ideally, a temperature change according to $T_i/T_f = A/B$.

The same conclusion is obtained when evaluating quantum-mechanically the energies of the various magnetic sublevels, over which a constant

Boltzmann distribution is assumed. However, for small B/A strong deviations from equidistance in the energy level spacing will occur at $\psi_H = 90°$, resulting in $T_i/T_f > A/B$.

In conclusion, for $A \gg B$ a considerable cooling of the nuclear spin system would result, which will be called rotational h.f.s. cooling henceforth.

2.3. *Effect of misalignment of the magnetic field.* In case $g_z A \gg g_x B$, a small deviation of ψ_H from 90° will result in a relatively strong increase of K with respect to $K_x = K(\psi_H = 90°) = B$.

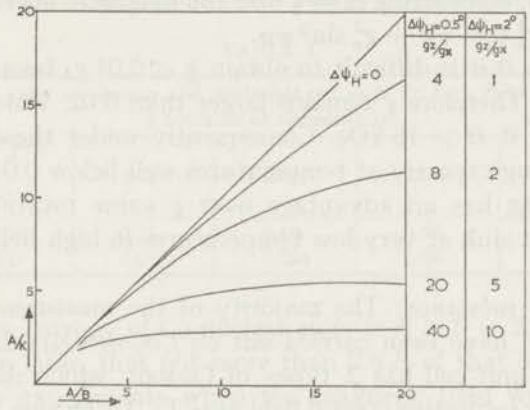

Fig. 1. Theoretical cooling ratio A/K as a function of A/B, the ratio of h.f.s. coupling constants in directions $\psi_H = 0°$ and $\psi_H = 90°$ of the magnetic field with respect to the z-axis. $\Delta\psi_H$ is the misalignment of the field from the position $\psi_H = 90°$.

In fig. 1 the quantity A/K has been plotted as a function of A/B with $\Delta\psi_H \equiv \psi_H - 90°$ and g_z/g_x as variable parameters; A/K equals near $T = 0$, in principle, the ratio of initial to final temperature T_i/T_f, called cooling ratio hence forth. The estimates for $\Delta\psi_H$ of 2° and 0.5° respectively, are determined by the experimental conditions in the following way.

In the case of a monoaxial salt with h.f.s. coupling constant $A > B$, it is required that $\boldsymbol{H}$ lies along the z-axis in the initial position ($K = A$) and in the xy-plane in the final position ($K = B$); this requirement is easily fulfilled with the apparatus described in section 3, except that the magnetic field has some inhomogeneity at the position of the sample, resulting in a possible misalignment of about 0.5°.

In the case of a salt in which the h.f.s. coupling is small along only one axis, one should align the field along this axis for maximal cooling; then, a misalignment of 2° of this axis out of the plane of the rotation of $\boldsymbol{H}$ cannot be excluded. The requirement $K = A$ for the initial position of the field may be relaxed considerably since the precise direction of $\boldsymbol{H}$ is relatively unimportant; for instance in case $A > B$, one wants $\psi_H = 0$, but $\psi_H = 30°$ gives $K/A > 0.75$, provided $g_z/g_x > 1$.

2.4. *Specific heat.* A considerable specific heat of the sample after rotational h.f.s. cooling will be present if $\Delta E_f \approx kT_f$ or equivalently $\Delta E_i \approx kT_i$. The latter requirement signifies that under the initial conditions an appreciable part of the nuclear spin entropy has been removed and considerable nuclear alignment or polarization is established by indirect cooling. This appears to be experimentally feasible in view of known magnitudes of h.f.s. constants and the temperatures (of about 0.02°K) obtained in indirect cooling processes. Let us compare this situation with rotational cooling on the basis of anisotropic g-values:

The g-value is, considering $S = \frac{1}{2}$ and the magnetic field at an angle ψ_H, given by $g^2 = g_z^2 \cos^2 \psi_H + g_x^2 \sin^2 \psi_H$.

Even for $g_x = 0$ it is difficult to obtain $g < 0.01\ g_z$ because of misalignment problems. Therefore g remains larger than 0.02, which signifies that $g\mu_B H > 0.02$°K if $H > 15$ kOe. Consequently under these circumstances there is no cooling capacity at temperatures well below 0.01°K. Thus h.f.s. rotational cooling has an advantage over g value rotational cooling for producing a heat sink at very low temperatures in high fields.

2.5. *Choice of substance.* The majority of the measurements, described in the following, have been carried out on $CoCs_2(SO_4)_2.6D_2O$, i.e. CoCs-tuttonsalt. The unit cell has 2 types of Co-ions, which differ only in the direction of their respective crystal field axes T_1, T_2, one ion being the mirror image of the other with respect to the K_1K_2-plane in the crystal (fig. 2).

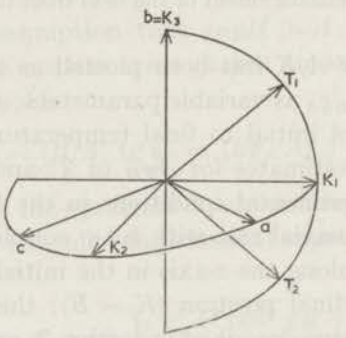

Fig. 2. Magnetic axes K_1, K_2, K_3 of Co-tutton salt; T_1 and T_2 are the directions of largest h.f.s. coupling for the two types of Co-ions respectively; a, b and c are crystallographic axes.

The tetragonal axes T are identical with the z-axes with respect to which the spin Hamiltonian is defined, and along which the g-value and h.f.s. constant A are larger than in a direction perpendicular to T, for instance the K_2-direction. The K_2-axis will be taken as x-axis hereafter.

It may be seen that in order to give the h.f.s. constant K a maximal value

for both ions simultaneously, the magnetic field has to be applied along the bisector of T_1 and T_2, i.e. along the K_1-axis, whereas only for $\boldsymbol{H}$ along K_2 both ions simultaneously give $K \approx B$. Therefore the orientation error $\Delta\psi_H = 2°$ of § 2.3 is applicable for our experiments. For CoCs-tuttonsalt $A/k = 0.042°\text{K}$ and $B < 0.1\ A$ [4]); $g(K_1) = 5.65$ and $g(K_2) = 2.9$ [3]).

The crystal has been deuterated since the large number of protons relative to the Co-nuclei might yield so much entropy to the Co-nuclear spin system as to prevent the temperature to drop below 0.01 °K, if a magnetic field of 20 kOe is applied. The entropy-yield of protons per mole Co for a field of 20 kOe is given as a function of temperature in table I.

TABLE I

Entropy yield of protons and deuterons per mole Co for a field of 20 kOe as a function of temperature

T°K / S/R	0.01	0.007	0.005	0.003
for 12 H	0.24	0.48	0.96	2.8
for 12 D	0.012	0.024	0.06	0.18

The maximum entropy of Co-nuclear spins is $R \ln 8 = 2.08\ R$.

It will be seen later, that not more than $0.6\ R$ of that entropy has been removed in the experiments when the magnetic field was in the initial position. If the proton or deuteron spin system keeps the same temperature as the Co-nuclear spin system when rotational h.f.s. cooling takes place, the reversible entropy yield of the protons at 0.01 °K is comparable in magnitude to the maximum amount of entropy, which can be absorbed by the nuclear spins of Co. Under irreversible conditions the situation may be worse, but, on the other hand, if the proton spin system were thermally isolated during the entire experiment, these considerations would be irrelevant.

3. *Experimental arrangement.* 3.1. *Apparatus.* The electromagnet*) gives a field of 18.5 kOe in a pole gap of 8 cm and has a cylindrical yoke with an outer diameter of 70 cm. The pole space is accessible through a few holes in the yoke, in these holes the magnetic field is smaller than 100 Oe everywhere and zero at one point. The magnetic field is horizontal and can be rotated in the horizontal plane over nearly 360°; since the magnet is mounted on top of a hydraulic lift, one can raise the position of the field relative to a fixed cryostat by 125 cm. Two scintillation counters are fixed to the magnet, such that they are diametrically opposed with respect to the centre of the magnet in a direction, which is perpendicular to the magnetic field.

*) The magnet was designed by Dr. D. de Klerk and built partially in the Kamerlingh Onnes Laboratory; its form is in some respects similar to the commerciably available magnets of A.D. Little Inc.

The centres of the NaI-scintillation crystals ($1\frac{3}{4}''$ ⌀, $2''$ long) have a distance of 16 cm to the sample and are connected by 30 cm long lucite light guides to the photomultipliers, which are placed outside the magnet yoke in a practically field free region and which are magnetically shielded by iron and μ-metal. The diametrical position of the two counters has the advantage that small displacements of the sample with respect to the magnet affect the sum of the two counting rates to a very small extent. The signals of the 6260 EMI-photomultipliers were fed into a RCL-256 channel analyzer, mainly in order to eliminate or to account for all effects of drift in the pulse

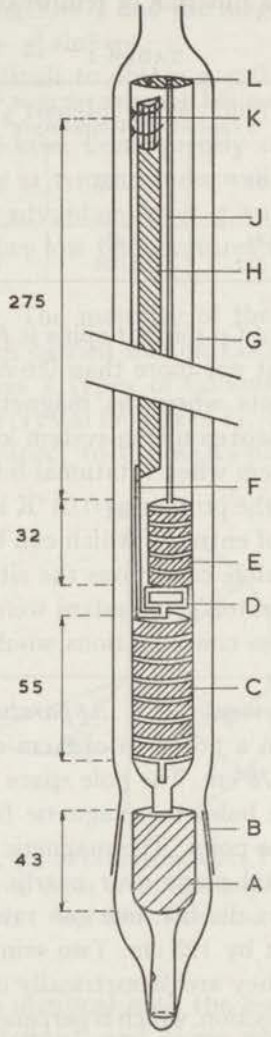

Fig. 3. Schematic diagram of the inner part of the apparatus. *A*: KCr-alum heat absorbing buffer, *B*: ground glass joint, *C* and *E*: slabs of KCr-alum with brass plates screwed on a central rod, *D*: stainless steel plate, *F* and *J*: copper rods, *H*: coil foil, *K*: sample, *G*: glass tube, *L*: plexiglass cap. Dimensions in mm.

height spectrum; a selective storage unit provided the possibility to analyse the signals of 4 counters simultaneously in 4 sections of 64 channels each, if necessary.

The cryostat consists, as usual, of glass dewars for hydrogen and helium and a glass walled vacuum space, on which primary and secondary coils for susceptibility measurements were wound. The vacuum space is closed at the bottom side by a ground joint, on which the inner part of the vacuum space is mounted. This inner part is shown in fig. 3 and consists of:

A, a K Cr-alum heat absorbing buffer, in which a glass tube, G, has been mounted, which serves for positioning the cooling salts C and E, and the sample, K. G is covered with coil foil (one layer of 0.1 mm diameter insulated copper wires, glued together and onto the tube G), which is connected via a copper wire, J, to a Cr-alum cooling salt, E. G serves as a thermal screen for the sample, into which the heat leak could in most cases be made lower than 0.01 erg/s. A second cooling salt, C, is isolated thermally from E by means of a rectangle of stainless steel, D. The purpose of the Cr-alum salt, C, is to cool the sample, K, indirectly via a copper wire, F, and coil-foil, H. K is glued with apiezon on one side of the coil-foil, which was made more rigid by fixing it to a thin quartz plate on the other side. This structure is fixed rigidly in the glass tube, G, with the aid of cotton threads, such that torsion of the sample in the magnetic field is negligible compared with the maximum acceptable values of $\Delta\psi_H$.

In later experiments the coil-foil was replaced by copper wire and a brass plate, giving slightly better heat contact with the sample, without undue eddy current losses when the field strength was varied or when the field was rotated.

3.2. *Crystal alignment.* The tutton salt single crystal was mounted with its ac-plane horizontally and its b-axis (K_3-axis) in the vertical direction,

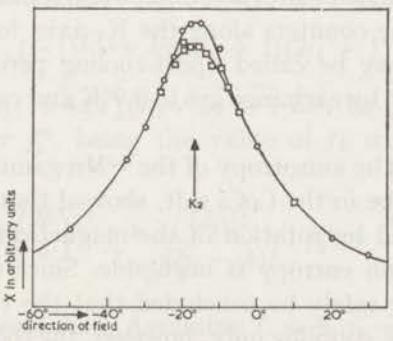

Fig. 4. Susceptibility of $CoCs_2(SO_4)_2.6D_2O$ as a function of the direction of the magnetic field ($H = 2.2$ kOe). The two series, marked with ○ and □ respectively, were measured rotating the field in opposite directions; the difference is due to a change in temperature of the sample.

in order to make a rotation of the field in the K_1K_2-plane feasible. The precise directions of K_1 and K_2, once the crystal was in a fixed position, were determined in an auxiliary experiment below 1°K. A magnetic field of 2200 Oe was applied to the sample, which was cooled by CrK-alum.

The magnetic susceptibility, χ, was measured in the vertical direction, while the direction of the magnetic field was varied in the K_1K_2-plane. As shown in the appendix $\chi \sim 1/gH$ where g refers to the K_1K_2-plane.

Therefore the maximum in χ will be expected to occur when the magnetic field is along the direction of minimum g, i.e. the K_2-axis. The accuracy of the measurement depended on the amount of CoCs-salt and varied between 0.5° to 3°; an example of the measurements is given in fig. 4.

3.3. *Experimental procedure.* The Cr-alum cooling salts were demagnetized from a field of 18 kOe and an initial temperature $T = 0.9$°K to a field of about 3 kOe and, consequently, a temperature of about 0.2°K. Then the magnet was raised about 35 cm in a few steps, while the field was further decreased, usually to values ranging from 600–1000 Oe; as a result the field was directed along the K_1-axis of the CoCs sample, whereas the Cr-alum was then essentially in zero field.

In the above manipulations a considerable part of the electron spin entropy of the sample was removed while the cooling salt was still at a relatively high temperature, therefore giving only a relatively small rise in entropy of the cooling salt. This procedure lasted for about 10 minutes.

In the next stage, called the "precooling period" nothing was changed, but one waited during 10–60 minutes for the transfer of part of the Co nuclear spin entropy from the sample to the Cr-alum; the progress of this entropy removal was monitored by the gamma ray counters when the sample contained ^{54}Mn or ^{60}Co.

The magnetic field was subsequently increased to values ranging from 5 to 18 kOe and rotated into the direction of the K_2-axis; the counting was resumed, now with the counters along the K_1-axis, for times ranging from 1 to 3 hours. This may be called "post-cooling period", after which the sample was warmed up by exchange gas to 0.9°K and calibrations were made.

3.4. *Main results.* The anisotropy of the ^{54}Mn gamma radiations, serving as a thermometer probe in the CoCs salt, showed that a cooling ratio T_i/T_f of 4 to 5 was achieved by rotation of the magnetic field at temperatures, where the electron spin entropy is negligible. Since moreover the g-value ratio $g_z/g_x = 2$ it may safely be concluded that the rotational cooling was due to anisotropic h.f.s. coupling only; however, the cooling ratio was smaller than the expected value, 10. These results were further corroborated by measurements of ^{60}Co gamma ray intensities, which showed the nuclear spins of the Co-ions to behave qualitatively according to the description

of § 2, i.e. they rotated under the influence of the rotating magnetic field, but lagged behind as a result of anisotropic h.f.s. coupling.

The results on ^{54}Mn in the post-cooling period showed the influence of relaxation times for the Mn nuclear spins, which apparently increased very strongly with the magnetic field strength. If the magnetic field strength decreased below 3 kOe, irreversible warm-up was observed, which is attributed to establishing heat contact with the lattice at these low fields.

^{137}Cs nuclei could be oriented at the lowest temperatures and it was found to be caused by electric h.f.s. coupling; peculiar relaxation phenomena were observed, which led to the conclusion that ^{137m}Ba has a negative nuclear quadrupole moment.

By reducing the thickness of the CoCs-crystals to 0.02 cm, the temperatures obtained in the precooling period could be reduced, so that also the final temperatures, T_f, were decreased to $T_f = 0.006°$K with fairly good reproducibility.

4. *Formulae for directional distribution of gamma radiation.* 4.1. *General formulae.* The directional distribution of the gamma radiation intensity, emitted from an ensemble of nuclei, which are oriented with respect to an axis of rotational symmetry, is given by the expression[5]:

$$W(\theta) = \sum_{k=\text{even}} \langle LLk0 | L1L - 1\rangle \, W(j_f j_i Lk; Lj_i) \, F_k(j_i)(2k+1)^{-\frac{1}{2}} \, Y_k^0(\theta) \qquad (4.1)$$

where $\langle LLk0 | L1L - 1\rangle$ is a Clebsch Gordan coefficient for gamma radiation of multipolarity L; W is a Racah-coefficient for recoupling of angular momenta L to j_i, j_f, the spins of the initial and final states of the nucleus; $F_k(j_i)$ is related to the orientation parameters[5] $f_k(j_i)$ according to

$$F_k(j_i) = \binom{2k}{k} j_i^k \left[\frac{(2k+1)(2j_i - k)!}{(2j_i + k + 1)!}\right]^{\frac{1}{2}} f_k(j_i). \qquad (4.2)$$

If $W(\theta)$ is normalized to $\int W(\theta)\, d\Omega = 4\pi$, an additional factor

$$(-1)^{L-1}\sqrt{4\pi}(2L+1)(2j_i+1)$$

is required in eq. (4.1); $\sqrt{4\pi}Y_k^0(\theta)/\sqrt{2k+1}$ can be replaced by $P_k(\cos\theta)$. We introduce further f_k^m, being the value of f_k when only the sublevel $j_z = j$ is populated

$$f_k^m(j_i) = \binom{2k}{k}^{-1} j_i^{-k} \frac{(2j_i)!}{(2j_i - k)!}\,; \quad f_2^m = \frac{2j_i - 1}{3j_i}. \qquad (4.3)$$

4.2. *^{137}Cs–^{137m}Ba radiation.* Assuming $L = 4$, $j_i = \frac{11}{2}$, $j_f = \frac{3}{2}$, we obtain from (4.1)–(4.3)

$$W(\theta) = 1 - \tfrac{17}{11}P_2\frac{f_2}{f_2^m} + \tfrac{81}{143}P_4\frac{f_4}{f_4^m} + \tfrac{1}{55}P_6\frac{f_6}{f_6^m} - \tfrac{28}{715}P_8\frac{f_8}{f_8^m} \qquad (4.4)$$

For relatively high temperatures $f_{k+2}/f^{m}_{k+2} \ll f_k/f^{m}_k$, thus the $P_2 f_2$ term is dominating; this is unfortunate in the sense that, for relatively small degrees of nuclear orientation, it is hard to distinguish between various possibilities for L, j_i and j_f.

It can for instance be shown, that the coefficient of $P_2 f_2/f^{m}_2$ is not changed by more than 25% if ($j_f = \frac{3}{2}$ remains fixed) $L = 4$, $j_i = \frac{9}{2}, \frac{7}{2}$ or $\frac{5}{2}$; or if $L = 5$, $j_i = \frac{13}{2}, \frac{11}{2}, \frac{9}{2}, \frac{7}{2}$; or if $L = 3$, $j_i = \frac{9}{2}$.

The distribution (4.4) is pertinent to the case of the 662 keV M4 radiation emitted in the decay of ^{137m}Ba, which very probably, has spin $\frac{11}{2}$, and decays to a ground state with spin $\frac{3}{2}$.

If it was assumed that the 662 keV radiation is "instantaneously" emitted after the β-decay of ^{137}Cs (in other words, if there were no reestablishment of thermal equilibrium during the 2.6 min half life of the 662 keV level), then f_k had first to be calculated for the spin of ^{137}Cs, $j_o = \frac{7}{2}$, and the change from $f_k(j_o)$ to $f_k(j_i)$ due to the beta decay had to be evaluated.

^{137}Cs decays predominantly by a 0.514 MeV beta-radiation, the spectrum of which shows a first forbidden unique shape[6]) and therefore presumably gives $|\Delta I| = 2$ and yes-parity change. This fits to the sequence of states in the single particle model: $f_{\frac{7}{2}} \xrightarrow{\beta} h_{\frac{11}{2}} \xrightarrow{M4} d_{\frac{3}{2}}$. For $\Delta I = -2$ and first forbidden beta decay the relation between $f_k(j_o)$ and $f_k(j_i)$ is:

$$f_k(j_i) = \frac{(j_o)^k\,(2j_o+1)!\,(2j_i+k+1)!}{(j_i)^k(2j_i+1)!\,(2j_o+k+1)!}\,f_k(j_o). \tag{4.5}$$

Assume that the nuclear orientation is produced by a combination of low temperatures and electric h.f.s. coupling, then f_2 may be evaluated as follows. The electric hyperfine structure coupling may be expressed by a Hamiltonian

$$\mathcal{H} = P\{j_z^2 - \tfrac{1}{3}j(j+1)\};$$

further, f_2 is the statistical average of the operator

$$O = j^{-2}\{j_z^2 - \tfrac{1}{3}j(j+1)\}.$$

Such an average is obtained from the density operator $\rho \equiv \exp(-\mathcal{H}/kT)$ by the well known relation

$$f_2 \equiv \langle O\rangle = (\mathrm{Tr}\,\rho O)/\mathrm{Tr}\,\rho.$$

Writing $\exp(-\mathcal{H}/kT) = 1 - \mathcal{H}/kT + \mathcal{H}^2/2k^2T^2$, one obtains

$$f_2 = -\tfrac{1}{45}\,\frac{(j+1)}{j}\,(2j-1)(2j+3)\,\frac{P}{kT}\left[1 - \tfrac{2}{21}(j^2+j-9)\,\frac{P}{kT}\right]. \tag{4.6}$$

Further $P = \frac{3}{4}e^2qQ/j(2j-1)$ where Q is the nuclear quadrupole moment and $eq = \partial^2V/\partial z^2$; V is the electrostatic potential at the nucleus. Neglecting the second term between brackets in (4.6), it is seen that f_2 is proportional to

$1/T$, in contrast to the $1/T^2$ dependence for magnetic h.f.s. splitting. Let us assume temporarily that $Q(^{137}\mathrm{Cs}) = Q(^{137\mathrm{m}}\mathrm{Ba})$. Then we want to compare the gamma ray directional distribution for the two distinct cases:

a. After β-decay of ^{137}Cs, the $^{137\mathrm{m}}$Ba nuclei come into thermal equilibrium with the environment and do not have a memory of the orientation of their parent nuclei;

or *b*. The population densities of the various magnetic sublevels of the $^{137\mathrm{m}}$Ba nuclei are entirely determined by those of the ^{137}Cs nuclei and by the preceding β-decay (perfect memory). The angular momentum carried away by the beta radiation and the change in nuclear spin determine the relationship which gives the new occupation numbers in terms of the old ones and the new orientation parameters follow from the old ones via eq. (4.5).

For both cases the same formula $W(\theta)$ applies, but the calculation of $f_k(j_1)$ is different for the two cases,

$$a.\quad f_2(j_1) = -\tfrac{1}{45}\,\frac{(j_1+1)(2j_1+3)}{4j_i^2}\,\frac{3e^2qQ}{kT} \tag{4.7}$$

$$b.\quad f_2(j_1) = \left(\frac{j_0}{j_1}\right)^2 \frac{(2j_1+2)(2j_1+3)}{(2j_0+2)(2j_0+3)}\, f_2(j_0) = \tag{4.8}$$

$$\frac{j_0^2(j_1+1)(2j_1+3)}{j_i^2(j_0+1)(2j_0+3)} \times (-\tfrac{1}{45})\,\frac{(j_0+1)(2j_0+3)}{4j_0^2}\,\frac{3e^2qQ}{kT}. \tag{4.9}$$

It is seen that $f_2(j_1)$ is the same in both cases and consequently $W(\theta)$ is the same as well for *a* and *b*. The gist of this remark is that a possible difference of anisotropy of $W(\theta)$ between *a* and *b* is entirely due to the difference in nuclear quadrupole moments and not to a change of spin values.

So far in the analysis, however, it is tacitly assumed that the axis of rotational symmetry, with respect to which f_k is defined, is also the same for cases *a* and *b*. In other words the principal axis of the tensor of the electric field gradient may not be equal for the Cs- and Ba-ion. If the field gradient is determined by the environmental charge distribution only and if the Ba-ion is not, due to the preceding β-decay, in a position different from that of the Cs-ion the principal axes are in the same direction.

4.3. *^{54}Mn-radiation*. From (4.1), (4.2), (4.3) it follows, that if $L = 2$, $j_0 = 3$, $j_1 = 2$, $j_f = 0$, then

$$W(\theta) = 1 - \tfrac{5}{7}\,\frac{f_2}{f_2^{\mathrm{m}}}\,P_2(\cos\theta) - \tfrac{2}{7}\,\frac{f_4}{f_4^{\mathrm{m}}}\,P_4(\cos\theta). \tag{4.10}$$

This formula gives the directional distribution of ^{54}Mn-nuclei, which are oriented with respect to an axis of rotational symmetry.

4.4. *Absence of rotational symmetry.* For the discussion of the results on ^{60}Co in § 7 we will need formulae for the directional distribution of gamma radiation, emitted from an ensemble of nuclei, which does not possess or exhibit rotational symmetry. For such cases De Groot and Cox[7]) have given the following expression:

$$W(\boldsymbol{k}_1) = \sum_{k,q} \langle L1L - 1 | LLk0\rangle\, W(j_f j_i Lk; Lj_i)\, \langle |j_i j_i kq\rangle\, \mathscr{D}^k_{q0}(\boldsymbol{S})$$

where $\langle |j_i j_i kq\rangle$ is the statistical tensor, defined by Fano[7])[8]) and

$$\mathscr{D}^k_{q0}(\boldsymbol{S}) = (-1)^q \sqrt{\frac{4\pi}{2k+1}}\, Y_{kq}(\theta, \varphi).$$

$\boldsymbol{k}_1$ is the direction of emission of the gamma radiation, making polar angles θ, φ with the coordinate system, in which the z-axis is the axis of quantization. For the evaluation of $\langle |j_i j_i kq\rangle$ we refer to Ambler[9]), who explicitly gives

$$\langle |jj\ 20\rangle = a_2 \langle j|3j_z^2 - j(j+1)|\, j\rangle = 3a_2 j^2 f_2 \tag{4.11}$$

$$\langle |jj\ 2 \pm 2\rangle = a_2 (\tfrac{3}{2})^{\frac{1}{2}} \langle j\, |j_\pm^2|\, j\rangle \tag{4.12}$$

$$\langle |jj\ 2 \pm 1\rangle = \mp\, a_2\, (\tfrac{3}{2})^{\frac{1}{2}} \langle j\, |j_z j_\pm + j_\pm j_z|\, j\rangle. \tag{4.13}$$

The expressions between bars, e.g. $|j_\pm^2|$ have firstly to be quantummechanically averaged for a certain magnetic sublevel (the expectation value has to be evaluated) and then a statistical average over the various magnetic sublevels is required.

In (4.11), (4.12), (4.13)

$$a_2 = 2\sqrt{5}[(2j+3)(2j+2)(2j+1)(2j)(2j-1)]^{-\frac{1}{2}} \tag{4.14}$$

such that, e.g.

$$\langle |jj\ 20\rangle = 3a_2 j^2 f_2 = F_2(j). \tag{4.15}$$

Further

$$Y_{20} = \tfrac{1}{4} \sqrt{\frac{5}{\pi}}\, (3\cos^2\theta - 1) \tag{4.16}$$

$$Y_{2\pm1} = \mp\, \tfrac{1}{2} \sqrt{\frac{15}{2\pi}}\, \sin\theta \cos\theta\, e^{\pm i\varphi} \tag{4.17}$$

$$Y_{2\pm2} = \tfrac{1}{4} \sqrt{\frac{15}{2\pi}}\, \sin^2\theta\, e^{\pm 2i\varphi} \tag{4.18}$$

$$Y_{00} = +\, (4\pi)^{-\frac{1}{2}} \tag{4.19}$$

More complicated formulae have to be added for $k > 2$, but we will restrict

ourselves to $k = 2$, which is justified at relatively high temperatures. Then

$$W(\theta) = \sqrt{4\pi}(2L+1)(2j_i+1)\langle L1L-1|LL00\rangle\, W(j_f j_i L0; Lj_i)\, a_0 Y_{00} +$$
$$+ \sqrt{4\pi}(2L+1)(2j_i+1)\,\langle L1L-1|LL20\rangle\, W(j_f j_i L2; Lj_i) \times$$
$$\times \sqrt{\frac{4\pi}{5}}\, 3a_2 j_i^2 \left[f_2 P_2(\cos\theta) \mp \frac{1}{2j_i^2}\,\langle j_z j_\pm + j_\pm j_z\rangle \cdot \sin\theta\cos\theta\, e^{\pm i\varphi} + \right.$$
$$\left. + \frac{1}{4j_i^2}\,\langle j_\pm^2\rangle \sin^2\theta\, e^{\pm 2i\varphi} \right]. \qquad (4.20)$$

The first term equals 1 since $a_0 = 1/\sqrt{2j_i+1}$, $Y_{00} = (4\pi)^{-\frac{1}{2}}$,

$$\langle L1L-1|LL00\rangle = (-1)^{L-1}/\sqrt{2L+1},$$

and

$$W(j_f j_i L0; Lj_i) = 1/\sqrt{2j_i+1}\sqrt{2L+1}.$$

Eq. (4.20) reduces to eq. (4.1) (apart from a normalization factor) if there is rotational symmetry about the z-axis; then $\langle j_z j_\pm + j_\pm j_z\rangle = \langle j_\pm^2\rangle = 0$ since $j_\pm = j_x \pm i j_y$. In the discussions of § 7 one always can take the xz-plane as a plane of symmetry; then

$$\langle j_z j_+ + j_+ j_z\rangle = \langle j_z j_- + j_- j_z\rangle.$$

and $\langle j_+^2\rangle = \langle j_-^2\rangle$ and the expression between brackets in eq. (4.20) becomes

$$G_2 \equiv \left[f_2 P_2(\cos\theta) - \frac{1}{j_i^2}\,\langle j_z j_+ + j_+ j_z\rangle \sin\theta\cos\theta\cos\varphi + \right.$$
$$\left. + \frac{1}{2j_i^2}\,\langle j_+^2\rangle \sin^2\theta\cos 2\varphi \right] \qquad (4.21)$$

where φ is zero along the x-axis.

For ^{60}Co quadrupole radiations, $L = 2$, $j_i = 4$, $j_f = 2$:

$$W(\theta) = 1 - \tfrac{1}{7}\tfrac{5}{7} N_2\, G_2 = 1 - \tfrac{6}{4}\tfrac{0}{9} G_2 \qquad (4.22)$$

since

$$N_2 = j_i(2j_i - 1)^{-1}.$$

However, since the change of nuclear orientation, due to the preceding beta decay, is determined by $N_2(j_i)\, f_2(j_i) = N_2(j_o)\, f_2(j_o)$, $W(\theta)$ may be expressed in terms of the $f_2(j_o)$ etc. according to

$$W(\theta,\varphi) = 1 - \tfrac{7}{6}\tfrac{5}{3} f_2 P_2(\cos\theta) + \frac{1}{2j_0^2}\,\langle j_z j_+ + j_+ j_z\rangle \sin 2\theta\cos\varphi +$$
$$+ \frac{1}{2j_0^2}\,\langle j_+^2\rangle \sin^2\theta\cos 2\varphi \qquad (4.23)$$

where f_2, $\langle j_z j_+ + j_+ j_z \rangle$ and $\langle j_+^2 \rangle$ have to be calculated as an average over the $2j_o + 1$ substates of the ^{60}Co nucleus ($j_o = 5$).

For ^{137}Cs–^{137m}Ba-radiation the absence of rotational symmetry does not need to be discussed, since deviations from rotational symmetry were not observed experimentally. For ^{54}Mn there is no reason to expect any significant deviation from rotational symmetry in the radiation pattern, since the Mn-ion has an isotropic g-value and the influence of the small crystal field splitting (§ 5.1) is overwhelmed by the electronic Zeeman splitting under all circumstances of this experiment (except in fig. 6, where a small change in counting rate is observed when increasing the magnetic field strength from 1.1 to 10 kOe).

5. *Results on ^{54}Mn.* 5.1. *Characteristics of the ^{54}Mn-thermometer.* The demonstration of rotational h.f.s. cooling requires a thermometer, which is insensitive to variation in magnitude or direction of the magnetic field; magnetic susceptibility measurements give, under these conditions, a very poor indication of the thermodynamic temperature. The anisotropy of ^{54}Mn(310 d) gamma radiations is expected to be a useful thermometer, since

a) there is only one gamma ray of 0.835 MeV, giving a pulse height spectrum which is uncontaminated with other radiations, consequently in spite of the rather poor resolution ($\approx 15\%$) of our light-guide counters, the intensity could be fairly accurately measured.

b) the h.f.s. coupling of Mn^{++} is isotropic and its magnitude is, in ionic salts, practically independent of the environment; this is a favourable aspect in view of the possibility that not *all* the Mn-ions are in well-defined lattice positions. For ^{55}Mn in many tutton salts the value $A = 0.0093$ cm^{-1} or $A/k = 0.0134$°K has been found[10]). Since $\mu\,(^{55}\text{Mn}) = 3.46\ \mu_N$ and $^{55}\text{I} = \frac{5}{2}$, while $\mu(^{54}\text{Mn}) = 3.30\ \mu_N$[11]) and $^{54}\text{I} = 3$, one calculates $A(^{54}\text{Mn})/k = 0.0104$°K.

A complication arises from the splitting of the $S = \frac{5}{2}$ electronic state by a crystalline field. This splitting, expressed by a DS_z^2-term in the spin Hamiltonian, ($D/k = -0.06$°K in the Cs tutton salt)[4]) has negligible influence in the presence of both a large magnetic field ($H > 3$ kOe) and low temperatures, so that $g\mu_B H \gg kT$ and practically only the $S_z = -\frac{5}{2}$ state is populated.

From the distance, $\Delta = 5A/2$ between successive h.f.s. energy levels one easily calculates the value of the nuclear orientation parameters f_2 and f_4 as a function of $1/T$.

c) the nuclear decay characteristics are well known and very simple (form. (4.10)):

$$W(\theta) = 1 - \tfrac{5}{7}(f_2/f_2^{\mathrm{m}})\, P_2(\cos\theta) - \tfrac{2}{7}(f_4/f_4^{\mathrm{m}})\, P_4(\cos\theta).$$

Here θ is the angle between the counter and the preferred direction of

nuclear orientation, which is also the direction of the magnetic field, irrespective of the relative directions of field and crystalline axes.

For $\theta = 0$ and $\pi/2$, the theoretical curves of W versus $1/T$ are given in fig. 5.

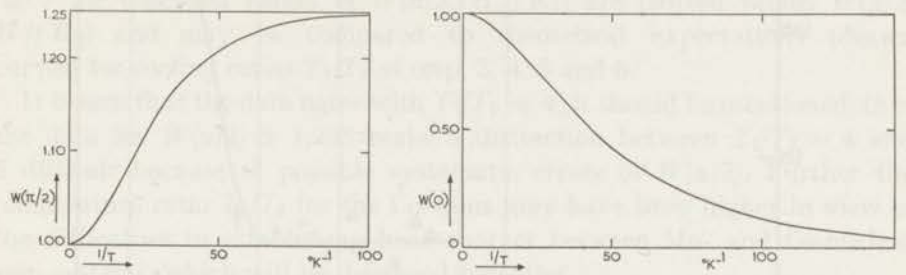

Fig. 5. Theoretical intensity distribution $W(\pi/2)$ and $W(0)$ of ^{54}Mn gamma radiation as a function of $1/T$, where T is the thermodynamic temperature. The angles 0 and $\pi/2$ refer to directions with respect to the preferred axis of nuclear alignment, i.e. the direction of the external magnetic field.

The results of nuclear orientation experiments on ^{54}Mn in other substances (e.g. CeMg-nitrate) and in the presence of appreciable magnetic fields are in reasonable agreement with the theoretical curve. It is seen that $W(\pi/2)$ reaches at $T = 0$ a maximal value of 1.25, where $W(\pi/2)$ is normalized to 1 at high temperatures; further $W(\pi/2)$ does not sensitively depend on T at low T, from which the limitations of the use of ^{54}Mn as a thermometer may be inferred. On the other hand, $W(\pi/2) - 1$ is still appreciable at $1/T = 20°K^{-1}$, allowing a temperature determination of the CoCs-sample in the precooling period.

Systematic errors in the observed $W(\theta)$ such as background and finite solid angles may be easily accounted for; however, misalignment of the counters or a contribution to the counting rate from gamma rays, which are scattered over small angles in the cryostat and hence do not exhibit the extremal anisotropy (particularly at $\theta = 0$), cannot be precisely evaluated. If the systematic errors add up unfavourably and are compounded with the statistical errors, the uncertainty in $W(\pi/2)$ may be as large as 0.5%.

5.2. *Rotational cooling.* $W(\pi/2)$ was measured both in the precooling period ($\boldsymbol{H}$ // K_1-axis) and in the post-cooling period ($\boldsymbol{H}$ // K_2-axis) as a function of time and for various field strengths. A typical result, obtained on a deuterated CoCs-sample, may be seen in fig. 6, where $W(\pi/2)$ is plotted versus time. It may be seen that $W(\pi/2) - 1$ increases in the precooling period as a result of the indirect cooling of the sample by the Cr-alum cooling salt. The value of $W(\pi/2)$ obtained after 60 minutes corresponds to $T = 0.055°K$, which is considerably higher than the temperature of the

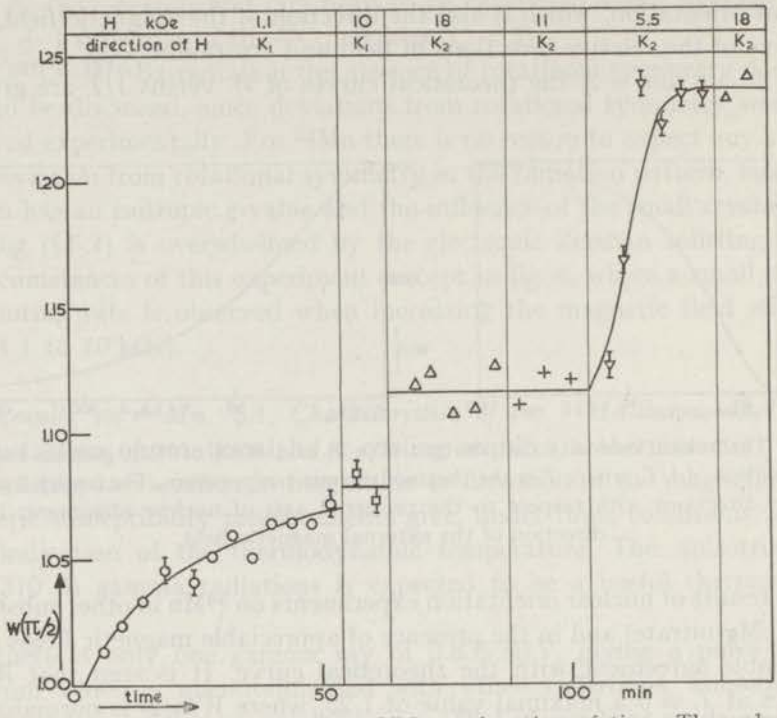

Fig. 6. Typical series giving $W(\pi/2)$ for ^{54}Mn as function of time. The values and directions of the applied magnetic fields are indicated on top of the figure.

Cr-alum. $W(\pi/2)$ does not change when the magnetic field is increased; this indicates that the electron spin entropy has been entirely removed. After rotational cooling $W(\pi/2)$ is somewhat higher, but approaches the value 1.25 only when the magnetic field is first reduced to a rather low value, $H = 5.5$ kOe. The rotational cooling, being due to the Co-spins, has apparently no effect on the ^{54}Mn-spins unless the magnetic field decreases its "hold" on the Mn^{++}-ions to some extent. However, once cooling of the ^{54}Mn-spins has been achieved, a subsequent increase of H to 18 kOe does

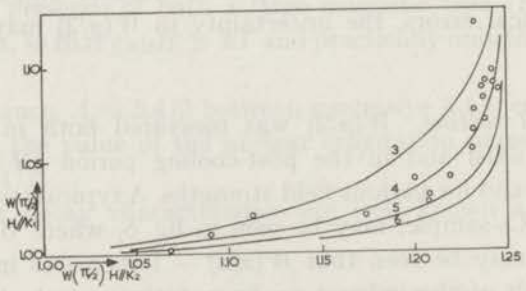

Fig. 7. $W(\pi/2)$ for ^{54}Mn before ($\boldsymbol{H} \,//\, K_1$) and after rotational cooling ($\boldsymbol{H} \,//\, K_2$). The drawn theoretical curves are obtained from fig. 5 assuming cooling ratios $T_1/T_f = 3$, 4, 5 and 6.

not change $W(\pi/2)$; such a change might have been expected, for instance, if electronic Zeeman splittings were responsible for the cooling effects.

A comparison of the $W(\pi/2)$-values for $\boldsymbol{H} \,//\, K_1$ with that for $\boldsymbol{H} \,//\, K_2$ gives, with the aid of fig. 5, a determination of the cooling ratio, T_i/T_f. In fig. 7 the observed values of $W(\pi/2,\ \boldsymbol{H} \,//\, K_1)$ are plotted versus $W(\pi/2,\ \boldsymbol{H} \,//\, K_2)$ and may be compared to theoretical expectations (drawn curves) for cooling ratios T_i/T_f of resp. 3, 4, 5 and 6.

It is seen that the data agree with $T_i/T_f \approx 4$; it should be mentioned, that the data for $W(\pi/2) > 1.235$ make a distinction between $T_i/T_f = 4$ and 5 difficult because of possible systematic errors in $W(\pi/2)$. Further the temperature ratio T_i/T_f for the Co-spins may have been higher in view of the difficulties in establishing heat contact between Mn- and Co-nuclear spin systems, which will be discussed hereafter.

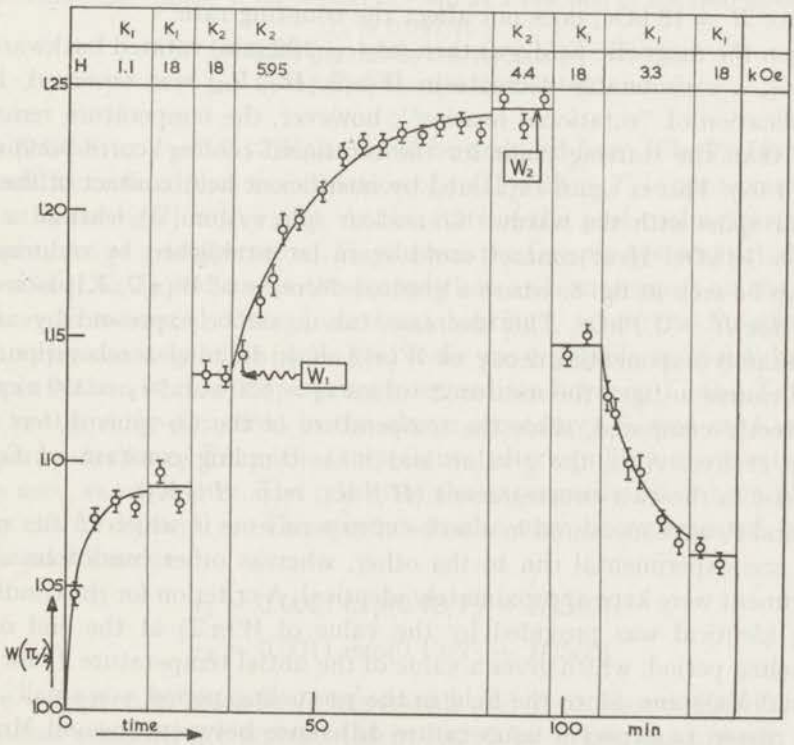

Fig. 8. Typical series demonstrating the occurrence of a relaxation time for $W(\pi/2)$ of ^{54}Mn. Directions and magnitudes of the magnetic field are indicated on top of the figure. The values W_1 and W_2 do not refer to K_1-respectively K_2-axes, but denote the value of $W(\pi/2)$ at the start and at the end of a relaxation time measurement for $\boldsymbol{H} \,//\, K_2$ and $H = 5.95$ kOe.

5.3. *Relaxation phenomena.* The occurrence of nuclear relaxation effects are illustrated in fig. 8, where again $W(\pi/2)$ is plotted versus time and where

the varying conditions of direction and magnitude of the magnetic field are indicated at the top of the drawing. The increase of $W(\pi/2, \boldsymbol{H} \,//\, K_2)$ to a value of 1.24 is less steep than in fig. 6, which is due to the somewhat larger field $H = 5.95$ kOe, compared to $H = 5.5$ kOe in fig. 6. For fields $H < 4.5$ kOe the counting rate $W(\pi/2, \boldsymbol{H} \,//\, K_2)$ becomes nearly 1.25 in a time less than that required for reducing the field and for counting. This indicates extreme sensitivity of the relaxation rate to the magnitude of H and makes it very probable that, in fig. 8, at $H = 4.4$ kOe the maximum value of $W(\pi/2, \boldsymbol{H} \,//\, K_2) \equiv W_2$ has been reached. Denoting the initial value by W_1, it is generally found that the dependence of $W(\pi/2)$ on time, denoted by $W(t)$, can be expressed by an exponential rise:
$W(t) = W_2 + (W_1 - W_2)2^{-t/\tau_2}$ where τ_2 is the relaxation time and where the index 2 refers to the K_2 direction. In fig. 8, $\tau_2 \approx 630$ s.

As mentioned before (fig. 5), raising the field strength to high values, for instance $H = 18$ kOe, does not affect the counting rate.

When the magnetic field was then (at $t = 100$ min) rotated backwards to $\boldsymbol{H} \,//\, K_1$, a considerable decrease in $W(\pi/2, \boldsymbol{H} \,//\, K_1)$ was observed, being an indication of "rotational heating"; however, the temperature remained lower than the starting point for the rotational cooling (corresponding to $W \approx 1.09$). This is again explained by insufficient heat contact of the Mn-nuclear spins with the warmer Co-nuclear spin system, at least in a field of $H = 18$ kOe. Heat contact could again be established by reducing H, as may be seen in fig. 8, where a gradual decrease of $W(\pi/2, K_1)$ is seen to occur for $H = 3.3$ kOe. This decrease can again be expressed by an approximately exponential decay of $W(\pi/2, K_1)$, defining a relaxation time τ_1. Of course in fig. 8 the measured values $\tau_2 = 630$ s and $\tau_1 = 330$ s cannot be directly compared, since the temperature of the Co-spins differs by a factor of five. Also, the g-value and h.f.s. coupling constant of Co are different in the two circumstances ($\boldsymbol{H} \,//\, K_2$, resp. $\boldsymbol{H} \,//\, K_1$).

τ_1 and τ_2 were measured in a series of experiments in which H was varied from one experimental run to the other, whereas other conditions of the experiment were kept approximately identical. A criterion for the conditions being identical was provided by the value of $W(\pi/2)$ at the end of the precooling period, which gives a value of the initial temperature T_i for both Co- and Mn-spins. Since the field in the precooling period was small, there is no reason to expect a temperature difference between Co- and Mn-spin systems. This is particularly true if it is assumed that the precooling rate is determined primarily by heat conductivity bottle necks.

Results of the measurements of τ_1 and τ_2 at $T_i \approx 0.05$°K are shown in fig. 9.

In order to determine the influence of the temperature on τ_1 and τ_2, measurements were carried out at a fixed field strength, but with varying time and field strength of the precooling period, resulting in variation

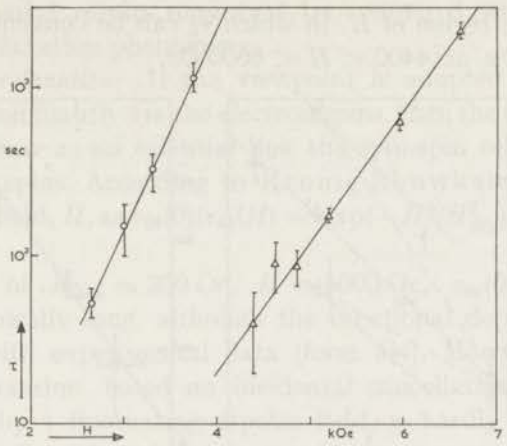

Fig. 9. Relaxation times, τ, for $W(\pi/2)$ of ^{54}Mn as a function of the field strength at $T_i = 0.047°$K.
○ field parallel to the K_1 axis (τ_1)
△ field parallel to the K_2 axis (τ_2)

of T_i ($0.04°\text{K} < T_i < 0.12°\text{K}$) as could be deduced from $W(\pi/2)$. However, it should be realized that a comparison of $\tau_1(T)$ with $\tau_2(T)$ is not as meaningful as that of $\tau_1(H)$ with $\tau_2(H)$. At the start of the post-cooling period the Mn-spins are at a temperature, T_i, whereas the Co-spin system had already been cooled to T_f and under these conditions τ_2 is measured; on the other hand, τ_1 is measured after "rotational heating", when the Co-spins are again approximately at T_i (since heat leaks are negligible, see § 6.4) but the Mn-spin system is at a temperature intermediate between T_i and T_f. Since T_f is not directly measured in the above procedure, T_i was used instead as a parameter for τ_2. For τ_1 the temperature, after equilibrium was established, is used as parameter. The results of the experiments have been plotted in fig. 10 for τ_1 and τ_2. The various results may be represented by the empirical formulae

$$\tau_1 = 0.0021 \exp(0.18/T_i + H/360) \tag{5.1}$$

$$\tau_2 = 0.0011 \exp(0.13/T_i + H/560) \tag{5.2}$$

where τ is given in seconds, H in oersteds and T in degrees Kelvin; these functional relations are represented in fig. 10 by drawn lines. As to τ_2, of which the measurements are relatively more accurate than those of τ_1, the field dependence may also be fitted to

$$\tau_2 \sim H^{10} \tag{5.3}$$

or to

$$\tau_2 \sim \exp(H/2600)^2. \tag{5.4}$$

That τ_2 can be fitted to various functional relationships is due to the very

limited accessible region of H, in which τ_2 can be conveniently measured: $50\text{ s} < \tau_2 < 3600\text{ s}$ at $4400 < H < 6600$ Oe.

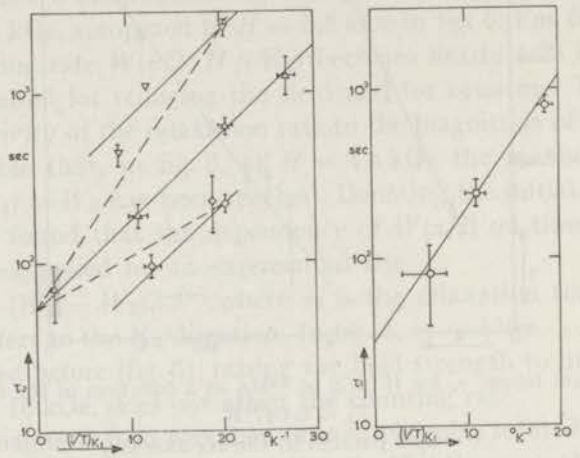

Fig. 10. Relaxation times for $W(\pi/2)$ of ^{54}Mn as a function of temperature. The drawn lines represent formulae (5.1) and (5.2). The dotted lines indicate the impossibility of fitting all the data by a H/T dependence.

▽ τ_2 $H = 6.70$ kOe ◇ τ_2 $H = 5.35$ kOe
△ τ_2 $H = 5.94$ kOe ○ τ_1 $H = 3.52$ kOe

Discussion. The qualitative features of the experimental results are clearly:

1) a strong dependence of τ on field strength
2) a relatively weak dependence of τ on the temperature T
3) the field strengths, for which roughly $\tau_1 = \tau_2$, are appreciably different.

A comparison between the field strength dependence and the temperature dependence, shows (fig. 10) that τ cannot be a function of H/T alone. The magnitude of the coefficient of $1/T$ in form. 5.1 and 5.2 suggests, that the temperature dependence is not determined by a Boltzmann distribution over the electronic Zeeman energy levels, (i.e. by $g\mu_B H/kT$) but rather by the Boltzmann distribution over the h.f.s. energy levels.

The fact that, in order to make $\tau_1 \approx \tau_2$, a stronger field is required in the K_2-direction than in the K_1-direction, may be related to the anisotropy in the g-value. It is remarkable that the field dependent factor in τ can be represented by $\exp(g_{Co} + g_{Mn})\, H/2750$ for both the K_1- and K_2-direction, according to form. (5.1), (5.2). Apparently τ is determined to a considerable extent by the electronic Zeeman splitting of both Co-ions and Mn-ions. This might indicate that heat contact between Co- and Mn-nuclear spins is established via both Co- and Mn-electronic spins acting as intermediaries. This occurs in spite of the extremely small population densities of the electronic Zeeman levels (except the lowest one, $S_z = -\frac{1}{2}$, $S_z = -\frac{5}{2}$ for Co and Mn respectively).

The experimental results may first be compared with existing interpretations of relaxation phenomena.

1. *Spin-spin-relaxation.* If the viewpoint is adopted that the nuclear spins relax predominantly via the electron spins, then the chain of relaxation events would show as an essential link the spin-spin relaxation time, τ_{ss}, of the electron spins. According to Kronig-Bouwkamp[12]), τ_{ss} depends on the external field, H, as $\tau_{ss}(0)/\tau_{ss}(H) = \exp(-H^2/H_{dip}^2)$, where H_{dip} is the dipolar field.

Substitution of $H_{dip} \approx 200$ Oe, $H = 6000$ Oe, $\tau_{ss}(0) = 10^{-9}$ s makes $\tau_{ss}(H)$ astronomically long, although the functional dependence is not in disagreement with experimental data (form 5.4). Moreover, the Kronig-Bouwkamp relaxation, based on incidental cancellation of the external magnetic field by a fluctuating dipolar field, is hardly applicable to the extremely ordered system of electronic spins in our experiment.

2. *Spin-waves.* The ordered state of the electronic spin system does not justify the introduction of spin-waves as a relaxation mechanism, since the mutual coupling among electronic magnetic moments is very much smaller than the Zeeman energy of the electronic moments individually.

3. *Phonons.* Although the lattice is practically emptied of phonons for $T < 0.05°$K, one might still be tempted to explain a Co-Mn-nuclear spin relaxation with the aid of an exchange of a (real or virtual) phonon. The only mechanism which possibly comes into play is the "direct process", in which a phonon is emitted spontaneously and subsequently absorbed, since stimulated emission is negligible if $g\mu_B H \gg kT_p$, T_p being the phonon temperature. For a Kramers salt Orbach[13]) gives a relaxation rate of the electron spins, $W = 1/\tau_p \sim H^5$ if, in addition to $g\mu_B H \gg kT_p$, also $g\mu_B H \gg kT_s$, T_s being the spintemperature i.e. if practically only the lowest electronic Zeeman levels are occupied.

Apart from order of magnitude considerations, it is seen that τ decreases with increasing H, in striking contradiction to experimental results. The introduction of virtual phonons will not alleviate this difficulty.

Direct interaction of the nuclear spins with the lattice will be negligible at these low temperatures and, moreover has, similarly, the wrong dependence on H.

4. *Indirect coupling of nuclear spins.* The most effective mechanism is presented by indirect coupling of the nuclear spins similar to the Rudermann-Kittel[14]) interaction in metals or to the Suhl-Nakamura[15]) interaction in magnetically ordered salts .This may be briefly stated as follows. The h.f.s. coupling energy of Co-ions will, for purposes of discussion, be assumed isotropic and equal to that of Mn. If we take the direction of the magnetic field as the z-axis of quantization, then the relevant part of the spin

Hamiltonian becomes

$$\mathcal{H} = \sum_{i=1,2} H_z S_z^{(i)} + \sum_{i=1,2} A S_z^{(i)} I_z^{(i)} + \sum_{i=1,2} B(S_+^{(i)} I_-^{(i)} + S_-^{(i)} I_+^{(i)})$$

where $B = A$ according to the assumptions, not only for Mn^{++} $(i = 1)$ but also for Co^{++} $(i = 2)$. The wave function describing one pair of Co–Mn-ions for $B = 0$ would be

$$\Psi = \psi_1(S_z^{(1)} I_z^{(1)})\, \psi_2(S_z^{(2)} I_z^{(2)}) = |S_z^{(1)}, I_z^{(1)}\rangle\, |S_z^{(2)}, I_z^{(2)}\rangle$$

For $B \neq 0$ this is modified in:

$$\psi_1(S_z^{(1)} I_z^{(1)}) = |S_z^{(1)}, I_z^{(1)}\rangle + \frac{Ba}{g\mu_B H} |S_z^{(1)} + 1, I_z^{(1)} - 1\rangle - \frac{Bb}{g\mu_B H} |S_z^{(1)} - 1, I_z^{(1)} + 1\rangle$$

where a and b are spin dependent factors of order unity (either a or b is zero for Co, where $S = \frac{1}{2}$). We now consider a perturbing interaction $\mathcal{H}_{\text{pert}}$, which will be of order of magnitude $g\mu_B H_{\text{dip}}$, and which contains, among others, the operators $S_+^{(1)} S_z^{(2)}$ and $S_z^{(1)} S_+^{(2)}$. It may easily be verified, that these operators induce transitions

$$\Psi_i = \psi_1(S_z^{(1)} I_z^{(1)})\, \psi_2(S_z^{(2)} I_z^{(2)}) \to \Psi_f = \psi_1(S_z^{(1)}, I_z^{(1)} - 1)\, \psi_2(S_z^{(2)}, I_z^{(2)} + 1)$$

Since $B/g\mu_B H \approx 10^{-2}$ and $H_{\text{dip}}/H \approx 10^{-2}$, one easily finds from the transition probability

$$W = \frac{2\pi}{\hbar} \int |\langle \Psi_f\, |\mathcal{H}_{\text{pert}}|\, \Psi_i \rangle|^2\, d\rho,$$

that $\tau_{\text{ind}} = 1/W \approx 0.1$ s, where τ_{ind} is the relaxation time due to indirect coupling of two nuclear spins. Further, $\tau_{\text{ind}} \sim H^4$.

This relaxation is too fast by two to three orders of magnitude and also does not give a sufficiently strong dependence on H. One may conclude, that the magnetic field provides an additional inhibiting factor in the energy-exchange between Co and Mn nuclear spins. The above formalism was introduced in order to show that the Ruderman-Kittel mechanism would predict relatively long relaxation times, which are strongly dependent on H, even when the differences between Co and Mn-ions are neglected in a first approximation. For instance the difference between the h.f.s. energy for Co and that for Mn may prevent this indirect coupling to be effective for a relaxation process, unless the h.f.s. levels are sufficiently broadened by the dipolar field as to make a flip-flop process feasible with conservation of h.f.s. energy. It may be expected that both the dipolar interaction energy of the electronic angular momenta and the energy differences of the various Co h.f.s. sublevels depend appreciably on the magnitude of H. This de-

pendence combined with the derived $\tau \sim H^4$ dependence, would make τ a very sensitive function of H and can in principle explain the experimental results.

The temperature dependence of τ cannot be easily taken into account, e.g. because of difficulties in relating the parameter T_1 to the thermodynamic temperature during the measurement of τ.

We feel that the experimental results are susceptible to a more precise theory, but this would require a more precise knowledge of the h.f.s. level splitting of the Co-ions under the combined influence of dipolar and external magnetic fields.

5.4. *Reorientation.* A few experiments were done on a ^{54}Mn sample, using a magnet with hollow poles, so that also the γ ray intensity in the direction of the field, $W(0)$, could be measured. The main purpose of this experiment was to obtain information about a possible disorientation of ^{54}Mn in the 0.835 MeV state with half life of 12 ps as a result of disturbing effect of the preceding K capture. Such a disorientation would have a much larger effect on $W(0)$ than on $W(\pi/2)$.

After rotational cooling and waiting for about one hour we found experimentally $W(0) = 0.105$ in a field of 5.3 kOe. After correction for the finite solid angle of the counter (-0.025), background (-0.006) and scattering by the cryostat and the magnet (-0.010) we find $W(0) = 0.065$. When there was uncertainty about the corrections we used the lowest absolute value, therefore it is possible that the true value of $W(0)$ is somewhat lower. From $W(0) \leqslant 0.065$ one deduces that at least 97.5% of the nuclear spins were in the lowest h.f.s. magnetic sublevel ($m = I_z = -2$) when emitting gamma radiation. On the other hand, from the known h.f.s. splittings one calculates that at a temperature of 0.006°K or higher there were no more than 99.5% of the spins in the lowest level before K-capture.

Consequently the population density of the lowest sublevel could have been decreased by at most 2%, as a result of the K-capture disturbance, which signifies a transition probability smaller than $1 \times 10^9\ s^{-1}$ for $\Delta I_z = +1$ transitions.

The time required to obtain the lowest values for $W(0)$ was much larger than corresponds to the characteristic time τ_2 mentioned in § 5.3. This might be ascribed to the fact that the redistribution over the ^{54}Mn nuclear energy levels here was observed in a much lower temperature region than in § 5.3. and from $W(0)$ instead of $W(\pi/2)$.

6. *Results on ^{137}Cs.* When ^{137}Cs nuclei were incorporated in the Co–Cs-salt and when rotational h.f.s. cooling was applied to the Co-nuclei, an anisotropy was found in the intensity of the 662 keV gamma radiation, which is emitted in the decay of the ^{137m}Ba daughter nuclei. The anisotropy

depended on the magnetic field strength and even changed sign at $H \approx 10$ kOe; at high fields ($H \approx 20$ kOe) the gamma rays were not preferably emitted in directions perpendicular to the field, as would have been expected for the case of "brute force" polarization of the radioactive nuclei of the diamagnetic Cs-ions in an external magnetic field. Therefore an auxiliary experiment was carried out which had the advantage that the gamma ray intensity distribution could be measured at arbitrary angles; the results of these measurements will first be presented, deferring the results of rotational cooling to § 6.2.

6.1. *Measurements in magnetically diluted Cu-tutton salts.* ^{137}Cs was built into single crystals of $MgCs_2(SO_4)_2.6H_2O$, $ZnCs_2(SO_4)_2.6H_2O$ and $Zn(NH_4)_2\,(SO_4)_2\,6H_2O$, in which 10% of the Mg resp. Zn-ions were replaced by Cu^{++}; it is known that quite low temperatures ($T \approx 0.01°K$) can be reached in these salts by simple adiabatic demagnetization. The initial temperature was 0.9°K for the Zn samples. The Mg sample was mounted in the apparatus described in fig. 3 so that indirect cooling was used before demagnetization. After demagnetization from a field $H = 18$ kOe to zero field, the intensity distribution, W, of the 662 keV gamma rays was measured in the K_1K_2-plane as a function of the temperature. At the lowest obtained temperatures $W(\rho)$, normalized to 1 at high temperatures, could be represented by the expressions, resp. for the three salts:

$$\text{Mg–Cs: } W(\rho) = 1.039 - 6.0 \times 10^{-2} \sin^2(\rho + 3°)$$

$$\text{Zn–Cs: } W(\rho) = 1.033 - 5.0 \times 10^{-2} \sin^2(\rho + 9°)$$

$$\text{Zn–NH}_4\text{: } W(\rho) = 1.0185 - 2.7 \times 10^{-2} \sin^2(\rho - 13°)$$

as may also be seen in fig. 11.

Here ρ is the angle between the direction of the counter and an axis, which subtends an angle of 31° with the crystallographic a-axis. The direction $\rho = 0$ practically coincides with the K_1-axis in the isomorphous $CoCs_2(SO_4)_2.6D_2O$ salt.

The radioactive heat caused a warm-up of the $Zn(NH_4)$ sample to $T = 0.1°K$ in about 15 min; the warming up rate was smaller for the Mg–Cs sample and negligible for the Zn–Cs sample. Since $W(\rho) - 1$ is small, according to form 4.4 only a f_2P_2-term needs to be considered and then the temperature dependence of $W(\theta, T)$ is represented entirely by the f_2-parameter, having no interference with the angular dependence.

The radiation intensity distribution was also measured with the counter in the K_1K_3-plane and was found for the Mg–Cs crystal to be $W(\sigma) = 1.039 - 0.0054 \sin^2\sigma$ where σ is the angle of the counter with respect to the K_1-axis.

The largest deviation of $W(\rho)$ and $W(\sigma)$ from the high temperature value

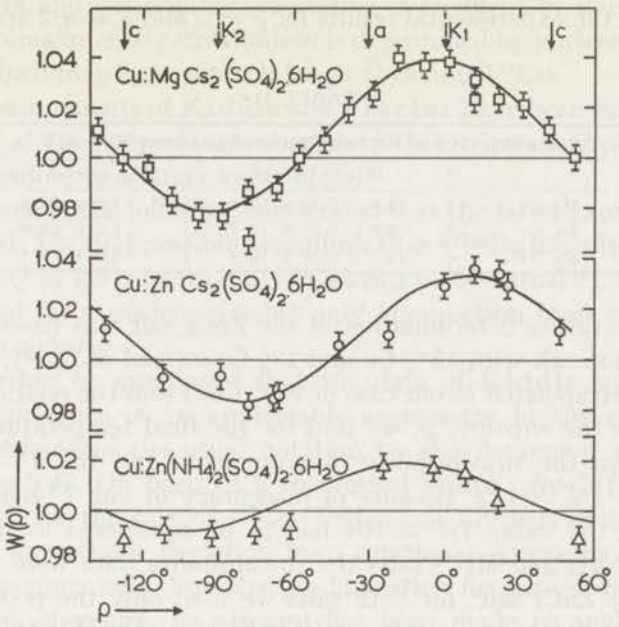

Fig. 11. Radiation intensity distribution $W(\rho)$ in the K_1K_2-plane for ^{137}Cs in diluted copper tutton salts. The K_1 and K_2 axis refer to CoCs-tutton salt.

1 is therefore found to occur near the K_1-axis and to be positive. Using this result and form. (4.4). one finds that the nuclear spins are preferably orientated in the K_2K_3-plane.

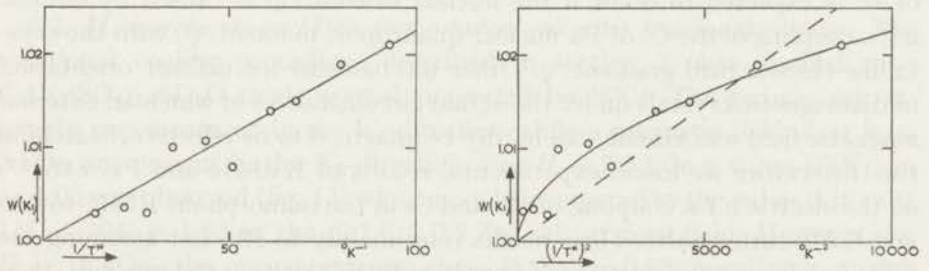

Fig. 12. Temperature dependence of $W(K_1)$ for ^{137}Cs in $Zn:Cu(NH_4)_2(SO_4)_2.6H_2O$. In both figures the same points are plotted demonstrating a $1/T^*$ dependence, which is indicated by the drawn lines, the dotted line giving a $(1/T^*)^2$ dependence. The statistical error in the counting rate results in an error of 0.2% for all points. For the normalizing point at $1/T^* = 0$ the statistical error is 0.08%.

Temperature dependence. $W(\rho) - 1$ was found to fit a T^{-1} dependence appreciably better than a T^{-2} dependence, as is shown in fig. 12 for one salt and one particular direction, $\rho = 0$, where $W(\rho) - 1$ reached almost its maximum value as a function of ρ. Adopting a $1/T$-dependence of $W(\rho, T)$

for all salts, the experimental results for $\rho = 0$ and $\rho = \pi/2$ are represented in table II.

TABLE II

Coefficients α of the temperature dependence $W = \alpha/T$		
	$W(\rho = 0) - 1$	$W(\rho = \pi/2) - 1$
Mg Cs	$(3.6 \pm 0.3) \times 10^{-4}$	-1.4×10^{-4}
Zn Cs	$(3.1 \pm 0.5) \times 10^{-4}$	-1.2×10^{-4}
Zn NH_4	$(2.3 \pm 0.3) \times 10^{-4}$	-0.8×10^{-4}

The temperature determination of the ZnCs salt was based on data on a ZnRb tutton salt with 13% Cu and 1% Co instead of Zn[16]; those results had to be extrapolated to our case of 10% Cu. From the relation of temperature, T, to the entropy, S, we find for the final temperature $1/T = 104$ whereas from the susceptibility measurements and the $T - T^*$ relation one obtains $1/T = 122$. Because of inaccuracy of our T^*-measurement of about 15%, the value $1/T = 104$ has to be considered as more reliable. For the $ZnNH_4$ and MgCs salts the susceptibility data were more reliable than for the ZnCs salt; for both salts we used only the points for which $1/T^* < 80$ in determinating the coefficients given in table II. From ref. 16 it follows that the difference between T and T^* should be less than 5% in this temperature region. The errors in $W(\rho) - 1$ versus T, given in table II, are partly due to the above mentioned inaccuracies in T, and partly due to the statistical inaccuracy in the counting rate.

Orientation mechanism. According to form. (4.6) and (4.4) a $1/T$-dependence of W is expected to occur if the nuclear orientation is caused by electric h.f.s. coupling of the Cs of Ba nuclear quadrupole moment, Q, with the crystalline electric field gradient, q. Other mechanisms for nuclear orientation in diamagnetic crystals under the actual circumstances in which an external magnetic field was absent, can hardly be imagined to be effective. Searching the litterature we found experimental results of Kiddle and Proctor[17] on the electric h.f.s. coupling of Rb and Cs in the isomorphous RbMg-tutton and CsMg-tutton salts. Their results refer mainly to Rb, but assuming the principal axes of the electric field gradient to be equal for the two ions, they estimate $q(\mathrm{Cs})/q(\mathrm{Rb}) = 2$. This would give $e^2qQ(^{137}\mathrm{Cs})/k = 1 \times 10^{-4}\,^\circ\mathrm{K}$, leading to $P/k = 3.6 \times 10^{-6}\,^\circ\mathrm{K}$.

On the other hand, a lower limit for the value of $|P|$ may be deduced from a comparison of our experimental results (table II) with theoretical formulae (4.4) and (4.6). This lower limit, $P/k \geqslant 1.2 \times 10^{-4}\,^\circ\mathrm{K}$, is obtained by assuming the external direction $\rho = 0$ to coincide with $\theta = \pi/2$ in (4.4) (i.e. assuming the nuclear spins to be preferably aligned along an axis in the K_2K_3-plane) since any other assumption would lead to a smaller value of $W(\rho = 0)$. The discrepancy of a factor of at least 30 between the quadrupole

resonance data and our nuclear orientation data might be due to:

1. The gamma intensity distribution is determined by nuclear orientation of ^{137m}Ba, which may have a much larger Q than $Q(^{137}\mathrm{Cs})$.

2. The measurements of Kiddle and Proctor have been made at room temperature; at low temperatures changes in the environment of the Cs ions may occur, leading to a larger value of q.

It will be seen in the following sub-section that the latter explanation has to be favoured. The first possibility requires that ^{137m}Ba has a large quadrupole moment, $Q \approx 1.5$ barn (that of ^{137}Cs being 0.050 barns) [18], which is not to be expected for a nucleus missing only one nucleon from an otherwise closed shell structure.

It may further be mentioned that the data of Kiddle and Proctor indicate the presence of an appreciable asymmetry in the electric field gradient, expressed in the usual notation by the parameter $\eta = (V_{xx} - V_{yy})/V_{zz} = 0.47$. On basis of a theoretical formula for $W(\theta, \varphi)$, which can be derived for the case of ^{137}Cs–^{137m}Ba and which is quite similar to eq. (4.23) an appreciable deviation from rotational symmetry might have occurred. Experimentally, however, no indication for such deviations have been observed, therefore, no attempt has been made to analyse the directional distribution of the gamma radiation with the aid of the directions of the electric field gradient tensor, as found by Kiddle and Proctor.

From the results mentioned in fig. 11 and table II it follows that the differences between the three salts are quite small, especially between ZnCs and MgCs. Therefore it seems justified to use the results on ZnCs for the temperature determination in CoCs tutton salt, as is done in § 6.4.

6.2. *Measurements on ^{137}Cs in Co-tutton salt after rotational cooling.* The rotational cooling procedure, described in section 3, was applied to a $CoCs_2(SO_4)_2.6D_2O$ single crystal, activated by ^{137}Cs. The gamma ray intensity was measured in the K_1-direction while a magnetic field of at least 3 kOe was present in the K_2-direction. For $H = 5.5$ kOe a value $W(K_1) = 1.03$ was observed (fig. 13) which may be compared to the value $W(\theta = 0, 1/T = 104) = 1.03$ in the (0.1 Cu, 0.9 Zn) salt at zero field. However, for $H = 18$ kOe, the measurements gave $W(K_1) = 0.98$, signifying a sign reversal of $W(K_1) - 1$ and consequently of the parameter f_2, in other words leading to a change of the preferred axis of nuclear orientation. A reduction of the magnetic field to values below 4 kOe caused an irreversible decrease of $W(K_1)$ towards the high temperature value 1, as found also for ^{54}Mn (§ 5). Variations in $W(K_1)$, induced by variation of the magnetic field strength in the region $5.5 \leqslant H \leqslant 18$ kOe, were, however, reversible within experimental accuracy; for instance changing H three times upwards and downwards between the above limits did not noticeably change the values of $W(K_1)$. However, the variation of $W(K_1)$ did not instantaneously follow the

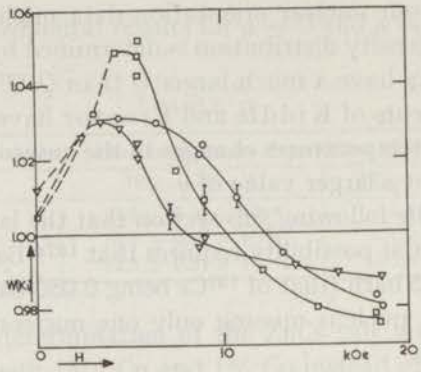

Fig. 13. The normalized γ ray intensity in the direction of the K_1 axis, $W(K_1)$ for ^{137}Cs in $CoCs_2(SO_4)_2.6D_2O$ as a function of the field strength H of a field which is applied in the direction of the K_2-axis.

○ crystal 2 mm thick.
□ crystal 0.2 mm thick
▽ crystal 2 mm thick, diluted Zn:Co = 3.5 : 1.
dotted curves: irreversible warming up
drawn curves: reversible region.

variation of H, but a recovery time $\tau_{\frac{1}{2}} = 100 \pm 50$ s was found at $H = 18$ kOe, while $\tau_{\frac{1}{2}} < 25$ s at $H = 5.5$ kOe.

These experiments were repeated on a crystal, in which part of the Co ions had been replaced by Zn(Co:Zn = 1:3.5), primarily with the intention to obtain lower final temperatures. This crystal gave practically the same results as the undiluted crystals, i.e. the extremal values of $W(K_1)$ as a function of H and also the recovery times were approximately the same, while the form of the curve of $W(K_1)$ versus H was slightly different (fig. 13).

A larger value of $W(K_1) - 1$, and therefore presumably a lower final temperature, was in fact achieved by confining the Co and ^{137}Cs ions to a layer of only 0.02 cm thickness, grown upon a crystal of $ZnCs_2(SO_4)_2.6H_2O$; this crystal gave $W(K_1) = 1.05$ at $H = 5.5$ kOe and $W(K_1) = 0.98$ at $H = 18$ kOe (fig. 13).

6.3. *Discussion.* An explanation of the behaviour of $W(K_1)$ as a function of the magnetic field strength (in the K_2-direction) as described in 6.2 may be given on basis of the following assumptions:

a. The nuclear orientation was primarily due to electric h.f.s. coupling, similar to that in the copper salts, described in 6.1.

b. The electric h.f.s. coupling constant, P, has the opposite sign for ^{137}Cs in the Cs-ion with respect to that for ^{137m}Ba in the Ba-ion.

c. In high magnetic fields the nuclear relaxation time of ^{137m}Ba is so long that one may consider the 662 keV gamma rays to be emitted virtually instantaneously after β-decay; consequently the directional distribution

of the gamma rays is then entirely determined by the ^{137}Cs nuclear orientation, referring to the case of "perfect memory" in § 4. In low fields, on the other hand, one assumes the nuclear relaxation time of the ^{137m}Ba-nuclei to be small compared with the 2.6 min. half life of the 662 keV state, referring to the case of no memory in § 4.

The concept of nuclear relaxation time is associated with the reestablishment of a Boltzmann distribution of the Ba nuclear spin system over the h.f.s. energy levels, which are, according to (*b*), assumed to be inverted with respect to that of the Cs-ions. Under these assumptions the reversal of sign of $W(K_1) - 1$ as a function of magnetic field strength is simply explained by saying that the positive $W(K_1) - 1$ values are attributed to nuclear orientation of ^{137m}Ba (for instance preferably in the K_2K_3-plane), while the negative $W(K_1) - 1$ values in high fields are due to nuclear orientation of ^{137}Cs (for instance, in contrast to ^{137m}Ba, preferably along the K_1-axis).

The value of $W(K_1) - 1$ in intermediate fields is determined by the contribution of the perfect memory decays relative to that of no-memory decays; this in turn is determined by the ratio of the relaxation time τ to the half life, $t_{\frac{1}{2}}$. For some value of $\tau/t_{\frac{1}{2}}$ of the order of 1, the reestablishment of thermal equilibrium may have proceeded just far enough from the initial negative T to the final positive temperature T as to give infinite temperature, leading to a zero value of $W(K_1) - 1$. The recovery time $\tau_{\frac{1}{2}}$ is related approximately to $t_{\frac{1}{2}}$ and τ according to $1/\tau_{\frac{1}{2}} = 1/\tau \ln 2 + 1/t_{\frac{1}{2}}$ giving $\tau_{\frac{1}{2}} = t_{\frac{1}{2}} = 156$ s in high fields and $\tau_{\frac{1}{2}} < 25$ s in small fields. In other words, in high fields the no-memory decays die out with a characteristic time equal to $t_{\frac{1}{2}} = 156$ s, while in low fields the perfect-memory-decays quickly replace the no-memory-decays according to a time constant $\tau < 25$ s, i.e. the nuclear relaxation time.

Since the nuclear relaxation mechanism of Ba-nuclei in this environment is unknown, a more precise analysis of the recovery time and $W(K_1)$ for intermediate values of $t_{\frac{1}{2}}/\tau$ encounters serious difficulties, primarily because the concept of a Boltzmann distribution seems rather inappropriate. From the experimental results it is not quite certain that the magnetic fields up to 18 kOe were in fact sufficiently high as to obtain the situation $t_{\frac{1}{2}} \gg \tau$ i.e. of perfect memory-decays only. Neither is it certain that the maximum in the W versus H curve is to be associated with "no-memory-decays only" since irreversible heating in small fields tends to obscure the truly saturated value. If we, however, assume that $W(K_1) = 0.98$ at $H = 18$ kOe and $W(K_1) = 1.05$ at $H = 5.5$ kOe are the "saturated" values and if we assume that for ^{137}Cs and ^{137m}Ba the directions of the electric field gradient are the same, it follows $f_2(^{137}\text{Cs}) \approx -0.4\, f_2(^{137m}\text{Ba})$. Apart from random displacements of the Ba-ions – which would wipe out the nuclear orientation entirely – no changes in the electric field gradient are expected, since the Sternheimer antishielding factors are nearly equal for Ba and Cs. One can

calculate that the magnetic field of 18 kOe, acting on the nuclear magnetic moment of ^{137}Cs, may have appreciably reduced f_2 (^{137}Cs). Therefore we conclude that the quadrupole moment Q of ^{137m}Ba has roughly the same absolute value as Q (^{137}Cs) $= +\ 0.050$ and is negative. The negative sign agrees with the nuclear shell model, since ^{137m}Ba has a neutron missing from a closed $h_{\frac{11}{2}}$ shell, while ^{137}Cs lacks one proton from the $g_{\frac{7}{2}}$-shell; the odd proton and odd neutron, are in principle associated to opposite signs of the nuclear quadrupole moments. An additional conclusion is that the nuclear relaxation time τ is strongly field dependent, but reaches values of the order of 10^2 s at much higher fields than was found in § 5 in the ^{54}Mn-behaviour. Also, if τ is expressed as $\tau \approx H^n$, the exponent n is certainly smaller than 10, as was found for ^{54}Mn.

6.4. *Temperature determination.* The results of 6.1 and 6.2, in conjunction with the data of § 5 allow one to determine the temperature in the post-cooling period, which may be compared to the temperatures in the precooling period. For this purpose we want to compare results of two crystals of 0.2 cm thickness, one activated with ^{137}Cs and the other one with ^{54}Mn, the other experimental conditions being identical. Also a comparison is made between measurements on ^{137}Cs (1.5 μC) and on ^{54}Mn (0.1 μC), which were grown simultaneously in one thin layer (0.02 cm). These results are given in table III where T_i is the temperature at the end of the precooling period, T_f is the temperature at the start of the post-cooling period. The data of ^{54}Mn are derived from fig. 5, whereas for ^{137}Cs a temperature calibration was provided by the data of table II on (Zn : Cu) $Cs_2(SO_4)_2\ 6H_2O$.

TABLE III

Comparison of reached temperatures						
		end precooling period		postcooling period $H = 5$ kOe		
		$W(K_2)-1$ (%)	$1/T_i(°K^{-1})$	$W(K_1)-1$ (%)	$1/T_f(°K^{-1})$	T_i/T_f
thick crystal	^{54}Mn	7.0 ± 0.7	17.5 ± 1.5	23.6 ± 0.4	70	4 ± 0.5
thick crystal	^{137}Cs			3.0 ± 0.2	100 ± 20	5.7 ± 1.2
thin layer	^{54}Mn	12.7	28 ± 2	24.2 ± 1.0	>65	>2
thin layer	^{137}Cs	−0.8 ± 0.4	(70 ± 30)	5.3 ± 0.3	170 ± 35	6.0 ± 1.2

In table III it is further assumed that W is saturated as a function of H at 5.5 kOe, i.e. only "no-memory-decays" and absence of irreversible heating is assumed. In calculating T_i/T_f we used for T_i always the data on ^{54}Mn. From this table it can be concluded that in a field of 5 kOe a temperature well below 0.01°K was reached. The value of $W(K_1) - 1 = 5.3\%$ for ^{137}Cs decreased during one hour by 0.4% (± 0.4%, statistical error), indicating that the low temperature of the nuclear spin system can be maintained for a long time. In fields higher than 5 kOe we could not measure temperatures because of relaxation phenomena both for ^{54}Mn and ^{137}Cs.

7. *Results on* ^{60}Co. 7.1. *Experiments.* The concept of rotational h.f.s. cooling on Co-ions is based on reduction of h.f.s. energy splitting under adiabatic conditions; although the temperature decreases, the populations of the various h.f.s. energy levels do not change and hence the degree of nuclear orientation of ^{60}Co would remain constant. However, the nuclear spins are rotated and this may be detected as a change in gamma ray anisotropy. This was investigated experimentally on the $CoCs_2(SO_4)_2.6D_2O$ crystals, in which ^{60}Co replaced part of the stable Co. The procedure of cooling was described in § 3 and the experiments were also similar to those described in § 5 on ^{54}Mn. However, the direction of the magnetic field was varied in steps from the K_1-axis to the K_2-axis, the field strength being constant, i.e. the gamma ray intensity was measured as a function of the angle of $\boldsymbol{H}$ with the K_1-axis, ψ_H^*.

The experiments were carried out on 3 different samples. For the first sample we used the large electro-magnet, so that the γ ray intensity could

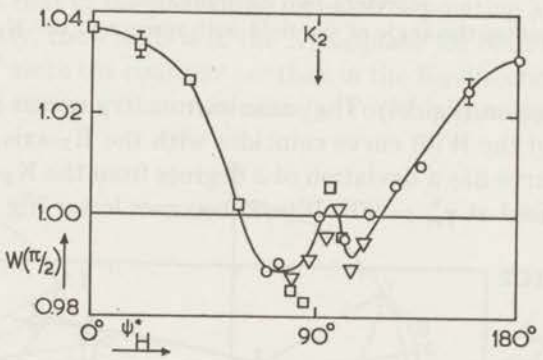

Fig. 14. The normalized γ ray intensity $W(\pi/2)$ of ^{60}Co in a direction perpendicular to the field as a function of the angle ψ_H^* between field and K_1-axis. The field strength is 18 kOe.
○: rotation of the field in the sense of decreasing ψ_H^*
□ and ▽: rotation of the field in the sense of increasing ψ_H^*.

be observed only in a direction perpendicular to the field, (i.e. $W(\pi/2)$) (fig. 14); for the other two samples a small magnet with hollow poles was used enabling a measurement of both $W(0)$ and $W(\pi/2)$ (fig. 15). The first sample was much thicker (2 mm) than the paramagnetic part of the other two samples which consisted of a 0.2 mm layer of CoCs-tutton salt on a ZnCs-tutton crystal. As a consequence, in the experiments on the latter samples lower temperatures were obtained since the thin layer could be precooled more efficiently than a thick crystal. The indicated position of the K_2 axis was found from the susceptibility data (§ 3.2).

The asymmetry of the $W(\pi/2)$ curves can not be due to heating up effects or rotation of the crystal since the same curve was found when reversing

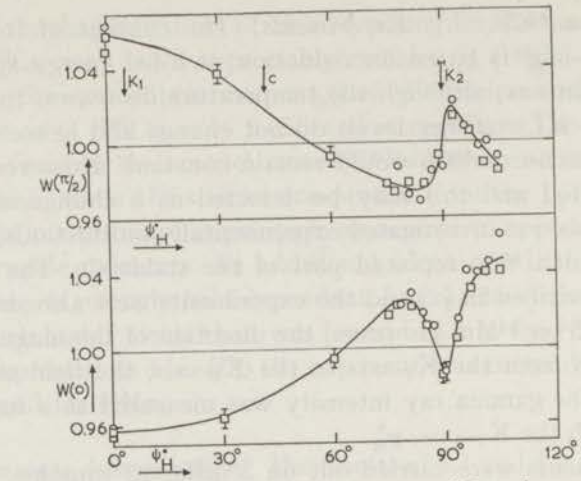

Fig. 15. The γ ray intensities of ^{60}Co in directions parallel and perpendicular to the field as a function of $\psi_H{}^*$ during rotation of a field of 5.2 kOe. The circles and squares represent two different runs.
$\psi_H{}^*$ denotes the angle of the field with respect to the K_1-axis.

the sense of rotation (fig. 14). The same asymmetry occurs for all samples. The minimum of the $W(0)$ curve coincides with the K_2-axis, the maximum in the $W(\pi/2)$ curve has a deviation of 3 degrees from the K_2-axis. When the field was decreased at $\psi_H^* = 90°$, $W(\pi/2)$ becomes lower (fig. 16).

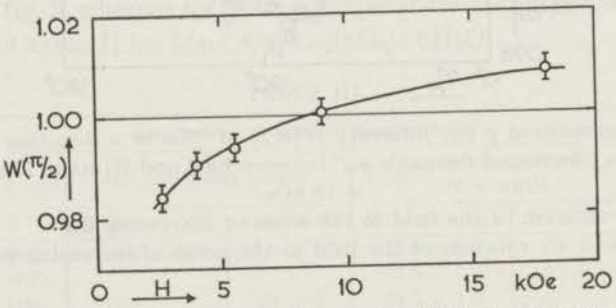

Fig. 16. $W(\pi/2)$ for ^{60}Co as a function of magnetic field strength H, H being along the K_2-axis.

7.2. *Calculation of γ ray anisotropy of ^{60}Co.* 7.2.1. *Semi-classical calculations.* The behaviour of the Co nuclear spins and of the directional distribution of the emitted ^{60}Co-gamma radiation may be analyzed as follows:

1) Considering the electron and nuclear spins as classical vectors, the formulae (2.2), (2.3) give the directons of these vectors with respect to the direction of the magnetic field, $\boldsymbol{H}$. The latter is defined by the angle ψ_H with respect to the tetragonal axis (z-axis) of the Co-ions, or, alternatively, by

the experimentally determined angle ψ_H^* with the K_1-axis, (the x-axis lies along the K_2-axis). The formulae relate the angle ψ_H to the angle ψ_N between the average direction of the nuclear spins and the z-axis.

2) Since the degree of nuclear orientation is sufficiently small in these experiments, the relatively small f_4P_4-terms may be omitted from the formula for the directional distribution of ^{60}Co gamma rays:

$$W(\theta) = 1 - \tfrac{2}{21}f_2P_2(\cos\theta) - \tfrac{6}{25}\tfrac{2}{2}f_4P_4(\cos\theta).$$

Here θ is the angle between the direction of the counter and an axis of rotational symmetry with respect to which f_2 is defined.

3) We assume *a*) that f_2 is always defined with respect to the average direction of the Co-nuclear spins and *b*) that f_2 remains numerically constant when the direction of $\boldsymbol{H}$ is varied.

Starting from the above assumptions, the calculation of the directional distribution, $W(\theta)$, of the ^{60}Co gamma rays is relatively simple. It has firstly to be remarked that in the precooling period $\boldsymbol{H}$ is pointing along the K_1-axis and consequently, the z''-axis is in the K_1K_3-plane for both types of Co-ions, so that $\theta = 90°$ since the counters are then in the K_2-direction. From $W(90°) = 1 + 0.595\,f_2$ one can then evaluate f_2. For this case $\psi_H = 40°$ and ψ_N

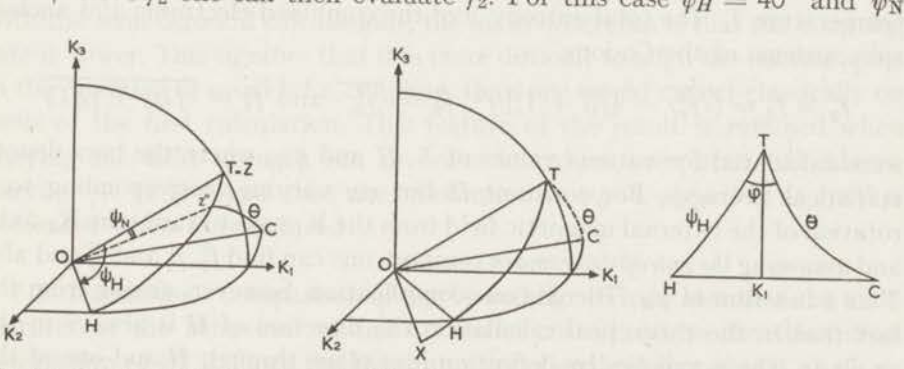

Fig. 17. Geometrical arrangement: The figure at the left side refers to the classical calculations, according to which the nuclear spins are aligned along the z''-axis, making an angle ψ_N with the z-axis (tetragonal axis, T) and an angle θ with the counter, C; H is the direction of the magnetic field. The middle and right figures refer to the quantum mechanical calculation. θ and φ are the polar angles of the direction of the counter with respect to T = z, φ being defined as the angle between the plane through T and C and the plane through T and H.

is only a few degrees, depending on the precise value $Ag_{//}/Bg_{\perp}$. From the experimental setting of the angle HOK_1 one determines ψ_H and from ψ_H, with the aid of (2.3), also ψ_N. In the triangle HCZ″ one can calculate θ from the known values of HOZ″, HOC = 90°, Z″HC = ZHK_1. The result of the calculations taking for the ratio $Ag_{//}/Bg_{\perp}$ = 12, 24 and infinity, are shown in fig. 18.

7.2.2. *Quantum mechanical calculation of* $W(\theta)$. The spin-Hamiltonian operator, $\mathcal{H}$, eq. (2.1), may be fairly simply put into matrix-form, using the (S_z, j_z) representation, where $j = I$ is the nuclear spin. In the following it will be assumed that $\boldsymbol{H}$ is always in the (x, z) plane, $H_y = 0$, and then all matrix-elements are real. The formulae for the matrix-elements were translated into Algol-code for the electronic computer Electrologica X1 of the Leiden-University; for numerical computation the constants

$$g_{//} = 6.45,\ g_{\perp} = 3.03,\ A/k = 0.0344°\mathrm{K},\ B/k = 0.0056°\mathrm{K}$$

$S = \frac{1}{2}$, $j = \frac{7}{2}$ were used in combination with varying values of the parameter H and ψ_H, where $H \cos \psi_H = H_z$, $H \sin \psi_H = H_x$. Then, with the aid of an existing Algol-program Symeve, the eigen values and eigen vectors of these matrices were calculated; the eigen vectors give the coefficients of the (S_z, j_z)-component wave functions in the expansion of the exact wave function Ψ_k, belonging to the k^{th} eigen value of the energy E_k. From the eigen vectors one can then calculate expectation values of, for instance, $\langle j_z^2 \rangle$, $\langle j_+^2 \rangle$ and $\langle j_+ j_z + j_z j_+ \rangle$ where $j_+ = j_x + i j_y$. After this quantum mechanical averaging for every energy level separately, a statistical averaging over the various energy levels was carried out for various values of the temperature T. The total entropy S of the combined electronic and nuclear spin systems of the Co-ions,

$$f_2 \equiv f_2^0 = \{\overline{\langle j_z^2 \rangle} - \tfrac{1}{3} j(j+1)\}/j^2,\ f_2^2 = \overline{\langle j_+^2 \rangle} \text{ and } f_2^1 = \overline{\langle j_+ j_z + j_z j_+ \rangle}$$

were calculated for various values of T, H and ψ_H, where the bars denote statistical averages. For constant H but ψ_H varying, corresponding to a rotation of the external magnetic field from the K_1-axis towards the K_2-axis, and *assuming the entropy to remain constant*, one can find f_2^0, f_2^1 and f_2^2 and also T as a function of ψ_H. There is one complication, however, arising from the fact that in the theoretical calculation the direction of $\boldsymbol{H}$ is always in the xz-plane. The x-axis lies by definition in a plane through $\boldsymbol{H}$ and one of the tetragonal axes of the Co-ions. This plane revolves around the z-axis when experimentally $\boldsymbol{H}$ is rotated from the K_1- to the K_2-axis.

The situation is drawn in fig. 17.

From $\sin K_1HT/\sin K_1OT = \sin HK_1T/\sin HOT \sin \psi_H$ and
$\sin HTC/\sin HOC = \sin K_1HT/\sin TOC$, one finds
$\sin HTC = \sin K_1OT/\sin \psi_H \sin TOC$.

Further $\cos TOC = \cos K_1OT . \cos COK_1 = \cos K_1OT \sin HOK_1$ and $\cos \psi_H = \cos K_1OT \cos HOK_1$ from which HOK_1 and TOC can be derived. We call $TOC \equiv \theta$ and $HTC \equiv \varphi$, which are the polar angles of the counter C with respect to the coordinate system xyz, in which f_2^0, f_2^1 and f_2^2 are calculated. Then formulae (4.23) may be applied for the evaluation of $W(\theta, \varphi)$, which can be compared to the experimental value $W(\psi_H^*)$. A result is shown in fig. 18 for a field strength $H = 5.5$ kOe and $A/B = 6$. When compared

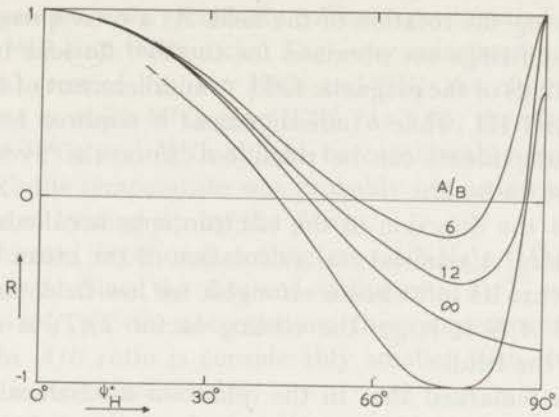

Fig. 18. Theoretical curves for the ratio R of the γ ray intensities $W(\pi/2) - 1$ when measuring with the field at an angle ψ_H with the K_1-axis to $W(\pi/2) - 1$ when measuring with the field parallel to the K_1-axis.

The three upper curves result from the calculation of § 7.2.1 for different values of A/B; the lower curve results from the quantum mechanical calculation of § 7.2.2. The theoretical curves have to be compared to the experimental data in fig. 14; $R = 0$ in this figure corresponds to $W(\pi/2) = 1$ in fig. 14.

with the semi-classical calculations, the main difference is that the counting rate is lower. This signifies that it is more difficult to align the nuclear spins in the direction of small h.f.s. coupling, than one would expect classically on basis of the first calculation. This feature of the result is retained when varying the field strength (or, in order to reduce computational labour, varying j). It is found that the maximum at $\psi_H = \psi^*_H = 90°$ is further decreased when H is reduced.

7.3. *Discussion.* Comparison of fig. 14 and fig. 18 indicates that the main features of the behaviour of the Co nuclei correspond to the theoretical description of § 7.2. Since the maximum rotational cooling occurs at $\psi^*_H = 90°$, we will discuss in the following some possible explanations of the discrepancies near $\psi^*_H = 90°$. The main discrepancies are:

I. It can be inferred from the data of § 5 and § 6 that the measured cooling ratio $T_i/T_f = 5$, while it was expected to be at least 10 since according to unpublished measurements of Miedema $A/B > 10$ (c.f. § 2).

II. The ratio of $W(\pi/2) - 1$ for $\psi^*_H \approx 90°$ to $W(\pi/2) - 1$ for $\psi^*_H = 0°$ is about 0.4, while the calculated values are 1.0 (§ 7.2.1.) and 0.6 (§ 7.2.2).

III. The γ radiation intensity is not the same for settings of the magnetic field which are symmetrical with respect to the K_2 axis, nor is it possible to designate a symmetry axis for both $W(0)$ and $W(\pi/2)$.

Those features can be related to the following situations which were not considered in § 7.2.

1°. Misalignment of the crystal; so that the field can not coincide with

the K_2 axis during the rotation of the field. As a consequence the smallest possible h.f.s. splittings are obtained for the two Co ions in the unit cell at different settings of the magnetic field. A misalignment of 10° is necessary to explain II and III, while 6° misalignment is required for explaining I; such large misalignments can be ruled out since the average mounting error was found to be 2°.

2°. In § 7.2.1 the direction of the electron spin is calculated neglecting the h.f.s. coupling. A semiclassical calculation of the effect of the electron spin indicates that its influence is strongest for low fields and large values of A/B. When A/B is large, the cooling factor T_f/T_i is completely determinated by the field.

It should be remarked that in the quantum mechanical calculation of § 7.2.2 the influence of the h.f.s. coupling on the electronspin is automatically included. From both models it can be concluded that the effect of a misalignment is considerably enhanced, such that I and II can be explained by much smaller misalignments than those mentioned in 1°. III. can not be explained by this assumption.

3°. Non-axial symmetry of the Hamiltonian. This situation is well known to occur for the Cu-tutton salts as well as for CoK-tutton salt[19)][20)]. If the x and y direction are not equivalent, e.g. $A > B_x > B_y$, and if none of these directions coincides with the K_2-axis the nuclear spins will be drawn towards the x-axis when the field is parallel to the K_2-axis. This model can explain III. Discrepancy I can also be explained by this model since Miedema measured essentially $A/B(K_2)$.

4°. Dipole-dipole interactions between the Co electron spins. From calculations of Uryû[21)] on the dipolar interaction in the Co-tutton salts, it can be shown that when the electron spins are mainly oriented along the K_2-axis there is a dipolar field of about 100 Oe acting along the K_1-axis. If one wants to orient the electron spins exactly in the direction of the K_2-axis it is necessary to compensate this dipolar field by an external field, that is, to rotate the field over a small angle with respect to the K_2-axis. Relative to this setting of the field the symmetry is not seriously affected. If one also includes the influence of the h.f.s. on the direction of the electron spin the situation is more complicated and difficult to evaluate.

In conclusion it can be remarked that the discrepancies between the experimental results and the models of § 7.2 can be explained by a combination of the effects mentioned in 1°, 2° and 3°. It is not excluded that also 1°, 2° and 4° might explain the experimental results.

From 2° and 4°, as well as from fig. 16 it follows that for the higher fields the Co nuclei are better aligned along the K_2-axis. Therefore it is possible that in high fields a lower temperature was obtained than that which was mentioned in § 5 and § 6.

§ 8. *Some negative results.* Similarly to the experiment on ^{137}Cs we tried to orient ^{134}Cs, ^{83}Rb and ^{86}Rb nuclei. The γ-ray anisotropies did not exceed the experimental error of 1%. For ^{134}Cs and ^{83}Rb the circumstances were the same as those in which ^{137}Cs gave $W(K_1) = 1.05$; therefore the quadrupole moment of ^{134}Cs and ^{83}Rb should be considerably smaller than for ^{137m}Ba. For ^{86}Rb the temperature was probably not as low as for the other samples because of heating up by the β-rays.

We also performed rotational cooling on $Co(NH_4)_2\,(SO_4)_2.6H_2O$ with ^{54}Mn as thermometer. Since the obtained cooling ratio $T_i/T_f \approx 2$ was smaller than for the Cs-salt we did not continue these experiments. This result suggests that the A/B ratio is considerably smaller than the value of 12 reported for Co in Zn-tuttonsalt.[19]).

Appendix.

Formula for the susceptibility of a paramagnetic substance in a perpendicular field:

We assume that the substance has anisotropic g values and spin $S = \frac{1}{2}$. The external field is denoted by $\boldsymbol{H}$ with components H_x and H_y and the measuring field by H_z. The spin hamiltonian is given by $\mathcal{H} = g_x\mu_B H_x S_x + g_y\mu_B H_y S_y + g_z\mu_B H_z S_z$. The energy levels are given by $E = \pm \frac{1}{2}W$. $W = (g^2\mu_B^2 H^2 + g_z^2\mu_B^2 H_z^2)^{\frac{1}{2}}$ in which $g^2H^2 = g_x^2H_x^2 + g_y^2H_y^2$. The magnetic moments of the two levels are $M_z = \pm\, \partial E/\partial H_z = \pm\, g_z^2\mu_B^2 H_z/2W$. For $T \neq 0$ a Boltzmann average has to be taken over the two Zeeman levels which multiplies the above M_z with a factor $\tanh(W/2kT)$. One finds then for the susceptibility

$$\chi_z = \frac{M_z}{H_z} = \frac{g_z^2\mu_B^2}{2W} \cdot \tanh \frac{W}{2kT}.$$

For $gH \gg g_zH_z$ it follows that

$$\chi_z = \frac{g_z^2\mu_B^2}{2g\mu_B H} \cdot \tanh \frac{W}{2kT}.$$

When rotating the field H in the xy plane under adiabatic conditions, $W/2kT$ is constant and therefore χ_z varies as $1/gH$.

References

1) Wheatley, J. C. and Estle, T. L., Phys. Rev. **104** (1956) 264.
2) Hobden, M. V. and Kurti, N., Phil. Mag. **4** (1959) 1092.
3) Private communication from D. Grijm.
4) Private communication from A. R. Miedema

5) De Groot, S. R., Tolhoek, H. A. and Huiskamp, W. J., Alfa, beta and gamma spectroscopy, ed. K. Siegbahn. (North Holl. Publ. Co., Amsterdam, 1964).
6) Yoshizawa, Y., Nucl. Phys. **5** (1958) 122.
7) De Groot, S. R. and Cox, J. A. M., Physica **19** (1953) 683.
8) Fano, U. and Racah, G., Irreducible tensorial sets, (Acad. Press, New York, 1959).
9) Ambler, E., Eisenstein, J. C. and Schooley, J. F., J. Math. Phys. **3** (1962) 118.
10) Bleaney, B. and Ingram, D. J. E., Proc. roy. Soc. **A205** (1951) 336.
11) Kedzie, R. W. and Jeffries, C. D., Bull. amer. phys. Soc. **3** (1958) 415 L 3.
12) Kronig, R. and Bouwkamp, C. J., Physica **5** (1938) 521.
13) Orbach, R., Proc. roy. Soc. **A264** (1961) 458.
14) Abragam, A., The principles of nuclear magnetism. (Oxford University Press, 1961).
15) Suhl, H., Phys. Rev. **109** (1958) 606.
16) Bleaney, B., Daniels, J. M., Grace, M. A., Halban, H., Kurti, N., Robinson, F. N. H. and Simon, F. E., Proc. roy. Soc. **221** (1954) 170.
17) Kiddle, R. E. and Proctor, W. G., Phys. Rev. **104** (1956) 932.
18) Bucka, H., Kopfermann, H. and Otten, E. W., Naturwissenschaften **45** (1958) 620.
19) Bleaney, B. and Ingram, D. J. E., Proc. roy. Soc. **A208** (1951) 143.
20) Bleaney, B., Bowers, K. D. and Ingram, D. J. E., Proc. roy. Soc. **A228** (1955) 147.
21) Uryû, N., J. phys. Soc. Japan **16** (1961) 2139.

CHAPTER II

SPIN-LATTICE RELAXATION OF ^{54}Mn NUCLEI IN CONCENTRATED PARAMAGNETIC CRYSTALS

Synopsis

Paramagnetic crystals and two diamagnetic crystals containing ^{54}Mn were indirectly cooled in the presence of a magnetic field to temperatures T in the region of 0.03 to 0.2°K. To cool effectively the nuclear spins of ^{54}Mn the presence is required of numerous paramagnetic ions with an energy splitting which is not larger than about $9\,kT$; *i.e.* the nuclear spin-lattice relaxation time becomes quite long when the electron spins are strongly ordered in a magnetic field. This was demonstrated for the following substances: $CoCs_2(SO_4)_2.6D_2O$; $(Ce_xLa_{1-x})_2Mg_3(NO_3)_{12}.24H_2O$ for $x = 1$ and 0.1; $Ni(NH_4)_2(SO_4)_2.6H_2O$ and $ZnCs_2(SO_4)_2.6H_2O$.

Further a lowering of the temperature by applying a large magnetic field was observed in the Ni salt. This is caused by the crossing of the Ni energy levels through cancelling of crystalline field energy and Zeeman energy.

1. *Introduction.* In previous experiments[1]) it appeared that indirect cooling of $CoCs_2(SO_4)_2.6D_2O$ crystals in which radioactive ^{54}Mn was included as a thermometer probe was much more difficult than could be expected on the basis of considerations on the heat capacity and the thermal conductivity. The experimental evidence suggested that long spin-lattice relaxation times were responsible for this slow cooling. In order to obtain more information about the nature of these phenomena we investigated ^{54}Mn in salts of two other paramagnetic ions, namely Ce and Ni. These two ions were chosen for the following reasons:

1. Since they have no hyperfine structure, the pattern of energy splittings is simple.

2. The energy splittings of these ions can be varied independently of the energy splitting of the Mn ion. This is feasible for Ce in $Ce_2Mg_3(NO_3)_{12}.24H_2O$ since the Ce ion has a strongly anisotropic g-value whereas a substituted Mn impurity has an isotropic g-value. Ni in $Ni(NH_4)_2(SO_4)_2.6H_2O$ has a large energy splitting in zero field, which can be decreased considerably by applying a magnetic field in an appropriate direction, whereas the splitting for the Mn ion is increased by the same field. We also studied what happens in the absence of paramagnetic ions, *i.e.* in diamagnetic crystals, for which we chose $ZnCs_2(SO_4)_2.6H_2O$ and $La_2Mg_3(NO_3)_{12}.24H_2O$.

When studying the ^{54}Mn relaxation phenomena in $(Ce_xLa_{1-x})_2Mg_3(NO_3)_{12}.24H_2O$ crystals as function of Ce concentration the results indicated the occurrence of strong deviations from thermal equilibrium for the more dilute crystals.

Therefore we only include a few results on a 10% Ce crystal, while the other phenomena will be discussed in a separate chapter.

2. *Apparatus and method.* We used the demagnetization apparatus described in § 3 of ref. 1. After demagnetization of the CrK-alum cooling salt to 0.02°K the magnetic field was applied to the sample, which was mounted in the top of the apparatus and in thermal contact with the cooling salt. The growth of the nuclear orientation of the ^{54}Mn nuclei was monitored by two scintillation counters, which measured the intensity of γ-rays emitted perpendicular to the magnetic field. This intensity is denoted as $W(\pi/2)$, it is normalized to unity at high temperatures. From $W(\pi/2)$ we derived with the aid of fig. 5 from ref. 1 the temperature of the ^{54}Mn nuclear spins.

In the analysis of the results we will mainly consider the value which $W(\pi/2)$ reaches after a long time, generally 2000 to 4000 s. In principle we might have obtained much information from the rate of change of $W(\pi/2)$. However, since the measured $W(\pi/2)$ has a rather large error of statistical origin, it is impossible to measure an accurate value of $W(\pi/2)$ in a short time interval. This excludes the possibility of a detailed analysis of the $W(\pi/2)$ *versus* time curve.

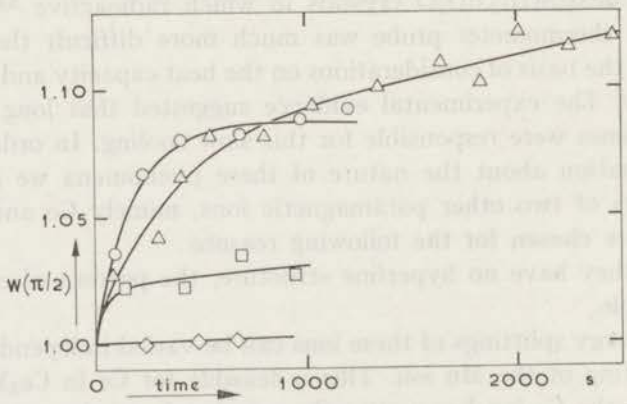

Fig. 1. $W(\pi/2)$ for ^{54}Mn in $CoCs_2(SO_4)_2.6D_2O$ as a function of time, when cooling this crystal in various fields H. Sample B.

△ $H = 0.66$ kOe □ $H = 2.2$ kOe
○ $H = 1.1$ kOe ◇ $H = 3.3$ kOe

3. *Experiments.* 3.1. $CoCs_2(SO_4)_2.6D_2O$. In fig. 1 we plotted the γ-ray anisotropy of ^{54}Mn as a function of the time from the beginning of the

cooling. Various magnetic fields are applied in the direction of the K_1-axis of $CoCs_2(SO_4)_2.6D_2O$. It can be seen that cooling in high fields proceeds faster than cooling in low fields.

The higher the field is, the lower is the stationary end-value of $W(\pi/2)$. In table I a survey of the dependence of the stationary values of $W(\pi/2)$ from the magnetic field is given. Two samples are included: sample A consisted of a 2 mm thick $CoCs_2(SO_4)_2.6D_2O$ crystal; sample B consisted of a 0.2 mm thick layer of $CoCs_2(SO_4)_2.6D_2O$ grown onto a $ZnCs_2(SO_4)_2.6H_2O$ crystal.

TABLE I

The values of $W(\pi/2)$ and the corresponding $1/T$ for ^{54}Mn nuclei after cooling in $CoCs_2(SO_4)_2.6D_2O$ crystals during a certain time in a field H applied in the direction of the K_1 axis

Sample	H kOe	Cooling time s	$W(\pi/2)$	$1/T$ °K^{-1}	H/T kOe°K^{-1}
A	0.66	3000	1.060*)	16.0 ± 1.0	10.6 ± 0.7*)
A	1.1	3000	1.067*)	17.1 ± 1.0	18.8 ± 1.0*)
A	1.5	3400	1.073	18.0 ± 1.0	27.8 ± 1.5
A	3.3	1200	1.015	7.5 ± 1.3	25 ± 5
A	8.8	800	1.009	6.0 ± 2.0	53 ± 17
B	0.66	2700	1.122*)	26.6 ± 1.0	17.6 ± 0.8*)
B	1.1	1200	1.087	20.5 ± 1.0	22.6 ± 1.0
B	2.2	1200	1.027	10.4 ± 1.0	22.9 ± 1.5
B	3.3	900	1.003	3.0 ± 3.0	15 ± 15

*) Stationary value not yet reached.

From this table it can be concluded that the lowest temperature which is reached by the ^{54}Mn spin system in a certain magnetic field is given by $H/T \approx 25$ kOe°K^{-1}. This corresponds to $g\mu_B H/kT \approx 10$ where $g = 5.65$ is the g-value of the Co ion for a field applied in the direction of the K_1-axis. It can be seen that the stationary values for the two samples do not differ considerably; the time which is needed to approach these values is, however, much longer for the thicker sample A.

3.2. $(Ce_xLa_{1-x})_2Mg_3(NO_3)_{12}.24H_2O$. The same experimental procedure is applied as on $CoCs_2(SO_4)_2.6D_2O$. The direction of the field with respect to the c-axis of the double nitrate crystals was set at various angles θ; the energysplitting of the Ce-ion is then given by $\Delta E = g\mu_B H$ in which $g = [(1.83)^2 \sin^2\theta + (0.02)^2 \cos^2\theta]^{\frac{1}{2}}$. The same behaviour of $W(\pi/2)$ as function of the field is found as for CoCs-tutton salt: a relatively slow cooling to low temperatures at low fields and a fast cooling which stops at a relatively high temperature for high fields. A summary of the values of $W(\pi/2)$ that were finally obtained is given in table II.

From this table it can be concluded that the temperature which can be

reached is determined much more by $g\mu_B H/k$ than by H alone. Also it follows that the temperatures which are reached in the dilute Ce-crystal are not as low as in the concentrated sample.

TABLE II

The values of $W(\pi/2)$ and the corresponding $1/T$ for ^{54}Mn nuclei after cooling in $(Ce_xLa_{1-x})_2Mg_3(NO_3)_{12}.24H_2O$ during a certain time in a field H applied in a direction which makes an angle θ with the c axis.

x	H kOe	θ	$g\mu_B H/k$ °K	Cooling time s	$W(\pi/2)$	$1/T$ °K^{-1}	$g\mu_B H/kT$
1.0	1.1	90°	0.136	3600	1.165*)	36 ± 3	4.7 ± 0.9*)
	2.2	90°	0.272	1800	1.149	32 ± 2	8.7 ± 0.7
	3.3	90°	0.408	3000	1.102	23 ± 1.5	9.5 ± 0.8
	4.4	90°	0.544	2800	1.064	16.5 ± 1.5	9.0 ± 1.0
	6.6	30°	0.408	2200	1.057	16.2 ± 1.5	6.5 ± 0.7
	13.3	15°	0.408	2000	1.074	18.4 ± 1.5	7.5 ± 0.9
	18.0	< 5°	< 0.185	3600	1.142*)	31 ± 2	< 5.7*)
0.1	1.1	90°	0.136	3000	1.102	23 ± 2	3.1 ± 0.4
	2.2	90°	0.272	3000	1.063	17 ± 2	4.6 ± 0.4
	3.3	90°	0.408	1500	1.038	12.5 ± 1.5	5.1 ± 0.4

*) Stationary value not yet reached.

3.3. $Ni(NH_4)_2(SO_4)_2.6H_2O$. Paramagnetic resonance of the Ni-ion (spin $S = 1$) in $Ni(NH_4)_2(SO_4)_2.6H_2O$ has been measured by Griffiths and Owen[2]). There are two ions in the unit cell which have different orientations of the axes x, y and z. The spin hamiltonian $\mathcal{H} = g\mu_B \boldsymbol{H}\cdot\boldsymbol{S} + DS_z^2 + E(S_x^2 - S_y^2)$ is defined with respect to these axes. Using the values of

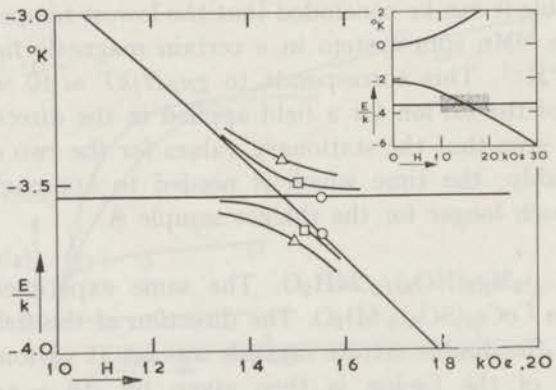

Fig. 2. The energy levels of Ni in $Ni(NH_4)_2(SO_4)_2.6H_2O$ as a function of the magnetic field H.

○ H applied in the direction of the y axis.
□ H in the yz plane, 1.7° from the y axis.
△ H in the yz plane, 3.4° from the y axis.

In the insert a general survey is given, the shaded region corresponds with the large figure.

the constants as measured by Griffiths and Owen at 90°K, namely $g = 2.25$, $D/k = -2.86$°K and $E/k = -0.69$°K, we calculated the energy levels for fields in the direction of the y-axis, and also for fields that make a small angle with the y-axis. The result is represented in fig. 2.

The investigated sample consisted of a 0.4 mm layer of $Ni(NH_4)_2(SO_4)_2.6H_2O$, into which the ^{54}Mn was incorporated, grown on a crystal of $Zn(NH_4)_2(SO_4)_2.6H_2O$. The sample was mounted with the Ni layer on the brass cooling plate. The x-axis of one ion of the unit cell was placed vertically so that the horizontal magnetic field could be rotated in the yz-plane for that ion.

Experiment. First we measured $W(\pi/2)$ of ^{54}Mn as a function of the direction of the field in the yz-plane (fig. 3).

It can be seen that $W(\pi/2)$ and therefore the temperature of the ^{54}Mn nuclear spins is strongly dependent on the direction of the field. The curve could be measured in both senses with fairly good reproducibility. The symmetry axis of this curve is assumed to give the direction of the y axis; all further measurements were done with the field in this direction.

We also varied the field strength, with the result that a maximum of $W(\pi/2)$ was obtained at $H = 15.5$ kOe.

The rate of indirect cooling was determined for various magnetic field strengths applied in the direction of the y-axis. The result is shown in fig. 4 from which it can be concluded that the value of $W(\pi/2)$ obtained for $H = 3.3$ kOe is definitely smaller than for higher fields.

Discussion. The occurrence of a large value of $W(\pi/2)$ at 15.5 kOe and a special direction of the field indicates that a low temperature is reached, caused by the reducing of the energy splittings of the Ni-ion. The presence of another Ni-ion in the unit-cell with different energy splittings does not interfere with this process since its splittings are very large compared to kT and therefore this system has no heat capacity.

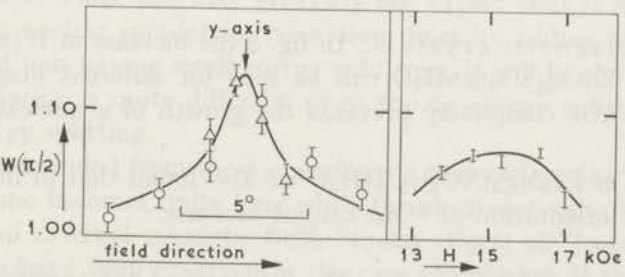

Fig. 3. $W(\pi/2)$ for ^{54}Mn in $Ni(NH_4)_2(SO_4)_2.6H_2O$ as function of field direction at $H = 15.5$ kOe (left hand side) and as function of field strength for H parallel to the y-axis (right hand side). The points denoted as ○ and △ were measured respectively going from left to right and from right to left.

Comparing the result of fig. 3 with the energy splittings given in fig. 2 it can be remarked that the minimum energy splitting occurs at a somewhat higher field than calculated. This indicates that the value of the crystal field splittings changes somewhat between 90° and 1°K. Also it follows that for a comparable change of the energy splittings (as calculated from fig. 2) by varying direction or strength of the field, the change in direction has an larger influence on $W(\pi/2)$ than the change in field-strength.

This indicates that the smallest energy splitting is reached for all ions at the same direction of the field but not at the same strength of the field; *i.e.*, for all ions the axes with respect to which the hamiltonian is defined coincide, but some spread in the crystal field parameters exists.

The result that for high fields the indirect cooling was to lower temperatures than was found for low fields can be attributed to the small energy splittings in the high fields.

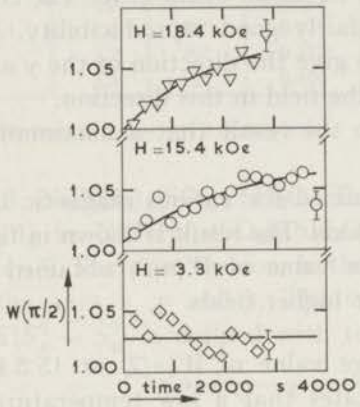

Fig. 4.

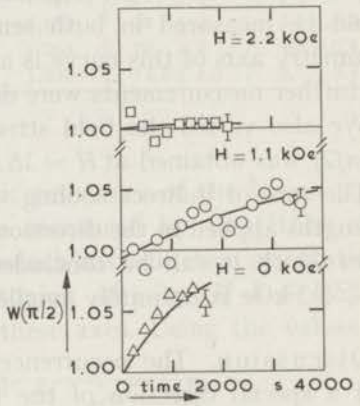

Fig. 5.

Fig. 4. $W(\pi/2)$ for ^{54}Mn as a function of time when cooling a crystal of $Ni(NH_4)_2(SO_4)_2.6H_2O$ in various magnetic fields parallel to the y-axis.
Fig. 5. $W(\pi/2)$ for ^{54}Mn as a function of time when cooling a crystal of $ZnCs_2(SO_4)_2.6H_2O$ in various magnetic fields.

3.4. Diamagnetic crystals. In fig. 5 the increase of $W(\pi/2)$ for ^{54}Mn included in $ZnCs_2(SO_4)_2.6H_2O$ can be seen for different magnetic fields. A field of 2 kOe completely prevents the growth of a nuclear orientation of ^{54}Mn.

For ^{54}Mn in $La_2Mg_3(NO_3)_{12}.24H_2O$ we also found that in fields of a few kOe nuclear orientation of ^{54}Mn cannot increase.

4. *Discussion and conclusions.* The influence of the specific heat of the paramagnetic ions on the cooling rate is observed for small energy splittings, where a considerable specific heat at low temperatures is present. When the energy splittings are increased the specific heat maximum shifts to higher

temperatures, where indirect cooling is easier and therefore proceeds faster. This results in an almost instantaneous cooling to the lowest attainable temperature at the high values of the energy splitting. The fact that the diamagnetic crystals, which have a much smaller specific heat than the paramagnetic crystals, gave the smallest cooling of the ^{54}Mn nuclear spins excludes an explanation of our result on the basis of the specific heat of the cooled substances. Therefore we ascribe our results to a relaxation bottleneck for the ^{54}Mn nuclear spins.

Generally, electron spins provide the best relaxation mechanism for nuclear spins. The result on the diamagnetic crystals indicate that the electron spin of an isolated Mn-ion does not provide an effective relaxation mechanism for the nuclear spin if a magnetic field of more than 2 kOe is present.

In concentrated paramagnetic crystals nuclear spins can relax via the electron spins of the numerous paramagnetic ions, provided that the energy splittings ΔE of these ions are not too high. To be more specific, it can be stated that the lowest temperature T which the ^{54}Mn nuclear spins can reach follows from $\Delta E = 10\,kT$ for $CoCs_2(SO_4)_2.6D_2O$ and from $\Delta E = 8\,kT$ for $Ce_2Mg_3(NO_3)_{12}.24H_2O$. For $Ni(NH_4)_2(SO_4)_2.6H_2O$ it is difficult to estimate ΔE since it depends critically on direction and magnitude of the magnetic field.

The results on the $(Ce_{0.1}La_{0.9})_2Mg_3(NO_3)_{12}.24H_2O$ crystal indicate that a dilute system of paramagnetic ions is less effective for relaxation than a concentrated system. Diluting ions can affect the relaxation in two ways:

a) the probability that a given Mn-ion has a Ce-ion as nearest neighbour is diminished and thus the strength of the coupling between the ions diminishes and

b) processes in which more than one Ce-ion participates become less probable. It may be mentioned that under the conditions of these experiments the Mn and Ce energy splittings are unequal. Apparently, under these conditions a fairly high concentration of ions with small energy splittings is required in order to give a reasonably short ^{54}Mn nuclear spin-lattice relaxation time. Thus, one may generally not expect that it is possible to shorten ^{54}Mn nuclear spin-lattice relaxation times by adding to the crystal a few percent ions having small energy splittings. It will be shown in ref. 3, that the situation is quite different when the Ce energy splitting is equal to a Mn energy splitting.

It can be concluded from these experiments that the nuclear spin-lattice relaxation time becomes quite long when the electronic spins are strongly ordered by an external magnetic field. Similar effects of "freezing" of the nuclear spins have been observed in the case of ordering of the electronic spins in antiferromagnetics[4) 5)].

REFERENCES

1) Lubbers, J., Miedema, A. R. and Huiskamp, W. J., Commun. Kamerlingh Onnes Lab., Leiden No. 341*b*; Physica **31** (1965) 153; Chapter I.
2) Griffiths, J. H. E. and Owen, J., Proc. roy. Soc. **A 213** (1952) 459.
3) Lubbers, J. and Huiskamp, W. J., Physica to be published; Chapter III.
4) Daniels, J. M., Giles, J. C. and Le Blanc, M. A. R., Can. J. Phys. **39** (1961) 53.
5) Miedema, A. R., Wielinga, R. F. and Huiskamp, W. J., Commun. Leiden No. 342*c*; Physica **31** (1965) 835.

CHAPTER III

SPIN-LATTICE AND CROSS RELAXATION OF ^{54}Mn NUCLEI IN DILUTE PARAMAGNETIC CRYSTALS

Synopsis

The relaxation of nuclei of radioactive ^{54}Mn in crystals of lanthanum magnesium nitrate is studied as a function of Ce concentration, magnetic field and temperature. The nuclear orientation is derived from the γ-ray anisotropy. Nuclear spin-lattice relaxation times of 10^1 to 10^5 s were measured and interpreted by electronic spin-lattice relaxation in conjunction with forbidden transitions, i.e. nuclear spin flips. Generally a Ce concentration of more than 1% is required in order to influence this relaxation significantly. When the sample is cooled at a fast rate, the Ce spins can induce forbidden transitions (e.g. $S_z = -\frac{5}{2}$, $I_z = +3 \rightarrow S_z = -\frac{3}{2}$, $I_z = +2$) in the Mn spin system, which process generates a population of the nuclear levels which strongly deviates from thermal equilibrium as was shown by the observation of anomalous nuclear orientation. An analysis of this process is given.

1. *Introduction.* For many years experiments on orientation of radioactive nuclei in paramagnetic crystals at low temperatures have been performed[1]). Most experiments have been done in concentrated paramagnetic crystals and at low magnetic fields. Under these conditions at least a local temperature equilibrium of the investigated substance is ascertained. If however the concentration of paramagnetic ions is low and/or a large magnetic field is present different spin systems and the lattice may preserve different effective temperatures for a long time. This has been clearly demonstrated in experiments on cross relaxation[2]), dynamic nuclear orientation[3]) and rotational cooling[4]). In the present paper we describe a series of measurements below 1°K on one particular system: ^{54}Mn in $(Ce–La)_2Mg_3(NO_3)_{12}.24H_2O$ with varying Ce concentrations. We are interested in the mechanisms by which the ^{54}Mn nuclear spins establish thermal contact with the lattice and with the Ce spin system. In particular our attention is focussed on the influence of magnetic field and Ce concentration on these processes. The magnetic field determines the Zeeman energy splittings of both Ce and Mn; since Ce has very anisotropic g-values it is possible to vary the Ce splitting between wide limits by rotating the magnetic field, the Mn splitting being only slightly affected by this rotation. Therefore we can study the influence of the magnetic field and of the

magnitude of the Ce energy splitting on the Mn more or less separately. The anisotropy of the Ce g-values gives also the opportunity of rotational cooling[5]), thus making a wide range of Ce spin temperatures accessible.

2. *Experimental arrangement.* The samples consist of slabs cut from single crystals of (Ce–La)Mg-nitrate. Typical dimensions are $4 \times 15 \times 20\,\text{mm}^3$. The Ce concentrations are given as the ratio Ce/(La + Ce) for the aqueous solution from which the crystals were grown. The following concentrations were investigated: 100, 10, 1, 0.1, and $\approx 0.03\%$ Ce. The 0.03% concentration was not added on purpose, but originates from the estimated Ce impurity in lanthanum nitrate. The chemicals used were supplied by Merck, who stated its content of other impurities as: maximum 0.02% Nd and 0.01% Pr. The same amount of Nd and Pr will be present in all crystals. Further a crystal of 0.01% Ce in BiMg-nitrate was grown in order to reach a lower Ce concentration.

Carrier free ^{54}Mn was used, the activity of a sample was of the orderofe magnitude of 5 μC. A small amount (max. 0.01%) of stable Mn can ha v been present in our samples, originating from the commercial magnesium nitrate.

The samples were mounted with their crystallographic c-axis in the horizontal direction in an apparatus which is described in ref. 4 in some detail.

Essentially this apparatus consists of the following parts: Inside a vacuum space, which is surrounded by liquid He, a KCr-alum cooling salt is mounted together with the sample in a glass tube (cf. fig. 1). The thermal contact between sample and cooling salt is made via a copper wire and a brass plate B. The temperature of B can be controlled by the heat flow from an induction heater to the cooling salt. The tin heat switch provides two widely different values of the thermal contact between the sample and the cooling salt, thus sample temperatures from 0.03 to 0.15°K and from 0.15 to 0.6°K are readily obtained without an undue heat input, which otherwise would rapidly obliterate the cooling capacity of the cooling salt. The temperature of plate B is measured by means of a CeMg-nitrate susceptibility thermometer.

A magnetic field in a horizontal direction can be applied to the sample by an electromagnet. The distance between sample and cooling salt is about 35 cm so that the field at the cooling salt is practically zero, while the field at the position of the thermometer is 10% of the field on the sample. The electromagnet, which has a maximal field of 18.5 kOe can be rotated around a vertical axis which coincides with the axis of our cryostat. By means of a hydraulic lift, a vertical displacement is also possible so that the centre of the magnet can be brought to the position of the cooling salt. On this electromagnet two scintillation counters are mounted, which measure the

intensity of the gamma-radiation emitted by the sample in a direction perpendicular to the magnetic field. A second electromagnet with hollow poles could be placed on top of the first magnet and then the gamma-ray intensities in directions parallel as well as perpendicular to its field could be measured. The maximum field of the second magnet was 5.5 kOe. In addition a coil which could produce a vertical field up to 200 Oe was wound on the cryostat. This arrangement enabled us to rotate the resulting magnetic field over a few degrees out of the horizontal plane, in order to compensate for a mounting error of the c-axis of the crystal.

Each experimental run was started with a demagnetization of the cooling salt by means of the 18 kOe magnet. Thereafter the magnet with the scintillation counters was placed around the sample. After this moment the experiment comprised variations in one of the following three parameters: the temperature T of the metal plate B, magnetic field strength H or the angle θ between $\boldsymbol{H}$ and the c-axis of the sample. The effect of these changes

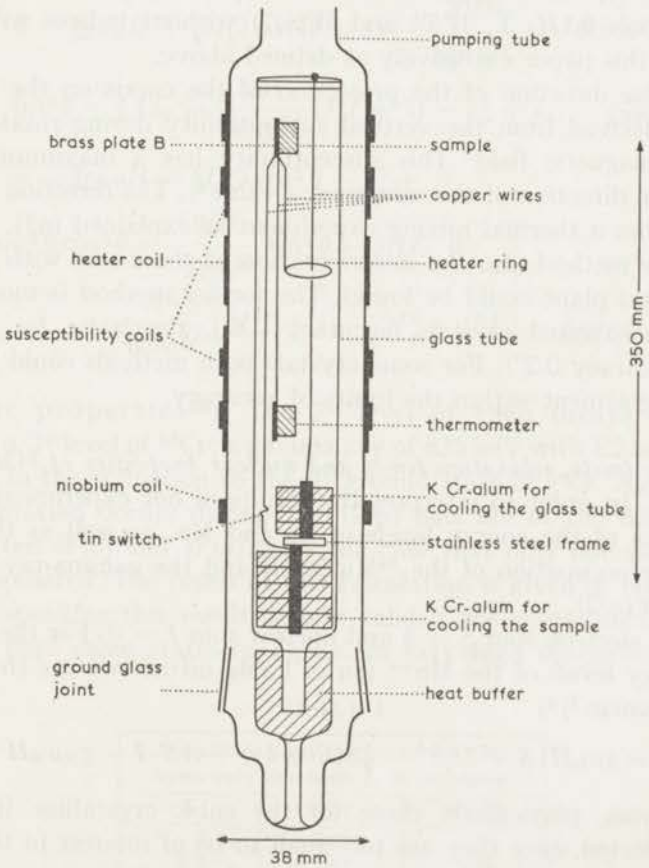

Fig. 1. Drawing of the inner part of the apparatus. The figure is to scale; horizontal and vertical scales differ a factor of 3.

on the nuclear orientation of ^{54}Mn was observed by measuring the intensities of the gamma-rays emitted in directions parallel and/or perpendicular to the magnetic field. These intensities are denoted as $W(0)$ and $W(\pi/2)$ respectively. Both W's are normalized to unity at high temperatures, i.e. in the absence of nuclear orientation. The normalizing intensities were measured at 0.9°K after each run at the same setting of θ and H as during the run. The influence of the magnetic field on the counters was always negligible. Corrections for finite solid angle of counter and sample and for background were not applied to W, unless this is explicitly indicated. These corrections were at most 4% of W-1.

In some experiments rapid changes of $W(0)$ occurred. By using our 256 channel analyser in its scaler time mode, a time resolution of $W(0)$ could be obtained which was only limited by the statistical fluctuations in the counting. Very large changes in $W(0)$ could be observed in 0.02 s, a 10% change in 1 s and a 1% change in 100 s. On the other hand, very slow changes in $W(0)$ could be observed accurately.

The symbols θ, H, T, $W(0)$ and $W(\pi/2)$ without indices will be used throughout this paper exclusively as defined above.

The precise direction of the projection of the c-axis on the horizontal plane was derived from the vertical susceptibility during rotation of the horizontal magnetic field. This susceptibility has a maximum when $\boldsymbol{H}$ points in the direction of the minimum g-value[4]). The direction could also be found from a thermal mixing experiment as explained in[6]). By means of the latter method also the misorientation of the c-axis with respect to the horizontal plane could be found. The former method is most suitable for the concentrated crystals (accuracy 0.5°), the latter for the dilute crystals (accuracy 0.2°). For some crystals both methods could be applied and gave agreement within the limits of accuracy.

3. *Energy levels, relaxation times and nuclear properties of ^{54}Mn and Ce.* Mn levels. In order to interpret the results of our experiments we need the positions of the energy levels of Ce and Mn, as well as the relation between the occupation of the ^{54}Mn levels and the gamma-ray intensities $W(0)$ and $W(\pi/2)$.

^{54}Mn has electron spin $S = \frac{5}{2}$ and nuclear spin $I = 3$. For the discussion of the energy levels of the Mn^{++} ion in LaMg-nitrate we use the following spin-hamiltonian[7]) [8])

$$\mathscr{H} = g\mu_B \boldsymbol{H}\cdot\boldsymbol{S} + D[S_\zeta^2 - \tfrac{1}{3}S(S+1)] + A\boldsymbol{S}\cdot\boldsymbol{I} - g_N\mu_N \boldsymbol{H}\cdot\boldsymbol{I}. \qquad (3.1)$$

Other terms, particularly those for the cubic crystalline field effects will be neglected since they are too small to be of interest in this investigation; the nuclear Zeeman energy term is of some importance only in the highest magnetic fields used.

There are 2 different types of lattice positions for Mn in the unit cell, which give different values of D. The ion with $D/k = -0.0070°\mathrm{K}$ occurs twice as frequently as the ion with $D/k = -0.0310°\mathrm{K}$[9]). The ζ-axis of both types of ions coincides with the c-axis of the crystals. g and A are isotropic and equal for both types of ions with values $g = 2.00$ and $A/k = -0.01025°\mathrm{K}$. The value of A is derived from A for stable ^{55}Mn: $^{55}A/k = -0.0129°\mathrm{K}$ and from the magnetic moment and spins of ^{55}Mn and ^{54}Mn respectively $^{55}\mu = 3.46\,\mu_N$, $^{55}I = \frac{5}{2}$ and $^{54}\mu = 3.30 \pm 0.06\,\mu_N$, $^{54}I = 3$[9]).

From the above Hamiltonian one can calculate the energy levels exactly by machine computations. It was found that sufficiently accurate values for the energy levels are obtained using the following expressions, which are obtained from perturbation theory. We use a representation in which the z-axis coincides with the magnetic field direction, which makes an angle θ with the crystallographic c-axis. Since we are mainly concerned with the lower levels $S_z = -\frac{5}{2}$ and $S_z = -\frac{3}{2}$ of ^{54}Mn only their positions are given:

$$E(-\tfrac{5}{2}, I_z) = -\tfrac{5}{2}g\mu_B H + \tfrac{5}{3}D(3\cos^2\theta - 1) - \frac{20D^2}{4g\mu_B H}\sin^2\theta\cos^2\theta +$$
$$- \frac{5D^2}{4g\mu_B H}\sin^4\theta - \tfrac{5}{2}AI_z - \frac{5A^2}{4g\mu_B H}[I(I+1) - I_z^2 + I_z] - g_N\mu_N H I_z \quad (3.2)$$

$$E(-\tfrac{3}{2}, I_z) = -\tfrac{3}{2}g\mu_B H - \tfrac{1}{3}D(3\cos^2\theta - 1) +$$
$$+ \frac{12D^2}{g\mu_B H}\sin^2\theta\cos^2\theta - \frac{9D^2}{4g\mu_B H}\sin^4\theta - \tfrac{3}{2}AI_z +$$
$$- \frac{A^2}{4g\mu_B H}[3I(I+1) - 3I_z^2 + 13I_z] - g_N\mu_N H I_z. \quad (3.3)$$

Nuclear properties[10]). The 3^+ level of ^{54}Mn decays by electron capture to a 2^+ level of ^{54}Cr; a gamma ray of 835 keV with E2 multipolarity is emitted in the transition to the 0^+ ground state of ^{54}Cr. Assuming that no disorientation occurs during the 12 ps half life of the 835 keV level, we calculated $W(0)$ and $W(\pi/2)$ for the case that only one sublevel I_z of ^{54}Mn is populated. The result of this calculation is given in table I.

Strictly speaking this result is only valid if the wave functions for the levels are pure eigen states of I_z, i.e. in very high magnetic fields. The

TABLE I

Normalized γ-ray intensities for ^{54}Mn when only one level I_z is populated

I_z	$W(0)$	$W(\pi/2)$
± 3	0.00	1.25
± 2	1.67	1.25
± 1	1.33	0.75
0	1.00	0.50

fields used by us approximate this condition sufficiently to warrant the validity of the table. In order to calculate the observed W's we have to sum over all levels, weighing each level in proportion to its occupation density.

Ce levels. The levels of Ce can be described by an effective spin $S = \frac{1}{2}$. Ce has no hyperfine structure. The distance between two levels is given by $E = g\mu_B H$ where $g = (g_{//}^2 \cos^2\theta + g_\perp^2 \sin^2\theta)^{\frac{1}{2}}$, $g_{//} = 0.0236$[11])[6]) and $g_\perp = 1.8264 \pm 0.0013$[12]).

Relaxation times. For purpose of discussion it is useful to distinguish in our sample the following subsystems: lattice, Ce electron spins, ^{54}Mn electron spins and ^{54}Mn nuclear spins. The electron spin systems are thermally coupled to the lattice, the lattice is thermally coupled to the metal plate on which the sample is glued. Suppose that any of the subsystems has an effective temperature different from that of the metal plate, then the rate at which equilibrium is restored can be found from the relevant relaxation times. In the following we give some estimates of the relaxation times for the temperature region of interest: $0.03 < T < 0.3$°K.

Considering the ^{54}Mn electron spins, it may be recalled that very few are present (something like 3×10^{-9} per mole La), hence their heat capacity is very low compared to that of the Ce ions. The large dilution also implies that no interactions between the ^{54}Mn ions are present. We feel that the measurement of Mr. v. Duyneveldt[13]) on a few percent stable Mn in LaMg-nitrate can give an order of magnitude estimate of Mn electron spin-lattice relaxation times. He found relaxation times $\tau = 0.8$ s and 0.7 s under the conditions $\theta = 90°$, $T = 1.3$°K and $H = 1$ kOe and 2 kOe respectively. From this temperature downwards the temperature dependence is probably that of the direct process: $1/\tau \propto \coth(g\mu_B H/2kT)$, thus we arrive at an electron spin relaxation time of the order of 10 s in the temperature region of our experiment.

Ruby *e.a.*[14]) measured the Ce spin-lattice relaxation time for samples of 2% and 0.2% Ce in LaMg-nitrate at $\theta = 90°$ and $H = 3.8$ kOe. For temperatures $0.3 < T < 1$°K they find a phonon bottlenecked relaxation time, τ_b, which is given by $1/\tau_b = p \coth^2(g\mu_B H/2kT)$, where $p = 2.4\ s^{-1}$ for the 0.2% sample and $p = 0.8\ s^{-1}$ for the 2% sample. At low concentrations one can expect $p \propto g^2H^2/c$ in which c is the Ce concentration, while at high temperatures the dependence of p on c will be weak, due to a simultaneous rise of heat capacity and line width of the Ce ions with c. For the direct relaxation process Ruby *e.a.* estimate $q > 20\ s^{-1}$ in $1/\tau_d = q \coth(g\mu_B H/2kT)$. Theoretically $q \propto g^3H^5$ according to Abragam[3]). The total spin-lattice relaxation time is found from $\tau = \tau_d + \tau_b$. For all situations studied by us we estimate $\tau < 50$ s, except for $\theta \approx 0°$ where τ may become much larger.

Also the thermal resistance between crystal and metal plate can give rise to a relaxation time. For the heat flow through the thermal resistance we found $\dot{Q} = 1 \times 10^5 (T_{cr}^4 - T^4).A$ erg s^{-1} in which T_{cr} and T are the temperatures of the crystal and of the metal plate, while A is their contact area in cm^2. This relation was found when we cooled in our apparatus a CeMg-nitrate crystal doped with Cu in magnetic fields of $0 < H < 800$ Oe and $0.1 > T > 0.02$°K. It may be remarked that possible effects of finite thermal conductivity of the crystal are included in the above mentioned heat resistance. Combining this heat flow with the heat capacity of our crystals, which was calculated from a Schottky type anomaly for the Ce ions, we calculated for the relaxation time $1/\tau \geqslant 11\, T^3/c$ s^{-1}. This $1/\tau$ is a function of $g\mu_B H$; the minimum value stated above is reached for $g\mu_B H \approx$ $\approx 2.4\, kT$. This relaxation time is rather short, except for high Ce concentrations: namely $c = 0.1$ and $c = 1$.

Comparing the Ce spin-lattice relaxation time with the relaxation time for the lattice-metal heat resistance, we find that the latter is only important if $c \approx 1$ or if $c \approx 0.1$ in low magnetic fields. In all other cases, the spin-lattice relaxation is the slower process and then also the Mn electron spin system will equalize its temperature to that of the metal plate at a rate determined by its own spin-lattice relaxation time.

4. *Thermal contact between* ^{54}*Mn nuclear spins and the lattice.* 4.1. Measuring method. A polarization of the ^{54}Mn nuclear spins was produced by rotational cooling or demagnetization (cf. ref. 6). Subsequently the magnetic field was set at the chosen value and direction. The temperature

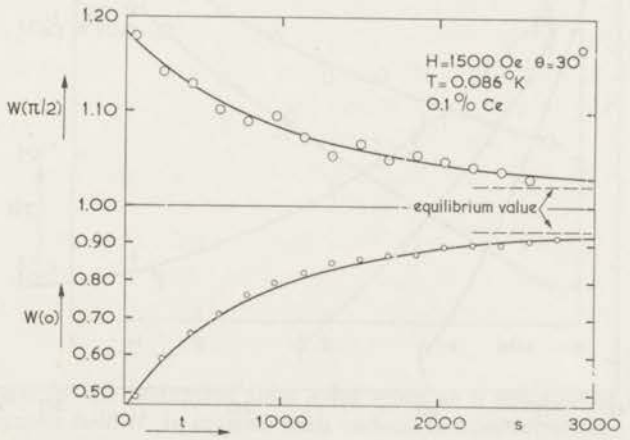

Fig. 2. Typical experimental run, showing the approach of the gamma-ray intensities $W(0)$ and $W(\pi/2)$ to equilibrium values as a function of time. The equilibrium values were calculated from the lattice temperature; the drawn lines are exponential curves with relaxation times $\tau(0) = 865$ s and $\tau(\pi/2) = 1040$ s respectively. Note the different scales for $W(0)$ and $W(\pi/2)$.

of the metal plate was increased to a certain value and then kept constant. The change in nuclear orientation was observed by measuring $W(0)$ and/or $W(\pi/2)$ as a function of time. In fig. 2 a typical result is shown. It can be seen that both W's approach equilibrium values W_{eq} nearly exponentially with a time constant τ. The inverse of the relaxation time $1/\tau = (dW/dt)/(W - W_{eq})$ will be used as a measure for the rate of change of the nuclear orientation. Generally the time constants for $W(0)$ and $W(\pi/2)$ are somewhat different, and are designated as $\tau(0)$ and $\tau(\pi/2)$ respectively.

The temperature of the metal plate was constant within a few percent during the measurements. A spread of 5% is found between the temperature determinations on different measuring days. From the measured temperatures we calculated the equilibrium value of $W(0)$ and $W(\pi/2)$, assuming that a Boltzmann distribution over the Mn levels will be reached. In a few series the measurements were continued until $t = 5\tau$ in order to find W_{eq} experimentally; the agreement between calculated and observed equilibrium values was satisfactory.

4.2. Results. Following the procedure outlined above, we measured the relaxation time τ for a number of crystals, field strengths, field directions and temperatures. The most complete survey was made for the 0.03% Ce crystal at $\theta = 30°$; the results are given in fig. 3. From this figure it is obvious that τ is strongly dependent on field and temperature; however,

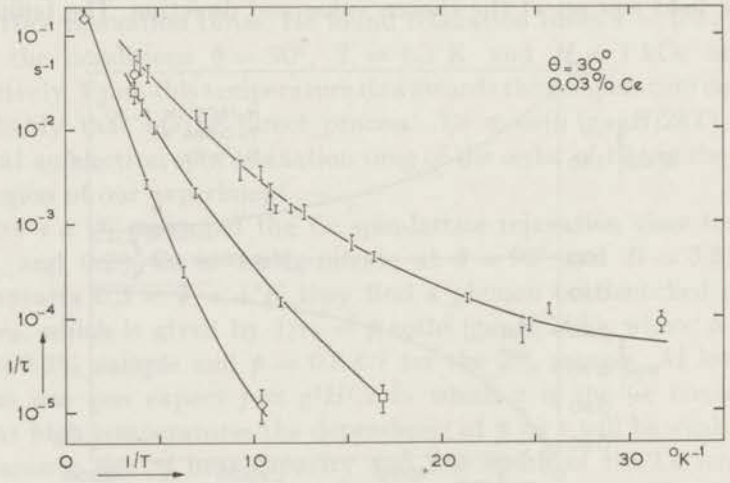

Fig. 3. The inverse of the relaxation time $\tau(0)$ for ^{54}Mn as a function of the inverse of the lattice temperature T for 3 magnetic fields.
○ $H = 1440$ Oe □ $H = 2710$ Oe ◇ $H = 4820$ Oe
The error bars give the uncertainty with which τ can be determined from the $W(0)$ vs time curve.

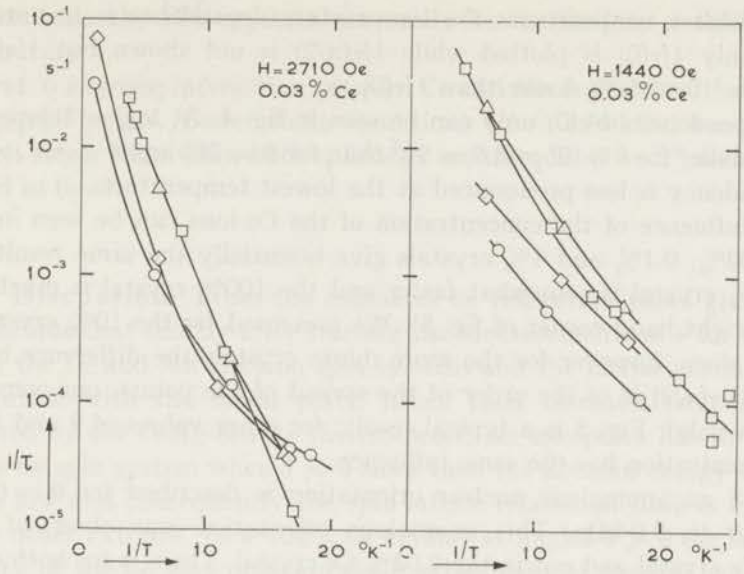

Fig. 4. The inverse of the relaxation time $\tau(0)$ for ^{54}Mn as a function of the lattice temperature T, plotted for various angles θ between magnetic field and c-axis.

○ $\theta = 0°$ ⊡ $\theta = 30°$ △ $\theta = 65°$ ◇ $\theta = 90°$

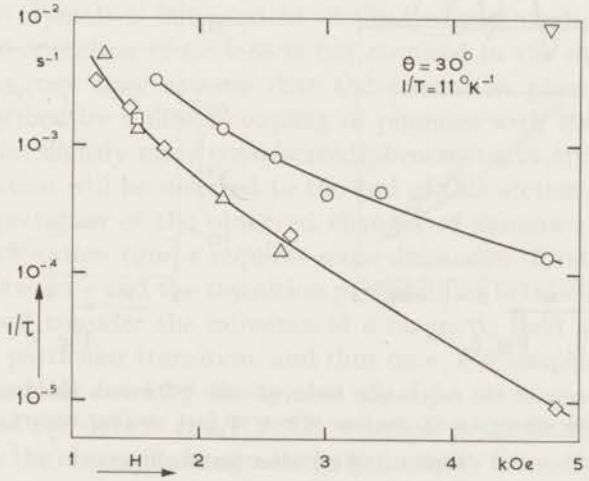

Fig. 5. The inverse of the relaxation time τ for ^{54}Mn as a function of the applied magnetic field H, in crystals with various Ce-concentration.

◇ 0.03% Ce $1/\tau(0)$
⊡ 0.1 % Ce $1/\tau(0)$
△ 1 % Ce $1/\tau(0)$
○ 10 % Ce $1/\tau(\pi/2)$
} $1/T = 11.0°K^{-1}$

▽ 100 % Ce $1/\tau(0)$ $1/T = 10$ to $20°K^{-1}$

at the lowest temperatures the temperature dependence is less steep. In fig. 3 only $1/\tau(0)$ is plotted while $1/\tau(\pi/2)$ is not shown but $1/\tau(\pi/2)$ is generally 10 to 50% lower than $1/\tau(0)$.

A dependence of $\tau(0)$ on θ can be seen in fig. 4. At higher temperatures $1/\tau$ is smaller for $\theta = 0°$ and $\theta = 90°$ than for $\theta = 30°$ and $\theta = 65°$, whereas this tendency is less pronounced at the lowest temperatures.

The influence of the concentration of the Ce ions can be seen in fig. 5. The 0.03%, 0.1% and 1% crystals give essentially the same result, while the 10% crystal is somewhat faster and the 100% crystal is much faster (upper right hand corner of fig. 5). We measured for the 10% crystal only $\tau(\pi/2)$; since, however for the more dilute crystals the difference between $\tau(0)$ and $\tau(\pi/2)$ is of the order of the spread of the points, our comparison remains valid. Fig. 5 is a typical result: for other values of θ and $1/T$ the Ce concentration has the same influence.

In § 5 an anomalous nuclear orientation is described for $\theta = 67°$ and $H = 2.0$ to 3.0 kOe. This anomalous orientation was observed in the 0.1% Ce crystal and not in the 0.03% Ce crystal. The τ is for both crystals a smooth function of H in this region of field strength (fig. 6). The difference

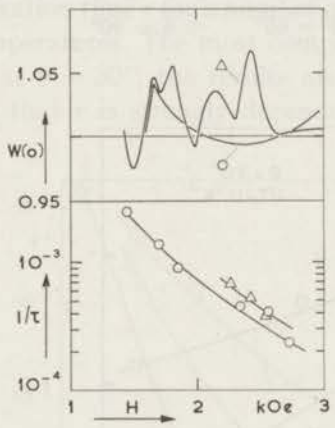

Fig. 6.

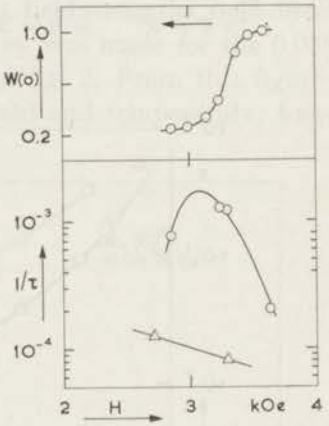

Fig. 7.

Fig. 6. The inverse of the relaxation time $\tau(0)$ for ^{54}Mn as a function of the field in the region where an anomalous effect at fast cooling occurs. $\theta = 67°$.

Top: $W(0)$ after fast cooling.
Bottom: $1/\tau(0)$
○ 0.03% $1/T = 12.0°K^{-1}$ △ 0.1% Ce $1/T = 10.8°K^{-1}$

Fig. 7. The inverse of the relaxation time $\tau(0)$ for ^{54}Mn as a function of the field in the region where $(AS)_{Mn} = (g\mu_B H)_{Ce}$ for the 0.1% Ce crystal.

Top: $W(0)$ during decreasing the field H at $\theta = 3.3°$.
Bottom: ○ $1/\tau(0)$ at $\theta = 3.3°$ $(1/T = 10.0°K^{-1})$
△ $1/\tau(0)$ at $\theta = 0°$ $(1/T = 8.6°K^{-1})$

in τ between the two crystals can easily be ascribed to a difference in temperature.

In ref. 6 a strong interaction between Ce and Mn is described for the case that $g_C\mu_B H = AS$. Under these conditions ($H = 3.26$ kOe, $\theta = 3.3°$) $1/\tau$ is much larger than when both splittings are unequal ($\theta = 0°$) as is demonstrated in fig. 7.

4.3. Discussion. From the estimates on relaxation times given in § 3 we conclude that shortly after starting the measurements of τ for the ^{54}Mn nuclei, the Ce and Mn electron spin systems and the lattice are in thermal equilibrium with the metal plate, hence their common temperature is indicated by the CeMg-nitrate thermometer. An exception has to be made for the Ce spin system when $\theta \approx 0$ since then the Zeeman energy of the Ce ions is low and consequently the spin-lattice relaxation time is long; also at the other extreme, in a 100% Ce crystal at angles $\theta \gg 0$ the large heat capacity of the Ce ions prevents rapid attainment of thermal equilibrium with the metal plate. Thus in the experiments to be discussed in the following, the observed nuclear relaxation rates correspond to the warm up time of a cold nuclear spin system to a warm lattice, while generally the Mn and Ce electron spins have the lattice temperature.

It was demonstrated in fig. 5 that the relaxation time of ^{54}Mn in magnetically dilute crystals is independent of the Ce concentration. Since apparently the co-operation of Ce ions is not required in the relaxation of Mn nuclear spins, one may assume that the relaxation phenomena of § 4.2 may be described by a direct coupling of phonons with Mn-ions. The discussion on the slightly more complicated phenomena in crystals with high Ce concentration will be deferred to the end of this section.

The interpretation of the observed changes of gamma ray intensity in terms of a relaxation time τ requires some discussion. First we will derive a relation between τ and the transition probabilities between the Mn levels, further we will consider the influence of a magnetic field and the phonon density on a particular transition, and thus on τ. For simplicity of notation we indicate a ^{54}Mn level by the symbol (S_z, I_z).

For most of our data is $g\mu_B H \gg kT$, where T is the lattice temperature, consequently the observed changes in the gamma ray intensity W correspond to changes in population density of the $(-\frac{5}{2}, I_z)$ levels only, since the $(-\frac{3}{2}, I_z)$ states and higher states remain unpopulated. In order to compare the measured $\tau(0)$ and $\tau(\pi/2)$ for $W(0)$, and $W(\pi/2)$ respectively, with the transition probabilities between various $(-\frac{5}{2}, I_z)$ levels, we calculated the behaviour of $W(0)$ and $W(\pi/2)$ as a function of time for a particular model. The following assumptions were made:

a) initially all nuclei are in the lowest state $(-\frac{5}{2}, -3)$;

b) the transition probability w_{ab} between levels $a(I_z)$ and $b(I_z + 1)$ is proportional to $(I - I_z)(I + I_z + 1)$;

c) the ratio of the upward and downward transition probabilities connecting two levels is given by a Boltzmann factor: $w_{a\to b}/w_{b\to a} = \exp(-AS/kT)$.

Such a model predicts that $W(0)$ is approximately an exponential function of time, while initially $W(\pi/2)$ deviates appreciably from an exponential behaviour. More precisely, the model predicts the following:

Suppose one calculates from the theoretical curves of $W(0)$ and $W(\pi/2)$ versus time a relaxation time according to the prescription $1/\tau = (dW/dt)/(W - W_{eq})$, in which W_{eq} is the gamma ray intensity for thermal equilibrium. Then it is found that $1/\tau(0)$ decreases as a function of time from $1.67w_{-3\to-2}$ to $1.00w_{-3\to-2}$, while $1/\tau(\pi/2)$ is initially zero and increases to $1.00w_{-3\to-2}$. These initial values could also have been found from inspection of table I.

These predictions are, at least qualitatively, born out by the experimental results, since it is seen in fig. 2 that $1/\tau(0) > 1/\tau(\pi/2)$ and that a slight decrease of $1/\tau(0)$ occurs while $W(0)$ increases. The conclusion is that the macroscopically observable $1/\tau(0)$ represents fairly well the transition probability between the $(-\frac{5}{2}, -3)$ and $(-\frac{5}{2}, -2)$ states, while $\tau(\pi/2)$ is a less valuable parameter. These results depend on the fact that the transitions $w_{-3\to-2}$ and $w_{+2\to+3}$ give a much larger jump in $W(0)$ than the other transitions and on the fact that the lowest h.f.s. levels $I_z = -3$ and $I_z = -2$ have the highest population density. It can easily be verified that the statements above allow the following simplification in the discussion to be presented. Omitting the levels $(-\frac{5}{2}, I_z)$ with $I_z \geqslant -1$ the nuclear spin system is a two level system $(-\frac{5}{2}, -3)$, $(-\frac{5}{2}, -2)$; the measured $\tau(0)$ is considered as a relaxation time for this two level system.

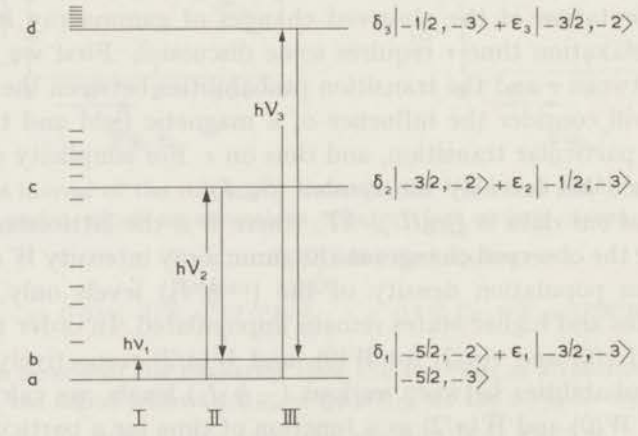

Fig. 8. Energy levels of ^{54}Mn and paths for relaxation by phonons between the levels a and b.

Our explanation of the behaviour of τ as a function of magnetic field strength and temperature is based on the assumption that phonons induce electronic spin flips, which in turn induce nuclear spin flips, via the hyperfine coupling. Simultaneous electronic and nuclear spin flips are well known in dynamic nuclear orientation experiments as "forbidden" transitions. The distinction between "forbidden" and allowed transitions is determined by the ratio of the respective transition matrix elements squared; this "ratio" is of the order of magnitude of $(A/g\mu_B H)^2$ and looses its meaning at small values of H (say $H < 1$ kOe in the case of Mn).

We propose, therefore, that the Mn nuclear spin relaxation rate is determined by the electron spin-lattice relaxation rate, multiplied by the ratio $(A/g\mu_B H)^2$. It is generally assumed[16]) that lattice vibrations interact with the Mn-electron spins through modulation of the predominantly cubic crystalline field and via spin-orbit interaction. The effective hamiltonian for this interaction is denoted as $\mathscr{H}_{SL}$. Phonons will induce transitions between states S_z and $S_z \pm 1$, $S_z \pm 2$. We will now discuss this in more detail with the aid of fig. 8.

A few comments on the figure may be appropriate

a. Only those levels relevant to our discussion have been drawn fully.

b. The corresponding wave functions are simplified, since only those admixtures from other states have been written, which lead to sizable transition matrix elements e.g. higher order perturbations and the influence of the crystalline field parameter D have been neglected.

c. We take $\delta_1 \approx \delta_2 \approx 1$, $\varepsilon_1 \approx \varepsilon_2 \approx \varepsilon_3 \approx A/g\mu_B H \equiv \varepsilon$, but more precisely, $\varepsilon_1 = \frac{1}{2}\sqrt{30}\varepsilon$, $\varepsilon_2 = \frac{1}{2}\sqrt{48}\varepsilon$, $\varepsilon_3 = \frac{1}{2}\sqrt{80}\varepsilon$.

We consider the following processes between levels a and b in fig. 8.

I. A direct transition between levels a and b under absorption of a phonon having energy $h\nu_1 = AS$. Such a nuclear spin-flip only is possible since the wave functions of levels a and b are not pure eigenfunctions of I_z, S_z, so that the electronic spin-lattice interaction $\mathscr{H}_{SL}$ has nonzero matrix elements, according to

$$\langle b|\,\mathscr{H}_{SL}\,|a\rangle = \varepsilon_1 \langle -\tfrac{3}{2}\,|\mathscr{H}_{SL}\,|-\tfrac{5}{2}\rangle \equiv \varepsilon_1 M_1.$$

II. An indirect transition a $\rightarrow$ b may occur via an intermediate state c, i.e. a real phonon having an energy $h\nu_2 \approx g\mu_B H$ is absorbed and a phonon of a slightly different energy is emitted (cf. Orbach process in electron spin-lattice relaxation). The matrix elements for the forbidden transition a $\rightarrow$ c and the allowed transition c $\rightarrow$ b are respectively:

$$\langle c|\,\mathscr{H}_{SL}\,|a\rangle = \varepsilon_2 \langle -\tfrac{1}{2}|\,\mathscr{H}_{SL}\,|-\tfrac{5}{2}\rangle \equiv \varepsilon_2 M_2$$

$$\langle b|\,\mathscr{H}_{SL}\,|c\rangle = \delta_1\delta_2 \langle -\tfrac{5}{2}\,|\mathscr{H}_{SL}\,|-\tfrac{3}{2}\rangle \approx M_1$$

III. Similarly, intermediate states, having predominantly $S_z = -\frac{1}{2}$ or

$S_z = +\frac{1}{2}$, may be connected to a and b, but obviously they become unimportant at low temperatures, except possibly $S_z = -\frac{1}{2}$, e.g. level d. Transitions $a \to d \to b$ require phonons of energy $h\nu_3 \approx 2g\mu_B H$, the respective matrix elements can easily be found from fig. 8 and are of the same order of magnitude as those for process II.

IV. It may be argued that transitions between a and b may also be induced via virtual intermediate states (quasi-Raman process), but an order of magnitude estimate shows, that this process can not compete with process II below 1°K.

Since the number of phonons of frequency ν is

$$p(\nu) \propto \nu^2 \bar{p}(\nu) \equiv \nu^2/[\exp(h\nu/kT) - 1]$$

the transition probabilities are given by (cf. ref. 15)

$$\begin{aligned} &\text{I.} \quad w_{a\to b} \propto \nu_1^3 \bar{p}(\nu_1)\, \varepsilon_1^2 M_1^2 \\ &\text{II.} \quad w_{a\to c} \propto \nu_2^3 \bar{p}(\nu_2)\, \varepsilon_2^2 M_2^2 \\ &\qquad w_{c\to b} \propto (\nu_2 - \nu_1)^3 [1 + \bar{p}(\nu_2 - \nu_1)]\, M_1^2 \\ &\qquad w_{c\to a} \propto \nu_2^3 [1 + \bar{p}(\nu_2)]\, \varepsilon_2^2 M_2^2. \end{aligned} \tag{4.1}$$

Assuming $\varepsilon \ll 1$ and $\nu_2 - \nu_1 \approx \nu_2$ we find for process II the net result:

$$w_{a\to b} = w_{a\to c} \cdot w_{c\to b}/(w_{c\to a} + w_{c\to b}) \propto \nu_2^3 \bar{p}(\nu_2)\, \varepsilon_2^2 M_2^2 \tag{4.2}$$

and similarly for III:

$$w_{a\to b} \propto \nu_3^3 \bar{p}(\nu_3)\, \varepsilon_3^2 M_1^2.$$

Apart from the unknown matrix elements involved, the difference between the transition probabilities for processes I, II and III lies only in the phonon frequencies $\nu_1 = AS/h$, $\nu_2 \approx g\mu_B H/h$ and $\nu_3 \approx 2g\mu_B H/h$.

Consequently, for each of the mentioned processes we expect a temperature dependence $1/\tau \propto w_{a\to b} \propto \exp(-h\nu/kT)$ in the region $h\nu > kT$, i.e. approximately straight sections are expected in the plot of $\log 1/\tau$ vs $1/T$.

TABLE II

Comparison between energy splittings calculated from the slope of the $\log 1/\tau$ vs $1/T$ line and from paramagnetic resonance data

θ	H Oe	Region of $1/T$ °K^{-1}	Splitting from slope °K	$(E_c - E_a)/k$ °K	$(E_d - E_a)/k$ °K
0°	1440	6–18	0.24		
30°	1440	4–12	0.43	0.25	0.46
65°	1440	6–12	0.35		
90°	1440	6–17	0.22		
30°	2710	4–17	0.67	0.42	0.80
65°	2710	6–12	0.67		
30°	4820	1– 6.5	1.21	0.70	1.37

In fig. 3 and 4 such straight sections are apparent and from the slope one can deduce the corresponding value of $h\nu$. In table II we present the values of these slopes compared to the energy differences between levels a and c and also a and d.

It is seen that phonons of energy $g\mu_B H$ and $2g\mu_B H$ are both important for the observed relaxation, although at $\theta = 0°$ and 90° only phonons of energy $g\mu_B H$ are required. The influence of θ so far has been neglected in the theoretical analysis, but both M and the values of ε and $E_b - E_a$ are, to a minor extent, dependent on the direction of the field with respect to the crystal axis (i.e. on θ).

At the lowest temperatures the relaxation rate decreases less steeply than according to $\exp(-g\mu_B H/kT)$, which may indicate that the direct process (I) prevails.

A further test of our model can be made by comparing $1/\tau$ at different field strengths, H, but at constant values of the phonon-density (Boltzmann-factor for the electron spins), i.e. constant $g\mu_B H/kT$. Since the phonon frequency ν is approximately proportional to H, eq. (4.2) predicts that $(1/\tau)(1/H)$ is a constant for fixed H/T.

TABLE III

Values of $(1/\tau)(1/H).10^6$ at $\theta = 30°$ for different magnetic fields and Boltzmann factors					
$g\mu_B H/kT$ / H Oe	1.34	2.01	2.68	4.02	5.36
4820	(7.9)	2.49	.71	.057	.007
2710	8.5	2.46	.73	.126	.012
1440	11.1	1.95	.57	.140	.042

Table III derived from fig. 3, shows this to be approximately true if $g\mu_B H/kT < 3$; the deviations at values $g\mu_B H/kT > 3$ can be explained by the presence of relaxation by phonons having frequency $\nu = AS/h$, which is most important in low magnetic fields.

For an order of magnitude estimate one may neglect the difference between matrix elements M_1 and M_2 (eq. (4.1)). From the theoretical work of Blume *e.a.*[16]) (eq. 23 loc. cit.) we derive for $w_{c\to b}$ in eq. (4.1):

$$w_{c\to b} = 0.01H^3/[1 - \exp(-g\mu_B H/kT)]\ \text{s}^{-1} \qquad (4.3)$$

where H is given in kOe.

It may be recalled that Blume *e.a.* relate the direct relaxation time to distortions of the octahedral complex of 6 oxygen atoms surrounding one Mn ion. The value of the coefficient in eq. (4.3) seems, however, not to depend very critically on the surroundings of the Mn ion, since we derive from measured relaxation times (§ 3.3) for dilute Mn in LaMg-nitrate a coefficient in eq. (4.3) which is only a factor 2 to 5 higher than the theoretical

estimate. Hence we apply eq. (4.3) to our experiment, taking into account the ratio of transition probabilities of forbidden and allowed transitions following eq. (4.2) and find for $H = 2.7$ kOe and $1/T = 11°K^{-1}$ $1/\tau = w_{a\to b} = 2 \times 10^{-5}\ s^{-1}$. This value agrees in order of magnitude with our experimental result (fig. 4).

We consider the agreement in order of magnitude between the measured and calculated values of τ as a further confirmation of the applicability of our model.

The conclusion is that the phonon density predominantly determines the nuclear spin lattice relaxation, the rate of which is given by the electron spin-lattice relaxation time multiplied by the ratio of forbidden and allowed transition probabilities.

Influence of the Ce ions. A concentration of 10% Ce gives an overall increase of the relaxation rate compared to the more dilute sample (cf. fig. 5). This might be due to a broadening of the energy levels of the Mn ions by magnetic interactions. Also a multiple Ce spin flip might become possible.

At a concentration of 100% Ce the Mn nuclear spin lattice relaxation time becomes quite short. It is very doubtful whether the point shown in fig. 5 represent an ordinary spin-lattice relaxation time, more probably it is the response time of a tightly coupled system of Ce spins, Mn spins and lattice to the heat, applied via a thermal resistance (e.g. the grease layer between crystal and the metal plate).

A low concentration of Ce spins (0.1%) still can strongly influence $1/\tau$. A necessary condition is that the Ce energy splitting is equal to a Mn energy splitting. In fig. 7 it is demonstrated that equalizing $g_C\mu_B H$ to AS strongly increases $1/\tau$.

In ref. 6 it is found that a relaxation time of the order of 10^{-2} s between Ce and Mn exists if their splittings are equal, therefore it can be assumed that both spin systems are in thermal equilibrium at $H = 3.2$ kOe. Consequently, the observed relaxation time must represent the relaxation of the Ce spins towards the lattice. From measurements of Ruby, Benoit and Jeffries[14]) it is possible to give an estimate of this relaxation time as is discussed in § 3.3. Under the conditions of this experiment $1/\tau_b = 0.6\ s^{-1}$ and $1/\tau_d \gtrsim 0.012\ s^{-1}$ is found. Comparing these figures with the relaxation time between Mn nuclear spins and the lattice $1/\tau = 10^{-4}\ s^{-1}$, observed at $\theta = 0°$, it is clear that a good thermal contact with the Ce ions shortens the Mn relaxation time. If the splittings of Ce and Mn are not exactly equal the spin-spin relaxation time will increase and influence the observed relaxation rate, giving decrease of $1/\tau$. This explains the observation of a maximum in $1/\tau$ as a function of the field.

In the situation of fig. 6 also a strong coupling between Ce and Mn exists.

This affects however only the $(-\frac{5}{2}, +3)$ and $(-\frac{5}{2}, +2)$ levels. A fast relaxation between these levels can be expected. Since the occupation of these levels is very small, when we measure τ, it is plausible that this coupling does not influence our result.

Conclusion. The nuclear spin-lattice relaxation of ^{54}Mn in magnetic fields of a few kOe is mainly due to simultaneous flips of the electron spin and of the nuclear spin, i.e. to forbidden transitions in the electron spin-lattice relaxation. This mechanism becomes ineffective for $g\mu_B H \gg kT$, (where T is the lattice temperature); the relaxation time is then very long.

In the presence of 10% or more Ce the ^{54}Mn nuclear relaxation time is shortened. Ce concentrations of 1% or less do not have a significant influence, unless the energy splittings of Mn and Ce are equal.

5. *Nuclear orientation by fast cooling.* 5.1. Introduction and experiment. In this section we will discuss how investigations similar to those of § 4, performed on the same samples and using almost identical techniques will lead to physically quite different results. We will first discuss the experimental procedure for obtaining those results.

A rapid cooling of the sample from $T \approx 0.5°$K to a temperature below 0.05°K was produced in the following way. While the heat switch in the lead between sample and cooling salt was open (nonconducting), a current was applied to the heater, thus the sample was heated to about 0.5°K. Thereafter a magnetic field H was applied and when it had reached the desired value and direction, the heat switch was closed and the heater current was interrupted. During and after the subsequent cooling of the sample the gamma ray intensities in directions parallel and perpendicular to the field, $W(0)$ and $W(\pi/2)$ respectively, were measured.

For a crystal containing 100% Ce only $W(\pi/2)$ was observed. $W(\pi/2)$ increased gradually with time to a certain value, which depended on field strength and the angle θ between the applied magnetic field and the c axis of the crystal. From $W(\pi/2)$ a temperature T_M of the ^{54}Mn nuclei could be calculated by assuming a Boltzmann distribution over the Mn energy levels. In a series of observations at $\theta = 15°$, 30° and 90° and field values $2 < H < 13$ kOe it was found that the temperatures at which $W(\pi/2)$ became stationnary are given by $g_C\mu_B H/kT_M = 8 \pm 1$. In other words: the cooling of the Mn nuclei practically stops when the Ce electron spins reach a certain degree of polarization (cf. also ref. 17).

For a crystal with 10% Ce similar observations were made at $\theta = 90°$, but the stationnary value of $W(\pi/2)$ was already reached for $g_C\mu_B H/kT_M \approx \approx 5 \pm 1$. However, for $\theta = 30°$ and $H = 2650$ Oe a remarkable result was found, namely $W(\pi/2) < 1.00$ which signifies, crudely speaking, that the nuclear spins are predominantly aligned in a plane perpendicular to H

instead of being polarized along H; consequently, a significant deviation from a Boltzmann distribution must have occurred. It was soon found that neither the particular value of θ nor that of H is essential for obtaining this strong deviation from Boltzmann equilibrium.

Very similar results were obtained when cooling crystals with 1% and 0.1% Ce. Here the stationnary values of $W(0)$ and $W(\pi/2)$ were reached in

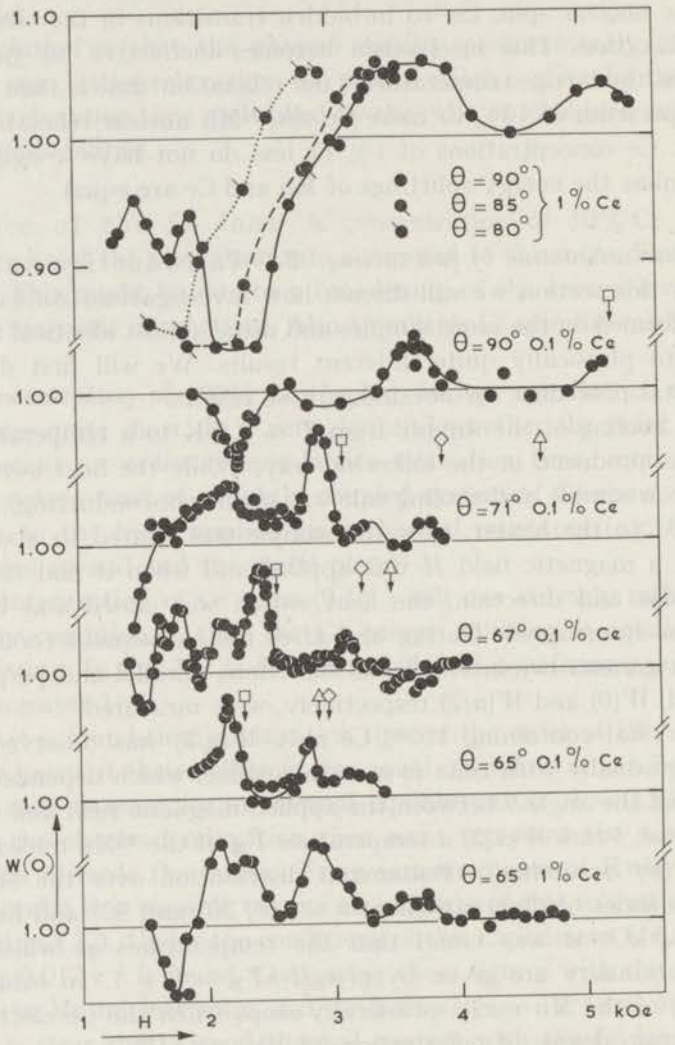

Fig. 9. The observed values of $W(0)$ after fast cooling as a function of the magnetic field strength H for various field directions and two different samples. The calculated positions of some transitions are indicated.

□ $(-\frac{5}{2}, +3) \rightarrow (-\frac{3}{2}, +2)$ for ions with $D/k = -0.007°\mathrm{K}$
◇ $(-\frac{5}{2}, +3) \rightarrow (-\frac{3}{2}, +1)$,, ,, ,, $D/k = -0.007°\mathrm{K}$
△ $(-\frac{5}{2}, +3) \rightarrow (-\frac{3}{2}, +2)$,, ,, ,, $D/k = -0.031°\mathrm{K}$

a short time (typically 40 s) and their values depended strongly on the magnetic field. The patterns which were obtained for some directions of the magnetic field are shown in fig. 9. When the angle was varied over a small interval the patterns obtained are almost identical when plotted versus $(g_M - g_C)\mu_B H$. Hence we ascribe the observed effect to an interaction between Ce and Mn.

The $W(0)$ and $W(\pi/2)$ versus H patterns are entirely determined by the field H which was present during the cooling. If after the cooling the field was altered in magnitude or direction, no significant variations in $W(0)$ and $W(\pi/2)$ occurred. It may be remarked, that $W(0)$ and $W(\pi/2)$ were only constant for $H > 1.5$ kOe; for smaller fields they gradually changed towards values which correspond to a low temperature Boltzmann distribution over the Mn levels.

For the 0.1% and the 1% Ce samples measurements were taken at $\theta = 90°$, 65°, 30° and 0°. Whereas at $\theta = 90°$ the 1% Ce sample gave large effects e.g. $W(0) - 1 = -0.16$ at $H = 2300$ Oe, the 0.1% Ce sample gave in the same field the much smaller effect $W(0) - 1 = -0.05$. At $\theta = 65°$ both samples gave comparable peak structures, only were the peaks for the 1% Ce sample broader than for the 0.1% Ce sample. For $\theta = 30°$ only a few measurements were taken since the peaks were narrow and difficult to reproduce. For $\theta = 0°$ no peaks, which could be associated with Ce were observed.

The 0.03% samples gave a few broad peaks at $\theta = 90°$ and $\theta = 65°$; since they did not show the $(g_M - g_C)\mu_B H$ dependence they have to be

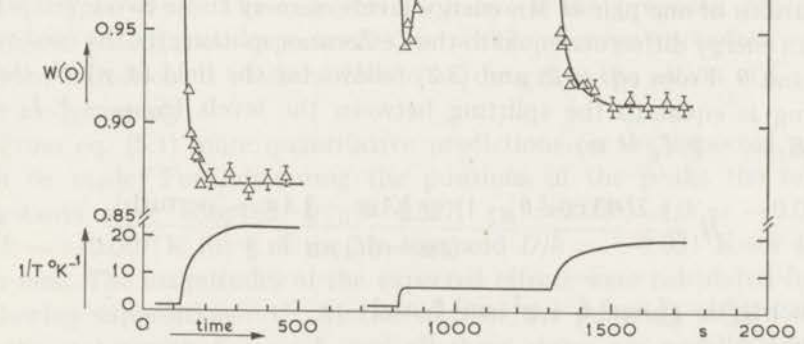

Fig. 10. Time dependence of $W(0)$ during and after cooling of the sample. At the top $W(0)$ is shown, at the bottom the temperature of the cerium magnesium nitrate thermometer is given. The left hand side of the figure represents a normal cooling, at the right hand side the temperature is decreased in two steps.

attributed to other ions than Ce e.g. impurities. They will not be discussed further.

Interesting information was obtained when we varied the cooling procedure. An example is given in fig. 10, where $W(0)$ is plotted as function of time for two different cooling procedures. On the left hand side a normal run is plotted. It can be seen that $W(0)$ reaches its final value within 100 s. On the right hand side of the figure a run is shown in which the temperature is decreased in two steps. At the first cooling the gamma ray intensity distribution becomes anisotropic, but this anisotropy vanishes in a few minutes; at the second cooling again an anisotropy effect is produced, which is however smaller than when the cooling had been performed in one step.

For some other peaks we measured the effects after cooling as a function of the temperature before the cooling started: generally it was found that less gamma ray anisotropy was obtained for an initial temperature $T \approx 0.2°\mathrm{K}$ than for the normal procedure in which initially $T \approx 0.5°\mathrm{K}$. Finally it may be remarked that a slow cooling did not produce the effect according to the above mentioned patterns of peaks, but rather effects of a few percent according to the Boltzmann distribution.

For the 0.1% Ce sample we varied the magnetic field over 100 Oe around 2250 Oe, during the first minute of the cooling at $\theta = 90°$. The same effect was observed as when the field had a fixed value in this region. This result indicates that inhomogeneous broadening is not the main origin for the width of the observed peaks.

5.2. Discussion. Model for explaining the patterns. First we will present an interpretation of the patterns, observed for the 0.1 and 1% Ce samples. Both the dependence on angle θ and on Ce concentration indicate an interaction between Ce and Mn during cooling. It is plausible to ascribe the observed effect to an energy exchange between Ce and the populations of one pair of Mn energy levels, namely those two levels which have an energy difference equal to the Ce Zeeman splitting for the used value of H and θ. From eq. (3.2) and (3.3) follows for the field at which the Ce splitting is equal to the splitting between the levels $(S_z = -\frac{5}{2}, I_z = n)$ and $(S_z = -\frac{3}{2}, I_z = m)$:

$$H = \frac{2D(3\cos^2\theta - 1) + \frac{3}{2}Am - \frac{5}{2}An + [\text{perturb}]}{(g_M - g_C)\,\mu_B} \tag{5.1}$$

in which $g_C^2 = g_{//}^2 \cos^2\theta + g_\perp^2 \sin^2\theta$ and

$$[\text{perturb}] = \frac{-32D^2\sin^2\theta\cos^2\theta + D^2\sin^4\theta - \frac{1}{4}A^2[2I(I+1) + 3m^2 - 13m - 5n^2 + 5n]}{g_M\mu_B H}.$$

A priori the energy exchange between Ce and Mn may lead either to downward or to upward transitions of the Mn (e.g. transitions a or b in fig. 11). The sign of the observed effect in $W(0)$ depends on this direction. Experimentally we observed for $\theta = 65°$ positive effects in $W(0)$ at the highest magnetic fields, for which $W(0)$ effects have been found. From eq. (5.1) we deduce, since $D < 0$, $A < 0$, $g_M > g_C$ and [perturb] is small, that the transition which occurs at the highest magnetic field is that having $n = +3$ and m as small as compatible with selection rules. With the aid of table I we conclude from the observed positive effects in $W(0)$ that the $n = +3$ level is depopulated, thus an *upward* transition $(-\frac{5}{2}, +3) \rightarrow (-\frac{3}{2}, m)$ is observed.

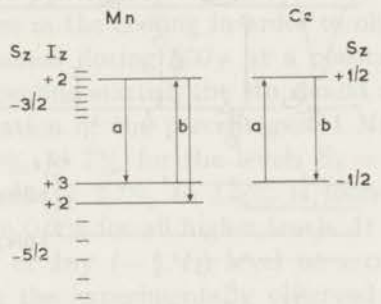

Fig. 11. Diagram of the energy levels of Mn and Ce with an indication of the proposed processes.

Presumably the population of the level $(-\frac{3}{2}, m)$ will be transferred to the $(-\frac{5}{2}, m)$ level by the normal spin-lattice relaxation of Mn but this will not be noticeable in our measurement of the gamma-ray anisotropies which depend only on m and not on S_z. The net result of the action of the Ce during its cooling is that the population of the $(-\frac{5}{2}, +3)$ level is transferred to the $(-\frac{5}{2}, m)$ level. The resemblance between the proposed process and dynamic polarization experiments, in which microwaves induce one forbidden transition, is obvious. Hence we designate the action of Ce on the Mn as "pumping".

From eq. (5.1) more quantitative predictions on the expected patterns can be made. For calculating the positions of the peaks the following constants were adopted: $g_{\perp C} = 1.827$, $g_M = 2.000$, $A/k = -0.0102°K$, $D/k = -0.007°K$ for $\frac{2}{3}$ of the Mn ions and $D/k = -0.031°K$ for $\frac{1}{3}$ of the Mn ions. The magnitudes of the expected effects were calculated from the following suppositions: 1°. At the start of the pumping all Mn ions are in the states with $S_z = -\frac{5}{2}$, and all these states are equally populated. 2°. Through the pumping the whole population of a level is transferred to a level $(-\frac{3}{2}, m)$ and subsequently goes to the $(-\frac{5}{2}, m)$ level.

In fig. 12 a comparison is made between calculated and observed peaks.

For this comparison we will mainly use the result of the 0.1% Ce sample, since in this crystal the sharpest peaks were observed. From eq. (5.1) it is anticipated that an appreciable number of peaks may overlap, and hence we will study only the most resolved structure in more detail. The experimental peaks at 2170 Oe ($W(0)$), 2260 Oe ($W(\pi/2)$ and 2810 Oe ($W(0)$) and $W(\pi/2)$ agree in relative positions and signs of the effects quite well with the theoretical peaks for the ions with $D/k = -0.007°K$.

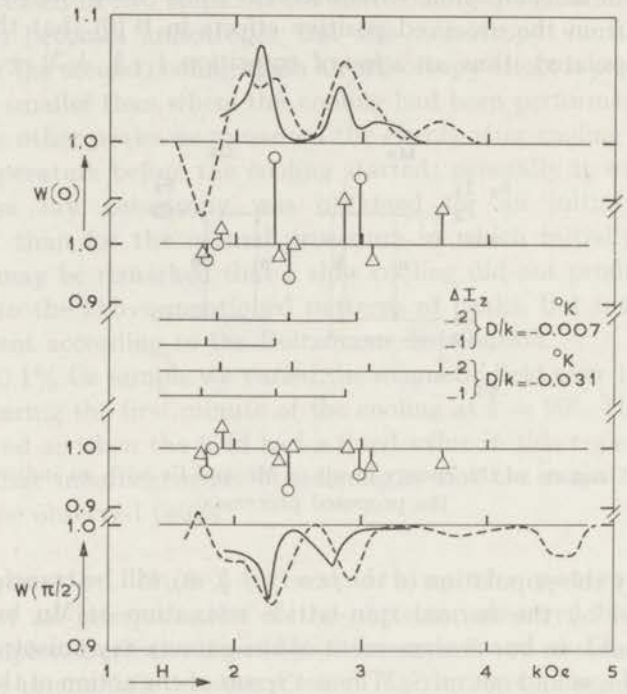

Fig. 12. Comparison between calculated and experimental peaks at $\theta = 65°$. Top and bottom respectively experimental $W(0)$ and experimental $W(\pi/2)$ values for the 0.1% Ce sample (drawn) and for the 1% Ce sample (dotted). In the middle the calculated positions of the transitions $(S_z = -\frac{5}{2}, I_z) \rightarrow (S_z = -\frac{3}{2}, I_z + \Delta I_z)$ are indicated. The expected magnitudes of the effect in $W(0)$ and $W(\pi/2)$ are indicated by ○ resp. △ for the ions with $D/k = -0.007°K$ resp. $D/k = -0.031°K$. The vertical scale is different from that used for the experimental points, its value rests on assumptions discussed in the text.

An overall discrepancy of 140 Oe is present, which might be due to errors in the theoretical calculations resulting from the use of an incomplete spin hamiltonian and the approximations of perturbation theory. Further it is possible that the constants used in the calculations are slightly incorrect. The peaks at 2170 and 2260 Oe respectively should clearly be identified with the transitions $(-\frac{5}{2}, +3) \rightarrow (-\frac{3}{2}, +2)$ and $(-\frac{5}{2}, +2) \rightarrow$ $\rightarrow (-\frac{3}{2}, 0)$ respectively for the ions with $D/k = -0.007°K$. As to the

peak at 2810 Oe in the $W(0)$ effect, both the transition $(-\frac{5}{2}, +3) \rightarrow$ $\rightarrow (-\frac{3}{2}, +1)$ for ions with $D/k = -0.007°\text{K}$ and the transition $(-\frac{5}{2}, +3) \rightarrow$ $\rightarrow (-\frac{3}{2}, +2)$ for the ions with $D/k = -0.031°\text{K}$ can be responsible. The $W(\pi/2)$ effect favours the former identification, which is further supported by the angular dependence of the distance between the two positive peaks in $W(0)$, as can be seen from fig. 9. Hence no effects of the ions with $D/k = -0.031°\text{K}$ can be clearly identified in the 0.1% Ce sample.

The 1% Ce sample shows also the above mentioned peaks, although they are considerably broadened. A further argument for the correctness of our model can be derived from fig. 10. It can be seen at $t \approx 1300$ s that cooling from a temperature $T = 0.16°\text{K}$ can still produce a change in $W(0)$ of 9%. From table I it can be concluded that at least $9/1.66 = 5.4\%$ of all Mn ions have to participate in the cooling in order to obtain this effect. Since the lattice was maintained during 500 s at a constant temperature $T =$ $= 0.16°\text{K}$, before the cooling started, the Mn should also have reached this temperature. A calculation of the percentages of Mn ions, which occupy a single level gave 19% to 7% for the levels $S_z = -\frac{5}{2}$, with I_z ranging from -3 to $+3$. Similarly 2.7% to 1.5% is found for the levels with $S_z = -\frac{3}{2}$ and less than 0.2% for all higher levels. It is then easily verified that e.g. deexcitation of any $(-\frac{3}{2}, I_z)$ level or a combination thereof is insufficient to explain the experimentally observed jump in $W(0)$. This argument confirms that the Ce transfers the Mn population from a $S_z = -\frac{5}{2}$ level to a $S_z = -\frac{3}{2}$ level.

The rate of vanishing of the anisotropy, observed in fig. 10 at $t = 900$ s, when the temperature was kept constant at $1/T = 6.6°\text{K}^{-1}$ is rather high when compared to the results given in § 4. From § 4 we estimate for $\theta = 90°$, $H = 2370$ Oe and $1/T = 6.6°\text{K}^{-1}$ a nuclear relaxation time $\tau = 700$ s, while fig. 10 gives $\tau \approx 50$ s. This fast relaxation can be explained by assuming that the transition probability for a particular forbidden transition is increased through the Ce; thus the relaxation time for that particular level, which was populated during the cooling, is short. However, at $1/T = 20°\text{K}^{-1}$ we did not observe a short relaxation time, hence apparently the Ce does not give an important increase in relaxation rate when all Ce ions are in their ground state.

From the above mentioned results it can be understood why a slow cooling did not produce anomalous nuclear orientation effects.

The coupling mechanism. It remains to be discussed which process is responsible for the coupling between Mn and Ce. Two mechanisms can be proposed:

a) the Ce produces numerous phonons of frequency $\nu = g_C \mu_B H/h$ which are absorbed by the Mn.

b) A simultaneous flip-flop between the Mn and Ce electron spins may be

induced e.g. by magnetic dipole interactions. The fact that the Ce can shorten the Mn nuclear spin relaxation time proves that the latter mechanism is present. There is, however, no experimental proof that the former mechanism is absent.

In the following we will give for both mechanisms an estimate of the order of magnitude of the effects in $W(0)$; numerical values will be given for $\theta = 65°$ and $H = 2.3$ kOe, under which conditions the process b indicated in fig. 11 takes place for $\frac{2}{3}$ of the Mn ions. The magnitude of the effect is determined by the time which is required for cooling the Ce, since only during this time the mechanism which polarizes the ^{54}Mn nuclei is operative. Ruby, Benoit and Jeffries[14]) have found that the spin-lattice-bath relaxation rate of the Ce is limited by a phonon bottleneck. It can be calculated that in our case, where the lattice temperature suddenly diminishes from $T = 0.5°$K to a much lower value the population of the highest Ce level decays approximately exponentially with a time constant τ_p. Taking the experimental values of Ruby *e.a.* for the linewidth and the mean phonon lifetime and multiplying the latter value with the ratio of the thickness of our crystals (0.3 cm) to the thickness of Ruby's crystals (0.1 cm) we calculate for the 1% Ce sample $\tau_p = 10$ s and for the 0.1% Ce sample $\tau_p = 3$ s.

For the phonon mechanism we used the inverse of the relaxation times given in fig. 4 as an estimate for the probability that phonons induce a transition with $\Delta I_z = 1$ in Mn. Then we calculate effects in $W(0)$ of only 2% resp. 0.6% for the 1% resp. the 0.1% Ce sample.

The magnetic dipolar interaction presumably induces flip-flop processes only between the electron spins of the Ce and Mn ions. However, transitions in which the nuclear spin of Mn changes with $\Delta I_z = 1$ or $\Delta I_z = 2$ have been observed. The occurrence of nuclear spin flips through a flip-flop between Mn and Ce electron spins can be understood from the circumstance that the wave functions of the Mn levels are not pure eigenstates of $|S_z, I_z\rangle$. Calculations following Bleaney and Rubins[18]) show that for the ions with $D/k = -0.007°$K at $H = 2.2$ kOe and $\theta = 65°$ the state $|S_z, I_z\rangle$ is for 10% admixed with $|S_z \pm 1, I_z \mp 1\rangle$ and for 1 à 3% with other wave functions e.g. $|S_z, I_z \pm 1\rangle$ and $|S_z \pm 2, I_z\rangle$. These admixtures give rise to transition probabilities of the order of 1 and 0.01% respectively for $\Delta I_z = 1$ and $\Delta I_z = 2$ transitions relative to the allowed transitions $\Delta I_z = 0$.

In the 0.1% Ce sample the average distance between a Mn ion and its nearest Ce neighbour is 50 Å. It can be calculated that, if the energy splittings of Mn and Ce are equal, the magnetic dipolar coupling induces a flip-flop rate of roughly 10^5 s^{-1} when the Mn makes an allowed transition $\Delta I_z = 0$; in case of forbidden transitions the flip-flop rate is estimated to be 10^3 s^{-1} and 10^1 s^{-1} for respectively $\Delta I_z = 1$ and $\Delta I_z = 2$. In the crystal with 1% Ce the distances between Ce and Mn are smaller, and hence the

flip-flop rates still higher than for the 0.1% Ce crystal. Since the Ce temperature changes only slowly when compared with the flip-flop rate, the ratio of the populations N_+ and N_- of the Mn levels $(-\frac{5}{2}, +3)$ and $(-\frac{3}{2}, +2)$ respectively (cf. fig. 11) is determined by the Boltzmann distribution over the Ce Zeeman energy levels, i.e. the Ce temperature. The transition $(-\frac{3}{2}, +2) \rightarrow (-\frac{5}{2}, +2)$ is the direct process in the Mn electron spin-lattice relaxation; for the transition probability we take the value which follows from eq. (4.4) and eq. (4.1) $w_M = 0.01\ H^3 = 0.1\ s^{-1}$. The number of Mn ions which is finally transferred to the $(-\frac{5}{2}, +2)$ level is given by $N_{pol} = w_M \int N_+(t)\, dt$. The Ce temperature and the number of Mn ions which has been transferred up to the time t determine $N_+(t)$; by numerical methods $N_+(t)$ and therefore N_{pol} can be calculated easily. For the 0.1% Ce sample we find that $N_{pol} = 0.1\ (N_+ + N_-)$. Since we consider only $\frac{2}{3}$ of the Mn ions, and initially only $\frac{1}{7}$ of them occupies the levels $(-\frac{5}{2}, +3)$ and $(-\frac{3}{2}, +2)$ the calculated effect in $W(0)$ is $\frac{2}{3} \times \frac{1}{7} \times 0.1 \times 167 = 2\%$. For the 1% Ce sample this figure is 6 %.

The above given calculations show:

1°. the dipolar flip-flop mechanism is probably more effective than the phonon mechanism in polarizing the Mn nuclei;

2°. the calculated effects for the flip-flop process agree in order of magnitude with the measured effects. The experimental effects are somewhat larger than the calculated ones, but this can easily be ascribed to the fact that both τ_p and w_M are not very well known.

Further it may be seen from our model that the value of the flip-flop frequency ν_f is unimportant as long as $\nu_f \gg 1/\tau_p$ and $\nu_f \gg 1/\tau_M \equiv w_M$. The magnitude of the observed effect is determined by the ratio τ_p/τ_M i.e. the cooling time of the Ce ions compared to the relaxation time of the Mn electron spins. The fact that no $\Delta I_z = 3$ transitions have been observed can be ascribed to a too long flip-flop time for these transitions.

Apart from the processes considered above, in which Ce induces a forbidden Mn transition, which is followed by an allowed transition, an effect on the gamma ray intensities can also be expected when the Ce induces an allowed transition $\Delta I_z = 0$, which is followed by a forbidden transition. A calculation similar to that given above shows that the latter processes are about a hundred times less probable than the former ones as far as the flip-flop mechanism is concerned. Thus these processes are relatively unimportant. The phonon mechanism, on the other hand gives only a slight difference between both types of processes.

Some remarks may be made about the ions with $D/k = -0.031$°K. The amplitude of the wave functions $|S_z \pm 1, I_z \pm 1\rangle$ admixed to a state $|S_z, I_z\rangle$ is for these ions much higher than for the ions with $D/k = -0.007$°K, i.e. up to 20% for $H = 2.3$ kOe and $\theta = 65°$. Hence the intensities of the forbidden lines $\Delta I_z = 1$ and $\Delta I_z = 2$ can be expected to be relatively

strong. It is questionable whether the distinction between "allowed" and "forbidden" intensities is very meaningful for these ions, which would imply that after an $(S_z = -\frac{3}{2}, I_z)$ level is occupied, many ways are open for deexcitation of this level. This could explain that for these ions not very distinct effects in $W(0)$ and $W(\pi/2)$ were found.

The higher Ce concentrations. When increasing the Ce concentration the following effects can be expected:

a) The probability is increased that strongly forbidden transitions are induced, so that they might become observable. At the same time the intensities in less forbidden lines can not be raised beyond saturation, i.e. when the initial level is completely emptied. Thus the patterns probably become more complicated.

b) The energy levels are broadened, hence the resonances may overlap and the total pattern may become poorly resolved.

c) The increased heat capacity of the Ce will make the cooling slower. This allows more time for competing relaxation mechanisms which can only operate as long as the electron spin are not in their ground states.

These three aspects together explain the experimental fact that upon increasing the Ce concentration, the line structures in $W(0)$ and $W(\pi/2)$ disappear and are replaced by effects in $W(0)$ and $W(\pi/2)$ according to a Boltzmann distribution over the Mn levels.

Further, in order to reach a distribution in accordance with a low temperature, relaxation via the Ce electron spins is required; apparently the Ce ions lose their capability to relax Mn nuclei when nearly all ions are in their ground state, i.e. for $g_C \mu_B H \gg kT$.

The utilization of magnetically concentrated compounds in earlier nuclear orientation experiments (and also the absence of appreciable magnetic fields) has presumably prevented the occurrence of large deviations from Boltzmann-equilibrium. The experiments reported in this paper suggest that one has to be careful in the interpretation ef e.g. gamma radiation anisotropies in terms of thermal equilibrium between nuclear spins and „the crystal".

Conclusion. It is found that polarization of ^{54}Mn nuclei can result from magnetic dipole-dipole coupling between Ce and Mn electron spins. It is essential for this mechanism that the Ce maintains a high temperature for one particular Mn splitting, the temperature of the other Mn splittings being much lower.

As a result the Ce spins act as a pump on the Mn spin system, inducing forbidden transitions e.g. from the level $(S_z = -\frac{5}{2}, I_z)$ to $(S_z = -\frac{3}{2}, I_z - 2)$, which is followed by a transition to the $(S_z = -\frac{5}{2}, I_z - 2)$ level. This leads to a population of the Mn nuclear levels which deviates strongly from a Boltzmann distribution. It is calculated that the magnitude of this

deviation is determined by the ratio of the spin-lattice-bath relaxation time of Ce and the spin-lattice-bath relaxation time of the Mn.

The operation of this mechanism is sensitively dependent on the matching of Ce and Mn energy levels, which leads to resonance like patterns in the gamma ray anisotropies of ^{54}Mn as a function of magnetic field strength and direction.

The effects of this mechanism were most clearly observed for Ce concentrations of 1% and 0.1%; at higher Ce concentrations the normal Mn nuclear-spin lattice relaxation prevails (cf. § 4).

REFERENCES

1) de Groot, S. R., Tolhoek, H. A. and Huiskamp, W. J., Alfa-, beta- and gamma-ray spectroscopy, ed. K. Siegbahn. (North-Holl. Publ. Co., Amsterdam, 1965.)
2) Bloembergen, N., Shapiro, S., Pershan, P. S. and Artman, J. O., Phys. Rev. **114** (1959) 445.
3) Abragam, A. and Borghini, M., Prog. low Temp. Phys. vol. **4** ed. C. J. Gorter. (North-Holl. Publ. Co., Amsterdam, 1964.)
4) Lubbers, J., Miedema, A. R. and Huiskamp, W. J., Physica **31** (1965) 153; Chapter I.
5) Wheatley, J. C. and Estle, T. L., Phys. Rev. **104** (1956) 264.
6) Lubbers, J. and Huiskamp, W. J., Physica to be published; Chapter IV.
7) Bleaney, B. and Ingram, D. J. E., Proc. Roy. Soc. **A 205** (1951) 336.
8) Brandt, B. M. M., van Ormondt, D. and Thalhammer, T., Phys. Letters **19** (1965) 549.
9) Kedzie, R. W. and Jeffries, C. D., Bull. Am. phys. Soc. **3** (1958) 415 L3. and unpublished preprint.
10) Nuclear Data Sheets, ed. K. Way. Ac. Press. New York.
11) Private communication of C. D. Jeffries given in [3]).
12) Private communication of H. J. Stapleton mentioned in [14]).
13) van Duyneveldt, A. J., private communication.
14) Ruby, R. H., Benoit, H. and Jeffries, C. D., Phys. Rev. **127** (1962) 51.
15) Abragam, A., The principles of nuclear magnetism. Clarendon Press Oxford, 1962. Chap. IX, Sect. IV.
16) Blume, M. and Orbach, R., Phys. Rev. **127** (1962) 1587.
17) Lubbers, J. and Huiskamp, W. J., Physica to be published; Chapter II.
18) Bleaney, B. and Rubins, R. S., Proc. Phys. Soc. (London) **77** (1961) 103.

CHAPTER IV

ROTATIONAL COOLING IN DILUTE PARAMAGNETIC CRYSTALS; THERMAL MIXING BETWEEN NUCLEAR AND ELECTRONIC SPINS

Synopsis

Rotational cooling in magnetic fields was performed with a few Ce electron spins ($\approx 10^{18}$/cm^3) included in lanthanum magnesium nitrate. When their energy splittings were made equal to the hyperfine structure splittings of ^{54}Mn nuclei (with a concentration of $\approx 4 \times 10^{12}$/cm^3) a fast ($\approx 10^{-2}$ s) thermal mixing was observed. A detailed investigation of this mixing process is presented; the mixing rate is quantitatively accounted for by magnetic dipole-dipole interactions. The obtained nuclear polarization of the ^{54}Mn nuclei was $\langle I_z \rangle / I > 97\%$ and could be maintained during at least 2000 s. The minimum g-value of Ce in lanthanum magnesium nitrate was found to be $g_{//} = 0.0235 \pm 0.0009$.

1. *Introduction and principle.* Establishment of thermal equilibrium between two nuclear spin systems by thermal mixing, also called cross relaxation, has been shown to be of considerable interest for the study of nuclear spin relaxation at low temperatures[1]). The rate at which thermal equilibrium is established is high if the energy level splittings of the two kinds of spins are equal, the rate for unequal splittings being much lower. This fast thermal mixing has also been found between protons and the electron spins of Yb[2]) and Ce[3]).

In the present paper we report thermal mixing between Ce electron spins and nuclear spins of ^{54}Mn in lanthanum magnesium nitrate. A survey of the energy levels and relaxation properties of these ions in magnetic fields is given in ref. 4, denoted as III henceforth. Since Ce has a small value of $g_{//}$ and ^{54}Mn has a fairly large hyperfine structure (h.f.s.) splitting, it is possible to equalize the Mn and Ce splittings in rather strong magnetic fields. The ^{54}Mn nuclear spin-lattice relaxation time can be made fairly long under these conditions. Therefore the ^{54}Mn nuclei form essentially an isolated system, which "sees" only the Ce spins at the transient crossing of energy levels, after which ample time is available to study the resultant nuclear orientation of ^{54}Mn.

The nuclear orientation is observed by measuring the anisotropy of the gamma rays emitted by ^{54}Mn. The gamma ray intensities are measured in directions parallel and perpendicular to the magnetic field and are respectively denoted by $W(0)$ and $W(\pi/2)$. The normalization is so chosen that $W(0) = W(\pi/2) = 1$ for unoriented nuclei. The known characteristics of the ^{54}Mn decay provide an experimentally verified correlation between the population densities of the Mn h.f.s. levels and $W(0)$ and $W(\pi/2)$ (cf. table I of III), consequently changes in $W(0)$ and $W(\pi/2)$ can be interpreted directly in terms of changes in population densities.

In the following we will designate a level by the symbol (S_z, I_z). From the formulae given in III it follows that thermal mixing between the Ce and the levels $(-\frac{5}{2}, I_z)$ and $(-\frac{5}{2}, I_z + 1)$ of ^{54}Mn can be expected if

$$(g_{//}^2 \cos^2\theta + g_{\perp}^2 \sin^2\theta)^{\frac{1}{2}} \mu_B H = |-\tfrac{5}{2}A - g_N \mu_N H + \tfrac{5}{2}A^2 I_z/(g\mu_B H - 4D)| \quad (1)$$

in which θ is the angle between the magnetic field $\boldsymbol{H}$ and the crystallographic c-axis, $g_{\parallel}$ and $g_{\perp}$ are the g-values of Ce, A is the h.f.s. splitting constant of ^{54}Mn, D is the parameter of the crystalline field splitting of ^{54}Mn, g is the electronic g-value and g_N the nuclear g-value of ^{54}Mn. The values of these constants are discussed in III § 3. Because of the last term in the right hand side of eq. (1) transitions between the upper h.f.s. levels of ^{54}Mn will occur at a somewhat higher value of the Ce splitting than for the lower levels; for a given pair of levels also a small difference is expected in crossing field or angle for the two different types of Mn ions in the unit cell.

Particularly interesting is the situation when thermal mixing occurs with a very cold Ce spin system. The Ce spin system can be brought to temperatures in the millidegree range, even while a magnetic field of many kOe is present by rotational cooling consisting of two steps:

a) precooling of the sample by the KCr-alum when the field is in a direction along which the g-value of Ce (g_C) is appreciable;

b) rotating the magnetic field towards a direction of small g_C, i.e. decreasing θ.

Since ample time is available for precooling and the spin-lattice relaxation time is short[5]), a good thermal equilibrium between lattice and Ce spins can be achieved in a). On the other hand, we require that in b) the Ce spins are sufficiently isolated from the lattice for studying energy exchange with the Mn spins and the resulting nuclear orientation. This lack of thermal contact between Ce and the lattice can be expected because of the anisotropy of the spin-lattice relaxation time (cf. III § 3); whether the isolation is sufficient has to be verified by experiment.

From eq. (1) we expect that the Ce splitting will "see" first the largest Mn h.f.s. energy difference (i.e. between the levels $(-\frac{5}{2}, 3)$ and $(-\frac{5}{2}, 2)$), resulting in a transfer of the population of the $I_z = 3$ level to the $I_z = 2$

level. Subsequently the population of the upper energy levels will be swept into the lower levels. This process will result in a stepwise change of $W(0)$, the theoretical prediction for a cerium temperature $T_C = 0$ is given in fig. 3 for a certain magnetic field. A large decrease in $W(0)$ is observed when the transition from $(-\frac{5}{2}, -2)$ to $(-\frac{5}{2}, -3)$ occurs. If $T_C \neq 0$, the upper h.f.s. levels remain populated but the population distribution over the levels after the above mentioned process is markedly different from a Boltzmann distribution. This results in a different relation between $W(0)$ and $W(\pi/2)$, as is shown in fig. 4. The model presented above will be designated as the "sweeping down" model.

2. *Experiments.* 2.1. Experiment in general. For details on the experimental setup and on the samples we refer to III. It is essential that a large magnetic field in a horizontal direction $\boldsymbol{H}_h$, as well as a small field in the vertical direction $\boldsymbol{H}_x$ may be applied to the sample. The field $\boldsymbol{H}_h$ can be rotated in a horizontal plane so that any angle θ between the total magnetic field $\boldsymbol{H} = \boldsymbol{H}_h + \boldsymbol{H}_x$ and the c-axis of the sample can be chosen. Independently of the magnetic field it is possible to change the temperature T of the metal plate to which the sample is glued over the region $0.03 < < T < 0.5°K$; the lattice temperature of the sample is generally equal to T. The symbols H, θ and T without indices will be used through this paper exclusively in the sense as defined above.

Unless otherwise stated all experiments were done on the LaMg-nitrate sample containing 0.1% Ce and carrierfree ^{54}Mn. Before each experiment the sample was heated to 0.4°K in zero field, in order to destroy the ^{54}Mn nuclear orientation of previous experiments. At $\theta = 30°$ a field of 3 or 5 kOe was applied and the sample was allowed to cool for a few minutes. In the mean time the metal plate reached a temperature of 0.03 to 0.05°K. Thereafter the field was rotated to a small value of θ.

The nuclear orientation of the ^{54}Mn remained small ($|W - 1| < 0.01$) until a certain value of θ was reached, where $W(\pi/2)$ increased and $W(0)$ decreased strongly. In fig. 1 the result of such an experiment is shown, in which θ was varied in small steps and $W(0)$ was measured after each step. We define a mixing angle θ_m as the angle in fig. 1 where $W(0)$ is halfway between its initial and final value. The angle θ_m depends on the applied magnetic field. In fig. 2 we show the experimentally found points together with two curves computed with the aid of eq. (1) for two different values of D and taking $I_z = -3$. A good agreement is found; in low magnetic fields however, the lines for both D values differ considerably and a comparison is less meaningfull. In this region also a line broadening may have some influence on the picture, as will be explained in the discussion.

The mixing region can also be reached by rotating a high field $\boldsymbol{H}$ to a value of θ somewhat larger than $\theta_m(H)$ and subsequently decreasing H.

From such a procedure the same relation between θ_m and H is found as given in fig. 2.

2.2. Maximum mixing field. From eq. (1) it follows that, if $g_{//} \neq 0$, for a certain magnetic field the Ce energy splitting is, for all θ, larger than the h.f.s. splitting of ^{54}Mn; i.e., no thermal mixing can occur.

In order to verify this expectation and to determine the value of $g_{//}$, we did an experiment in the strong magnet. The main problem is to circumvent the complication of a possible, unknown misalignment of the crystal.

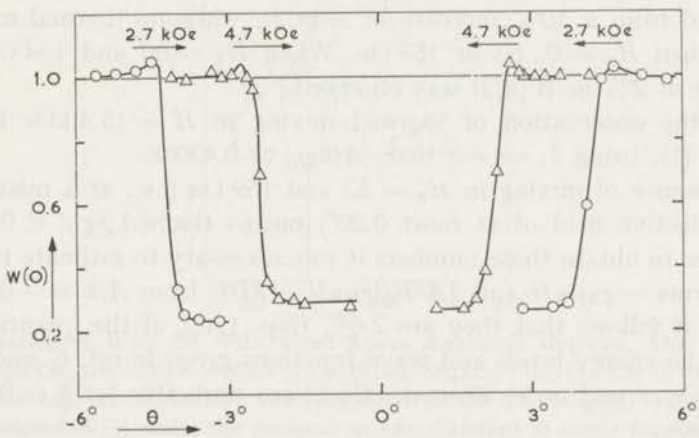

Fig. 1. Four typical series showing $W(0)$ for ^{54}Mn in (0.1% Ce–La)Mg-nitrate when the angle θ between magnetic field H and c-axis was decreased in small steps. Steps were taken every 30 s.

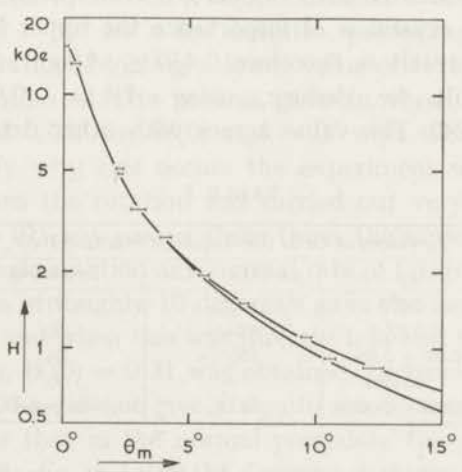

Fig. 2. Relation between field strength H and mixing angle θ_m. The dashes represent the measurements; the two drawn lines give the results of the theoretical calculations from eq. (1) for the two different types of Mn ions.

The following experimental procedure was therefore adopted. After a few minutes precooling at a large value of θ, the horizontal field $\boldsymbol{H}$ was rotated 1.5° further than the position where the field was closest to the c-axis of the crystal. A small vertical field $\boldsymbol{H}_x$ was present during this rotation. The lowest value of θ which is reached during this procedure is determined by $\boldsymbol{H}_x/\boldsymbol{H}$ and by the misalignment of the c-axis of the crystal with respect to the plane of rotation of the field $\boldsymbol{H}$. All values of θ higher than this minimum value are covered during the rotation. The quantity $W(\pi/2)$ was measured before and after rotation.

For $H = 15.4$ kOe thermal mixing was observed when $H_x = 106$ Oe as is deduced from a 10% increase of $W(\pi/2)$, while no thermal mixing occurred when $H_x = 0$, 53 or 159 Oe. When $H_x = 80$ and 134 Oe only a small rise of 2% in $W(\pi/2)$ was observed.

From the observation of thermal mixing in $H = 15.4$ kOe it follows from eq. (1), using $I_z = -3$ that $|A/kg_{//}| > 0.430$°K.

The absence of mixing in $H_x = 53$ and 159 Oe (i.e., at a misalignment of the effective field of at most 0.20°) means that $|A/kg_{//}| < 0.445$°K.

In order to obtain these numbers it was necessary to estimate the values of the terms $-g_N\mu_N H$ and $\frac{5}{2}A^2I_z/(g\mu_B H - 4D)$; from $A/k = -0.01025$°K (III, § 3) it follows that they are 2.6% resp. 1.4% of the quantity $-\frac{5}{2}A$.

From the energy levels and wave functions given in ref. 6, one deduces that for Ce second order Zeeman effects are negligible for $\theta = 0$, even at $H \approx 15$ kOe.

A few remarks on possible systematic errors in our result which are not included in the above limits have to be made. It is conceivable that mixing already starts before crossing of energy levels occurs. In this case $|A/kg_{//}|$ may be somewhat smaller than calculated. If a spread in direction of the c-axis through the crystal is of importance the upper limit of $|A/kg_{//}|$ decreases. Our final result is therefore $0.430 \lesssim |A/kg_{//}| < 0.445$°K.

From this result we deduce, using $A/k = -0.01025 \pm 0.0002$°K, $0.0226 < g_{//} \lesssim 0.0243$. This value agrees with other determinations of $g_{//}$.

TABLE I

$g_{//}$ values of Ce in $(Ce–La)_2Mg_3(NO_3)_{12}.24H_2O$		
$g_{\parallel}$	Ce : (Ce + La)	Reference
< 0.031	100%	7)
< 0.07	dilute	8)
0.05 ± 0.05	100%	6)
0.0236	–	9)
0.0235 ± 0.0009	0.1%	this paper

2.3. Detail of mixing curve. In fig. 1 it can be seen that $W(0)$ rises before the strong decrease is found. This rise was for $H < 5$ kOe always found when the rotation steps were taken small enough.

The sweeping down model predicts a similar, but somewhat more complicated behaviour. This behaviour has been observed best in low magnetic fields and at a low Ce concentration; an example is given in fig. 3.

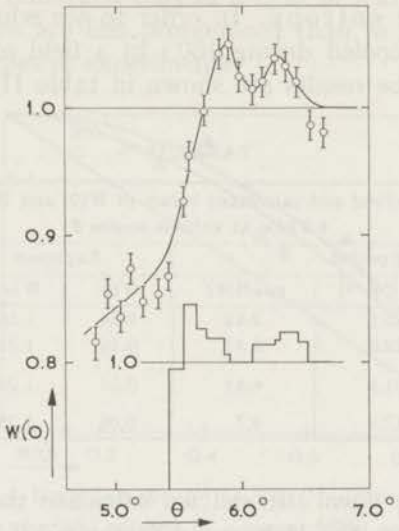

Fig. 3. Variation of $W(0)$ for ^{54}Mn when θ was decreased stepwise. The magnetic field H is 1950 Oe; the sample is (0.01% Ce–Bi)Mg-nitrate. The thin line at the bottom represents the expectation for the sweeping down model for complete orientation on a tenfold reduced $W(0)$ scale; the presence of two different D terms for the Mn ions gives rise to 2×6 steps, of which two coincide.

2.4. Repeated cooling. When, immediately after rotational cooling, the field was returned to $\theta = 30°$, $W(0)$ increased a few percent. If one leaves the field at $\theta = 30°$ for a few minutes, precooling is repeated and then at the next rotational cooling a lower value of $W(0)$ at $\theta = 0°$ could be obtained. Repetition of this process gave in three successive cycles e.g. 0.178, 0.091 and 0.087 for $W(0)$ at $\theta = 0°$ with the 0.1% Ce sample.

In order to clarify why this occurs the experiment was varied in the following ways. When the rotation was carried out very slowly, or when the region $\theta = 0° \leftrightarrow 10°$ was passed three times the same decrease of $W(0)$ was found as in a single rotation at a normal rate of 1 degree/s. On the other hand, a fast rotation of roughly 10 degrees/s gave the much smaller anisotropy $W(0) = 0.51$, and when this was directly followed by a slow passage of the mixing region, $W(0) = 0.21$ was obtained. Increasing the precooling time from 180 to 600 s did not give a significant decrease in $W(0)$. These experiments indicate that in the normal procedure the rate of mixing or the precooling of the Ce are not the limiting factors; much more they suggest a finite heat capacity of the Ce in comparison with the heat capacity to be cooled. At a fast rotation not enough time for mixing is available.

The results given above are for the 0.1% Ce sample. For a 0.03% sample the values of $W(0)$ at $\theta = 0°$ after two successive slow rotational coolings with intermediate precooling were 0.559 and 0.313 respectively.

2.5. Changing Ce entropy. In order to see whether the Ce entropy is important, we precooled during 180 s in a field of 4.8 kOe, applied in various directions. The results are shown in table II.

TABLE II

Comparison between observed and calculated values of $W(0)$ and $W(\pi/2)$ after precooling in 4.8 kOe at various angles θ

Precooling period				Expected		Observed	
θ	$g\mu_B H/k$ (°K)	$1/T$ (°K^{-1})	$g\mu_B H/kT$	$W(0)$	$W(\pi/2)$	$W(0)$	$W(\pi/2)$
10°	0.102	23.5	2.42	0.34	1.160	0.51	1.157
15°	0.151	22.5	3.41	0.16	1.213	0.24	1.223
30°	0.303	21.5	6.51	0.01	1.250	0.18 0.14	1.234 1.232
70°	0.570	17.1	9.7	0.00	1.250	0.14	1.241

For the "sweeping down" model we calculate the expected values of $W(0)$ and $W(\pi/2)$ from the Boltzmann factor $g\mu_B H/kT$ of the Ce ions.

From this table it can be seen that, even for the highest angles θ, ^{54}Mn is not completely polarized, although nearly complete polarization would be expected from the Boltzmann factor. An explanation of this discrepancy will be given in the discussion (§ 3.1). For the small angles $\theta = 10°$ and $\theta = 15°$, $W(0)$ is higher than for $\theta = 30°$ and $\theta = 70°$, which can be attributed to the incomplete polarization of the Ce ions in the precooling period at small θ values, which follows from the Boltzmann factor.

2.6. Relation between $W(0)$ and $W(\pi/2)$. The experiments described in 2.4 and 2.5 gave us an opportunity to test the supposition that a deviation from the Boltzmann distribution over the ^{54}Mn levels occurs after mixing. In fig. 4 the open points give the results of sections 2.4 and 2.5 in a $W(0)$ vs $W(\pi/2)$ diagram. There is no systematic difference between the points obtained in different experiments. It can be seen that the result is intermediate between what is to be expected from the "sweeping" down model and from a Boltzmann distribution. If the "sweeping down" model is modified in the sense that the Ce has thermal contact with two successive Mn splittings at once, i.e. with three Mn levels, a very different curve is obtained (cf. fig. 4). The experimental result for $H = 4.8$ kOe is intermediate between the "sweeping down" model for 2 levels and that for 3 levels.

Instead of cooling the ^{54}Mn spin system by a cold Ce spin system, also the reverse process of warming up a cold ^{54}Mn spin system by a warm Ce

spin system has been studied and leads e.g. to the closed points in fig. 4 which show also that substantial deviations from a Boltzmann distribution exist.

Finally it can be remarked that in a field of 2 kOe the deviations from the Boltzmann curve are less pronounced than in 5 kOe, as can be seen in fig. 4 for both types of experiments.

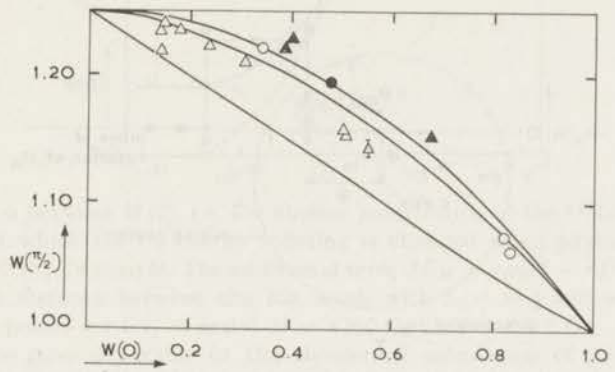

Fig. 4. Relation between $W(0)$ and $W(\pi/2)$ for ^{54}Mn in (0.1% Ce–La)Mg-nitrate. Open points are obtained by thermal mixing of a warm ^{54}Mn nuclear spin system with a colder Ce spin system; closed points are obtained by thermal mixing of a cold ^{54}Mn nuclear spin system with a warmer Ce spin system. In both cases mixing was obtained by decreasing θ. All points have equal statistical errors which are shown for only one point. The three curves are calculated for from bottom to top resp.: sweeping down model, modified sweeping down model in which Ce "sees" two Mn h.f.s. splittings at a time, Boltzmann distribution.
○ and ● $H = 2.0$ kOe
△ and ▲ $H = 4.8$ kOe

2.7. Time dependence. As was remarked in 2.4 the mixing was not complete when the mixing region was passed at a fast rate.

A controlled mixing rate was realized with help of the vertical field $\boldsymbol{H}_x$, which rotates the effective magnetic field $\boldsymbol{H} = \boldsymbol{H}_x + \boldsymbol{H}_h$ out of the horizontal plane in which the field $\boldsymbol{H}_h$ of the strong magnet lies. In our experiment H_x was always much smaller than H. Mixing occurs if the effective magnetic field makes an angle θ_m with the c-axis, thus on a circle in the polar diagram of fig. 5. The radius of this circle depends on H following the relation shown in fig. 2. In this experiment the mixing is performed in the following way. First the field $\boldsymbol{H}_h$ is rotated from a large value of θ to a point outside the mixing region (a), where the vertical field is switched on. The horizontal field is rotated a few degrees further, then the coil for the vertical field is short circuited so that H_x decays to zero. During this decay the mixing region is passed. The field H_{xm} at which mixing occurs is determined in a separate experiment in which H_x is slowly decreased and $W(0)$ is recorded simultaneously with H_x. The time constant τ for the

decay of the field H_x depends on the ratio of self-inductance and resistance of the coil circuit. By addition of self-inductances and resistances the region $10^{-3} < \tau < 10^{-1}$ s was covered. Manually the region of τ between 1 and 10 s could be reached. The τ value was determined in a separate experiment by observing respectively the field and the field variation with the aid of a Hall Gauss meter and a pick up coil on an oscilloscope.

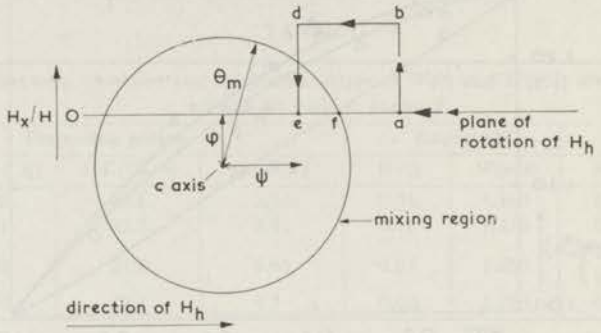

Fig. 5. Polar diagram giving the directions of the effective magnetic field $\boldsymbol{H} = \boldsymbol{H}_h + \boldsymbol{H}_x$ with respect to the c-axis of the crystal, during the mixing procedures of § 2.7 and 2.8.

The rate at which the mixing region is passed can be expressed by the rate of change dE_C/dt of the energy splitting of the Ce. From the relations $E_C^2 \equiv (g_{//}^2 \cos^2\theta_m + g_\perp^2 \sin^2\theta_m)\,\mu_B^2 H^2$; $\theta_m^2 = (\varphi + H_x/H)^2 + \psi^2$ (cf. fig. 5); $dH_x/dt = H_{xm}/\tau$; $g_{//}^2 \ll g_\perp^2$ and the condition $0.03 < \theta_m \ll 1$ it follows

$$dE_C/dt \approx g_\perp \mu_B H_{xm}(\theta_m^2 - \psi^2)^{\frac{1}{2}}/\theta_m \tau.$$

The quantity ψ can be derived from the setting of the magnet and an experiment as shown in fig. 1 which defines the direction of the projection of the c-axis on the horizontal plane, the value of θ_m follows from H with the aid of fig. 2 and hence dE_C/dt can be calculated.

The experiment described above was carried out with the 0.1% Ce sample for three different magnetic fields H_h. At each field various values of τ were used, and $W(0)$ (after the mixing) was measured.

The results are shown in fig. 6 where $W(0)$ is plotted vs $(\Delta E_M)^2\, dE_C/dt$. The term $\Delta E_M = g_M \mu_B H - 4D$ represents the electronic energy splitting of the Mn. It can be seen from fig. 6 that the inclusion of this term in the abscissa makes the points for different fields coincident.

The reason for this will be analyzed and the theoretical curve will be explained in the discussion (§ 3.2).

Some scatter in the points is present. This may be due to heat leaks into the Ce system during the time that the mixing is prepared.

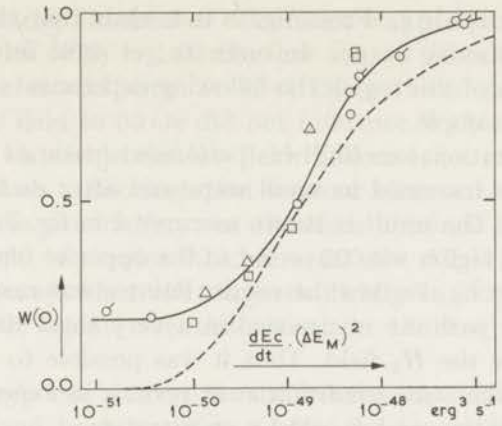

Fig. 6. Relation between $W(0)$, i.e. the nuclear polarization of the ^{54}Mn ions, and the rate dE_C/dt at which the Ce energy splitting is changed when passing the mixing region for the 0.1% Ce sample. The additional term $\Delta E_M = g\mu_B H - 4D$ on the abscissa represents the distance between the Mn levels with $S_z = -\frac{5}{2}$ and with $S_z = -\frac{3}{2}$. Experimental points are for: ○ and ◑ $H = 4760$ Oe □ $H = 1500$ Oe △ $H = 840$ Oe. The dotted line gives the result of the theoretical calculation of § 3.2. The value 10^{-49}erg^{3}s^{-1} corresponds for $H = 4760$ Oe with a time of 0.05 s to sweep through the mixing region ($2.4 \rightarrow 1.9^0$ in fig.7).

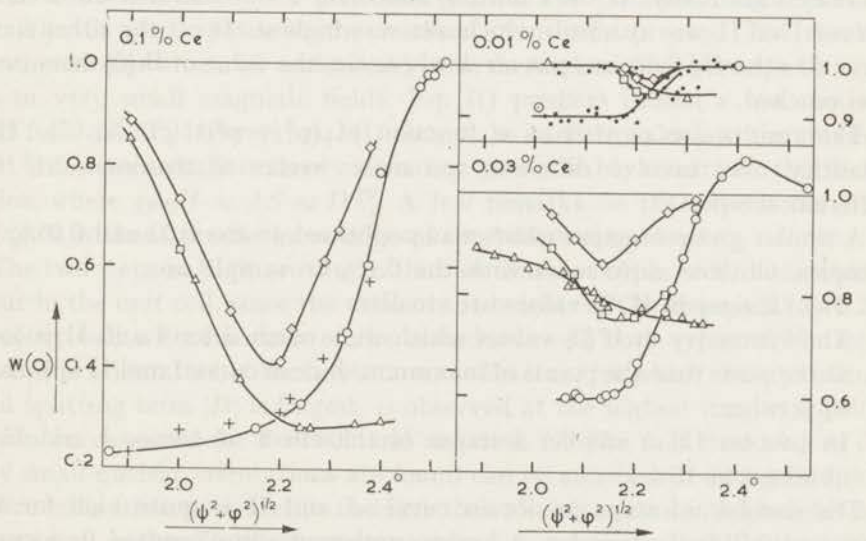

Fig. 7. The result of three different mixing procedures for three samples.
I. ○ passing through the mixing region in the normal sense (decreasing θ).
II. △ passing through the mixing region in the opposite sense (increasing θ).
In I and II the passage was done stepwise, after each step 30 s was allowed to measure one point.
III. The field was set at a fixed angle $(\psi^2 + \varphi^2)^{\frac{1}{2}}$. The value of $W(0)$ after 15 s is indicated by ◇, after 300 s by □. For the 0.1% Ce sample the mixing region was slowly left in the outward direction after 40 s, the resulting values of $W(0)$ for various initial positions are denoted by +.

2.8. Line broadening. From fig. 1 it is clear that there is a certain region where the mixing occurs. In order to get some information on the origin of the width of this region the following experiments were performed with the 0.1% Ce sample.

I. A normal rotational cooling was performed (path a f e in fig. 5). The mixing region was traversed in small steps and after each step $W(0)$ was measured for 30 s. The result is shown as curve I in fig. 7.

II. The mixing region was traversed in the opposite sense (path e f a in fig. 5). Curve II in fig. 7 gives the result. Point e was reached along path a b d e, where the path d e was passed in a very short time by switching off the current for the $\boldsymbol{H}_x$ field. Thus it was possible to start in point e under essentially the same condition as in point a in experiment I: i.e. no Mn nuclear orientation and a cold Ce spin system.

III. A point in the mixing region (point f in fig. 5) was suddenly reached by switching the $\boldsymbol{H}_x$ field off at an appropriate setting ψ of the $\boldsymbol{H}_h$ field. The switching time was so short, that virtually all nuclear polarization was generated at the point f.

This experiment was done for a number of settings of ψ.

It was observed that initially $W(0)$ decreased rapidly; then this rate decreased gradually. If the counting lasted for a few minutes the level of curves I or II was reached, whichever was highest. If on the other hand after 40 s the $\boldsymbol{H}_x$ field was put on slowly again, the value of $W(0)$ on curve I was reached.

The results are plotted as a function of $(\psi^2 + \varphi^2)^{\frac{1}{2}}$ (cf. fig. 5). This quantity may involve different systematic errors of maximal 0.1° for different samples.

A similar group of experiments was performed on the 0.03 and 0.01% Ce samples. Obvious differences with the 0.1% Ce sample are:

1. The changes in $W(0)$ values are smaller.
2. The symmetry in $W(0)$ values which were reached for I and II is lost; at the same time the points of maximum slope of curve I and II approach each other.
3. In process III a smaller fraction of the effect of curves I and II is obtained in 15 s.

The number of steps to obtain curves I and II is quite high for the 0.03 and 0.01% Ce samples. A lower number of steps resulted in a curve which gives higher $W(0)$ values. For the 0.1% Ce sample no difference was observed between curves I obtained in 5 or in 15 steps.

2.9. Demagnetization. When the sample was precooled for some minutes in a magnetic field of a few kOe, a nuclear orientation could be produced by temporarily reducing the field strength to a low value. An investigation of this process for the 0.03% Ce sample at $\theta = 30°$ showed

the following features. The nuclear orientation was produced in two discrete steps; starting with $W(0) = 1.00$ the first step at $H = 370 \pm 20$ Oe gave $W(0) = 0.85$, the second step at $H = 250 \pm 15$ Oe gave $W(0) = 0.58$. Reduction of the field to 30 Oe did not influence $W(0)$ anymore; if, however, one minute elapsed in this low field $W(0)$ rose; i.e. nuclear orientation was destroyed. Such a disorientation was not observed when $H > 90$ Oe. The largest nuclear orientation was therefore obtained by temporary reduction of the field to a value $90 < H < 250$ Oe. All $W(0)$ values quoted above were measured when the magnetic field was increased to a value higher than 1 kOe again; the time spent in the low field region was generally 10 s.

Carrying through this process for different values of θ, i.e. going from 1 kOe to 30 Oe and back again to 1 kOe, the lowest $W(0)$ values were found for $\theta = 40°$ and 50°, while for $\theta = 0°$ and 90° the nuclear orientation was small.

The orientation procedure as described above gave for the 0.01% Ce sample less nuclear orientation than for the 0.03% Ce sample; e.g. $W(0) = 0.86$ was found in a run which was made as closely as possible identical with a run which gave $W(0) = 0.58$ for the 0.03% Ce sample.

The influence of the Ce concentration on the obtained result proves that the Ce participates in the nuclear orientation process. The results mentioned above can be understood as a thermal mixing between Ce and Mn in very small magnetic fields. Eq. (1) predicts indeed a low mixing field for $\theta = 30°$, however, eq. (1) cannot be used to calculate the mixing field since perturbation theory does not give reliable results in this field region where $g\mu_B H \approx AS \approx DS_z^2$. A few remarks on the experiment can be made without precise knowledge of the ^{54}Mn energy levels.

The two steps in $W(0)$ are due to the two different types of Mn ions which occur in the unit cell, since the ratio of the heights of the steps is 0.15 : 0.27 agreeing well with the ratio of the abundancies of both types of Mn ions 1 : 2. The orientation of the less numerous Mn ions, for which the crystalline field splitting term $|D|$ is largest, is observed at the highest magnetic field, as can be expected for $\theta = 30°$ and negative D. The fact that at $\theta \approx 0°$ only small nuclear orientations are found can be ascribed to a long Ce spin-lattice relaxation time and to the fact that mixing occurs in high fields at these small angles. Both circumstances lead to relatively high Ce temperatures at the moment of mixing. For $\theta = 90°$ these arguments do not apply. Possibly the smallness of the orientation when the field was in this direction can be explained by the impossibility to match the splitting of Ce and the splitting of the Mn levels $I_z = -3$ and $I_z = -2$, because of the influence of the negative D term in the spin-hamiltonian.

The depolarization which occurred when some time elapsed at 30 Oe indicates that the nuclear spin-lattice relaxation time of ^{54}Mn in this field

is of the order of 10^2 s, whereas in a field of 90 Oe this relaxation time is evidently much longer. The relatively short relaxation time in 30 Oe might be due to thermal contact of the Mn ions with the Ce dipolar energy system, which in turn might have a good thermal contact with the lattice.

2.10. Maximum nuclear polarization. An effort was undertaken to observe a very low value of $W(0)$ after repeated rotational cooling in 4.8 kOe with the 0.1% Ce sample. The distance between one $W(0)$ counter ($1\frac{3}{4}'' \times 2''$ NaI(Tl)) and the sample was increased to 23 cm. After correction for the 2.2% background $W(0) = 0.033$ ($\pm$ 0.004 statistical error) was found. In determining this figure only the upper half of the photopeak in the pulse-height spectrum was used in order to reduce the counted contribution of compton scattered radiation, which does not have maximal anisotropy. The correction for the solid angle of the counter in these conditions is 0.0095 ± 0.0010, the final result is therefore $W(0) = 0.024 \pm 0.005$.

From this result it can be concluded: a) the disturbance of the nuclear orientation after K-capture during the 12 ps half life of the 835 keV ^{54}Cr level is quite small; at most 1.2% of the Cr ions can have changed their state from $I_z = -2$ to $I_z = -1$.

b) At least 97% of the ^{54}Mn ions can be polarized by thermal mixing. If a Boltzmann distribution for the ^{54}Mn ions is assumed, i.e. if nearly all ions which are not in the $I_z = -3$ state are in the $I_z = -2$ state, a nuclear polarization $\langle I_z \rangle / I = 99.5 \pm 0.1\%$ and a temperature $T = 6.1 \pm 0.3$ m°K are calculated from $W(0) = 0.024 \pm 0.005$.

3. *Discussion.* The model given in 1 explains the observation of a thermal mixing (2.1), the dependence of the mixing angle θ_m on H (2.1 and 2.2) and the occurrence of deviations from the Boltzmann distribution (2.3 and 2.6). In this discussion we will extend the model by considering: a) the heat capacities involved; b) the speed of mixing; c) the effects of broadening of the mixing region.

3.1. Heat capacities. The experiments mentioned in 2.4 strongly suggest a finite ratio of the heat capacity of the Ce spin system and that of the system to be cooled. An estimate of the number of Ce spins which "cool" one ^{54}Mn nucleus can be obtained in the following way. The lowest experimental value of $W(0)$ obtained in a single rotation of the 0.1% Ce crystal is $W(0) = 0.14$ This number has to be corrected for counter solid angle and background to $W(0) = 0.11$. Now we assume that the experiment started with a completely polarized Ce spin system and an unpolarized ^{54}Mn nuclear spin system before mixing and that thermal equilibrium according to a Boltzmann distribution exists after thermal mixing. Then we find from $W(0) = 0.11$ that $AS/kT = 2.73$ after mixing, which means

that on the average each Mn ion has given off 2.93 quanta AS. After mixing only a fraction $\exp(-2.73)/\{1 + \exp(-2.73)\} = 0.061$ of the Ce ions is in the upper state, therefore it takes $2.93/0.061 = 48$ Ce ions to cool one Mn ion. Making a calculation for the sweeping down model for one Mn ion in contact with a finite number of Ce spins, during which process the temperature of the Ce spins rises at the successive mixings, it is found that 84 Ce ions are required in order to give $W(0) = 0.11$. According to 2.6 and 3.3 the true process is intermediate between the sweeping down model and the establishment of a Boltzmann equilibrium, therefore it can be estimated that each Mn ion is cooled by roughly 60 Ce ions.

In a 0.1% Ce crystal these 60 Ce ions are distributed over 60.000 La lattice places. In the used crystal of 3.3 g approximately 4 μC ^{54}Mn was present, thus a concentration $^{54}\text{Mn/La} = 2.5 \times 10^{-9}$. The heat capacity of such a dilute spin system is extremely low, thus it should have been easy to cool the Mn spin system at once. On the other hand, a parasitical heat capacity may arise from paramagnetic impurities with h.f.s.-splittings. A concentration of 1×10^{-5} impurities would give an explanation of the observed effects of finite heat capacity. For instance Pr or stable ^{55}Mn (both have larger h.f.s. splittings than ^{54}Mn) might be responsible for this effect.

A similar calculation as above for the value $W(0) = 0.56$, obtained with the 0.03% Ce sample, gives that one ^{54}Mn is cooled by 11.5 Ce spins in the Boltzmann model. The calculated impurity content of this crystal is then nearly the same as above.

The heat capacity of the lattice is very small at these low temperatures and can be ignored. The heat capacity of the protons in a field of a few kOe, however, is considerable. If the numerous protons had been in thermal contact with the 0.1% Ce spin system, low temperatures could not have been reached. The conclusion is that the protons are thermally isolated from the ^{54}Mn and the Ce spins. This isolation is not surprising in view of the large discrepancy between the h.f.s. energy-splittings of ^{54}Mn, namely, $AS/k = 26$ millidegrees, and the Zeemansplittings $g\mu_N H/k$ of the protons, which is, even in a field as large as 15 kOe, only 3 millidegrees.

3.2. Mixing time. So far we have discussed the heat capacities involved but not touched on the interaction causing energy exchange between Ce and Mn ions. The high dilution makes distances between ions quite large, e.g. we calculate a 200 Å radius for the sphere containing the 60.000 La lattice places, on which the Ce ions are situated which cool one Mn ion. In spite of this we will show, hereafter, that dipolar coupling between Ce and Mn ions is still sufficiently strong to explain the observed speeds of mixing.

In 2.7 measurements are given on the nuclear polarization as a function of the speed of crossing of energy levels which may be utilized for the

comparison with calculated mixing speeds based on dipolar interactions between Ce–Mn. In order to present this calculation we consider first a typical Ce–Mn pair, which can be characterised by its distance r and the angle α between their connection line and the magnetic field $\boldsymbol{H}$. The initial state is where the Ce spin is in the ground state $S_z = -\frac{1}{2}$ and the Mn levels $S_z = -\frac{5}{2}$, I_z are equally populated. We ask for the probability w that h.f.s. energy, particularly between the $S_z = -\frac{5}{2}$, $I_z = -2$ and $S_z = -\frac{5}{2}$, $I_z = -3$ states of the Mn ion is transferred as Zeeman energy to the Ce ion. There exists a certain homogeneous broadening of the Ce and Mn energy splittings and w depends on the overlap of both distributions. The overlap and thus w is a function of time in our experiments since the centroid of the cerium energy splitting E_C is varied in time, while the centroid of the manganese splitting E_M is almost constant. The fraction of the Mn nuclei which is not oriented in this process is determined by $p = \int w(t)\,\mathrm{d}t$, as can be seen from the following calculation. Consider for the sake of simplicity the Mn as a two level system; the occupation number of the levels $I_z = -2$ and $I_z = -3$ is designated by n_2 and n_3 respectively, thus $n_2 + n_3 = 1$. From the definition of w follows: $\mathrm{d}n_3/\mathrm{d}t = wn_2 = w(1 - n_3)$. This can be integrated to $-\log(1 - n_3) = \int w\,\mathrm{d}t = p$ thus $(n_2)_f/(n_2)_i = \mathrm{e}^{-p}$ where f and i stand for final and initial. The only terms in the magnetic dipole coupling which can give energy transfer from Mn to Ce under the condition of conservation of energy are $S_+^C S_-^M$ and $S_+^C I_-^M$. Since the contribution of the $S_+^C I_-^M$ term is small compared to the $S_+^C S_-^M$ term, the following expression can be given for w:

$$w = \frac{2\pi}{\hbar} |\langle \psi_f | g_M \mu_B H_d S_+^C S_-^M | \psi_i \rangle|^2 \rho(E_C, E_M)$$

$$g_M \mu_B H_d = -\tfrac{1}{4} g_M g_C \mu_B^2 r^{-3}(1 - 3\cos^2\alpha)$$

$$|\psi_i\rangle = |-\tfrac{1}{2}; -\tfrac{5}{2}, -2\rangle + \varepsilon\,|-\tfrac{1}{2}; -\tfrac{3}{2}, -3\rangle$$

$$|\psi_f\rangle = |+\tfrac{1}{2}; -\tfrac{5}{2}, -3\rangle$$

$$\varepsilon = \frac{A}{2(g_M \mu_B H - 4D)} \langle \pm\tfrac{1}{2}; -\tfrac{3}{2}, -3 | S_+^M I_-^M | \pm\tfrac{1}{2}; -\tfrac{5}{2}, -2\rangle = \frac{A\sqrt{30}}{2(g\mu_B H - 4D)}$$

In the symbol $|S_z^C; S_z^M, I_z^M\rangle$ the Ce electron spin, the Mn electron spin and the Mn nuclear spin occur consecutively. It should be mentioned that in the above expressions for g_C the g-value in a direction perpendicular to the external field has to be used; since θ is small $g_C \approx g_\perp$. The quantity $\rho(E_C, E_M)$ corresponds with the density of final states and can be derived from the homogeneous broadening of the Ce and Mn energy levels, which is probably due to the surrounding protons. Suppose that the distributions for Ce and Mn resp. are given by the normalized distribution functions

$f(E - E_C)$ and $h(E - E_M)$ centered about E_C and E_M. Then evidently

$$\rho(E_C, E_M) = \int f(E - E_C)\, h(E - E_M)\, dE.$$

In our experiment E_M is constant and E_C varies in the crossing region approximately linearly with time; the crossing speed may be indicated by $\dot{E}_C$. In $w(t)$ only ρ depends on time and therefore the integration of w with respect to time (in order to obtain p) can easily be performed:

$$\int \rho\, dt = \frac{1}{\dot{E}_C} \int \rho\, dE_C = \frac{1}{\dot{E}_C} \iint f(E - E_C)\, h(E - E_M)\, dE\, dE_C =$$

$$= \frac{1}{\dot{E}_C} \int h(E - E_M)\, dE = \frac{1}{\dot{E}_C}.$$

This result is valid independently of the shape of the distribution functions as long as $\dot{E}_C$ is a constant over the region which contributes significantly to the integral.

From the above formulae p is found:

$$p = \frac{5\pi}{8\hbar} \varepsilon^2 g_M^2 g_C^2 \mu_B^4 r^{-6} (1 - 3\cos^2\alpha)^2 \cdot \frac{1}{\dot{E}_C}. \qquad (2)$$

For further calculations we have to consider the fact that Mn has 7 h.f.s. levels instead of two as assumed above. For complete orientation of the Mn the above described process has to occur six times. It can be expected that the dipole-dipole interactions give rise to a faster flip-flop rate between Ce–Ce than between Ce and Mn. Hence the Ce ion of the Ce–Mn pair considered above will return to its ground state after a Ce–Mn flip-flop in a time which is short compared to the time needed for the next Ce–Mn flip-flop. Thus the initial conditions (i.e. Ce in its ground state) is very probably restored before the next Ce–Mn flip-flop. Hence the above calculation is applicable to all flip-flops, apart from a spinfactor in ε which gives:

$$\tfrac{1}{6}p = \tfrac{1}{6}p_{3\to 2} = \tfrac{1}{10}p_{2\to 1} = \tfrac{1}{12}p_{1\to 0} = \tfrac{1}{12}p_{0\to -1} = \tfrac{1}{10}p_{-1\to -2} = \tfrac{1}{6}p_{-2\to -3}.$$

Using the sweeping down model, the final populations of the h.f.s. levels can be calculated from the above mentioned flip-flop probabilities p; with the aid of table I of III $W(0)$ is found. In fig. 8 the relation between $W(0)$ and p is given.

The result of fig. 8 will be schematized in the following way: the Mn ions which have a Ce neighbour for which $p > 1.2$ will be oriented and give $W(0) = 0$; the Mn ions which do not have a Ce neighbour with $p > 1.2$ will not be oriented and give $W(0) = 1$. Furthermore we average over α: $\overline{(1 - 3\cos^2\alpha)^2} = \frac{4}{5}$. These simplifications allow the following statement. The overal $W(0)$ is determined by the fraction of Mn ions which have no Ce neighbour within a distance R while R is derived by solving $R = r$

from $p = 1.2$ (eq. (2)). The following formula for $W(0)$ is found:

$$W(0) = (1 - c)^{4\pi R^3/3V} \tag{3}$$

in which c = Ce concentration and V is the volume of the unit cell of the crystal devided by the number of La places in the unit cell. Formula (3) is valid if the Ce : La dilution is random and if R is larger than a few times the dimensions of the unit cell.

From (2) and (3) it follows that

$$W(0) = \exp\left\{\frac{4\pi}{3V} g_M g_C \mu_B^2 A \sqrt{\frac{25\pi}{8\hbar(dE_C/dt)(g_M\mu_B H - 4D)^2}} \cdot \ln(1 - c)\right\} \tag{4}$$

From this formula the dashed line in fig. 6 is calculated. The above theoretical description correctly predicts a) the order of magnitude of dE_C/dt at which half of the ions participate in the mixing b) the order of magnitude of the width of the region in which $W(0)$ depends strongly on dE_C/dt and c) the field dependence which is present in the term ΔE_M. This result is more satisfying since no adjustable parameters to fit theory and experiment are present.

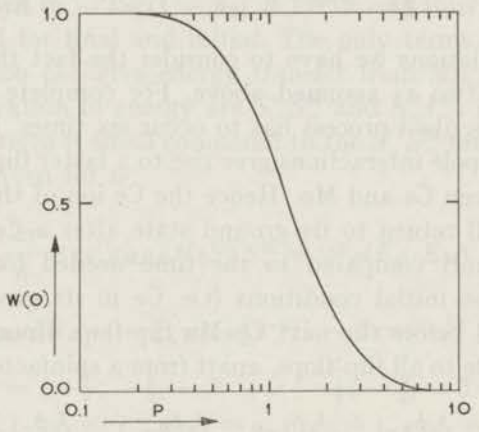

Fig. 8. Calculated theoretical relation between $W(0)$ and the parameter p, which is inversely proportional to the rate at which the mixing region is passed.

Two deviations exist between theory and experiment. a) At the side of low dE_C/dt the experimental values of $W(0)$ do not approach zero. In § 3.1 this was explained by the presence of a parasitical heat capacity of impurity ions. b) At $W(0) \approx 0.8$ the experiment gives a slower mixing than the theory. This might be due to the fact that in the theoretical calculation the discrete structure of the lattice is neglected. It can be expected that this effect is most important for the Mn ions which have their nearest Ce neighbour at small distances, e.g. at the highest dE_C/dt values. For these ions also the energy transfer between their Ce neighbour

and other Ce spins might become the bottleneck in the heat transfer. Thus a more elaborate calculation of our model might improve the agreement of theory with experiment. It can be concluded that the dipolar coupling between *Ce* and *Mn electron spins* explains the observed mixing rates between *Ce electrons* and *Mn nuclei* quite well.

Furthermore, it is hard to find satisfactory alternative solutions for explaining the experimental data, e.g. a model based on the interaction of Mn and Ce spins via the lattice (phonons) would predict cross relaxation times which are too long by many orders of magnitude compared to the data, and also the predicted dependence on fieldstrength H would be very different from the experimental result. Also coupling between Ce and Mn via exchange is improbable. From the fact that at least 97% of the Mn ions can be cooled in a 0.1% Ce crystal, it follows, assuming random dilution, that even Mn ions which have their nearest Ce neighbour at 78 Å distance, can participate in the mixing procedure.

From eq. (4) it can be concluded that at a decrease of Ce concentration lower dE_C/dt values, i.e. longer mixing times are required to give complete mixing. This was also experimentally found (cf. § 2.4 and 2.8).

3.3. Line broadening effects. The occurrence of thermal mixing is determined by the difference δ in energy splittings between a Mn ion and its nearest Ce neighbour. At a given setting of the magnetic field (H, θ) different ions in the sample will have different δ values. This spread in δ gives rise to an inhomogeneous broadening of the mixing region. Further also homogeneous broadening can be expected: mixing already occurs when for a given Ce–Mn pair δ is unequal to zero.

The presence of both types of broadening can be seen in fig. 7. First we will discuss the result on the 0.1% Ce sample. The finite slopes of curves I and II are due to inhomogeneous broadening. The presence of inhomogeneous broadening also explains that in experiment III finally (points denoted by +) the same $W(0)$ values are found as in I. In both experiments the same part of the inhomogeneous broadened region is traversed, although in opposite directions, and thus the same Mn ions are oriented.

If one waits 30 s at $\theta = 2.2°$ most Mn ions are oriented; this proves that the width of the homogeneous broadening is larger than the width of the inhomogeneous broadening.

When comparing the more dilute samples with the 0.1% Ce sample, we observe that the width of the homogeneous broadening decreases more strongly than the width of the inhomogeneous broadening. The decrease of both types of broadening with decreasing Ce concentration explains that the details of the mixing curve are best observed in the most dilute crystal (§ 2.3). The fact, that in low magnetic fields the spacing of the different transitions is largest, because of the term $A^2/g\mu_B H$ in eq. (1), explains

that the details of the mixing curve were most clearly observed in low magnetic fields. The presence of a considerable homogeneous broadening explains that in the sweeping down model mixing between Ce and several Mn. h.f.s. levels at once is found (cf. § 2.6).

3.4. Conclusion. The practicability of the thermal mixing (cross relaxation) between electron spins and nuclear spins is firmly established. A large nuclear polarization can be obtained in this way simply by changing the direction or magnitude of an external magnetic field. The use of two dilute spin systems has the advantage that the thermal contact is very selective and that spin-lattice relaxation times are very long. Thus the nuclear polarization can be maintained for a long time, also when the lattice temperature is not very low. A lower limit on the dilution is set by the impurity content of the sample and by the rate of mixing. The latter can be calculated from the magnetic dipolar interactions between the spins. The characteristics of the thermal mixing between Ce and Mn are of general interest for the study of relaxation of nuclei which belong to magnetic ions under conditions of paramagnetic saturation.

REFERENCES

1) Abragam, A. and Borghini, M., in Prog. low Temp. Phys. vol. **4** ed. C. J. Gorter. (North-Holl. Publ. Co., Amsterdam 1964.)
2) Langley, K. H., Jeffries, C. D., Phys. Rev. Letters **13** (1964) 808.
3) Robinson, F. N. H., Phys. Letters **4** (1963) 180.
4) Lubbers, J. and Huiskamp, W. J., Physica, to be published; chap. III.
5) Ruby, R. H., Benoit, H. and Jeffries, C. D., Phys. Rev. **127** (1962) 51.
6) Leask, M. J. M., Orbach, R., Powell, M. J. D. and Wolf, W. P., Proc. Roy. Soc. **A 272** (1963) 371.
7) Wheatley, J. C. and Estle, T. L., Phys. Rev. **104** (1956) 264.
8) Hudson, R. P., Kaeser, R. S. and Radford, H. E., Proc. 7th int. Conf. low Temp. Phys. p. 100 (University of Toronto Press 1961.)
9) Private communication from Jeffries, C. D. mentioned in ref. 1.

SAMENVATTING

Het doel van de in dit proefschrift beschreven onderzoekingen is geweest een methode te vinden volgens welke grote kernspinpolarisaties verkregen kunnen worden. Hiertoe is getracht een lage temperatuur te realiseren in een preparaat dat zich tevens in een sterk magneetveld bevindt. Hierbij is gebruik gemaakt van een tweetraps adiabatisch koelproces. In de eerste fase wordt een koelzout adiabatisch gedemagnetiseerd, dat vervolgens gebruikt wordt om het preparaat af te koelen dat zich in een sterk magneetveld bevindt. Het preparaat bestaat uit een éénkristal waarin zich, naast de te orienteren radioactieve kernen, paramagnetische ionen met een anisotrope spin-hamiltoniaan bevinden. Door de richting van het veld te veranderen, kunnen de energiesplitsingen van deze ionen verkleind worden, wat tot een verdere temperatuur verlaging leidt. Deze laatste fase van het koelproces wordt draaikoeling genoemd. De bereikte temperatuur wordt afgeleid uit de anisotropie van de γ-straling, die door de radioactieve kernen wordt uitgezonden.

Reeds bij de eerste experimenten bleek dat bij aanwezigheid van sterke magneetvelden lange relaxatietijden optreden, zowel tussen de spinsystemen en het rooster, als tussen de verschillende spinsystemen onderling. Voor een aantal systemen zijn de kernspinrelaxatietijden bestudeerd.

In hoofdstuk I wordt de methode van draaikoeling door middel van anisotrope hyperfijnstructuur-koppeling besproken. In experimenten met cobalt-caesium-tuttonzout werd een temperatuur van 0,006°K bereikt, zoals bleek uit de kernorientatie van ^{54}Mn en ^{137}Cs. De grootte van het gebruikte magneetveld beinvloedde de relaxatietijd tussen cobalt en de radioactieve kernen sterk; de mate van herorientatie van het 2,6 min. niveau van ^{137m}Ba, dat aangeslagen wordt in het verval van ^{137}Cs, kon dientengevolge beinvloed worden. Een experiment met ^{60}Co bevestigde in grote trekken het voor deze koelmethode gegeven model.

In hoofdstukken II en III worden onderzoekingen over de relaxatieverschijnselen voor ^{54}Mn kernen besproken. De metingen van hoofdstuk II demonstreren dat het warmtecontact tussen kernspins van ^{54}Mn en het kristalrooster in geconcentreerde paramagnetische zouten voornamelijk verloopt via de electronenspins van de talrijke paramagnetische ionen. Dit

warmtecontact wordt zeer slecht als de electronenspins sterk gepolariseerd worden. Bij verdunning van de paramagnetische ionen wordt het bovengenoemde mechanisme spoedig ineffectief, zodat dan het warmtecontact alleen via de electronspin van het Mn zelf verloopt (hoofdstuk III). Een model voor dit proces wordt voorgesteld.

In de loop van de metingen aan ^{54}Mn in verdunde ceriummagnesiumnitraat kristallen werden anomale kernpolarisaties gevonden, d.w.z. polarisaties die niet te beschrijven zijn met een thermische verdeling over de hyperfijnstructuur niveaus van Mn. Deze polarisaties blijken veroorzaakt te kunnen worden door een proces waarbij de Ce ionen overgangen tussen bepaalde Mn niveaus induceren.

In hoofdstuk IV wordt aangetoond dat draaikoeling ook voor een verdund systeem van Ce ionen uitvoerbaar is. Essentieel hierbij is dat een lange spinrooster relaxatie tijd optreedt als de Ce splitsing klein is. Als de Zeemansplitsing van de Ce ionen gelijk gemaakt wordt aan de hyperfijnstructuursplitsing van Mn ontstaat een goed warmtecontact tussen beide spinsystemen. Gebruikmakend van dit goede warmtecontact kon na draaikoeling van het Ce een grote kernspinpolarisatie voor het Mn bereikt worden. Een model voor het mechanisme van dit warmtecontact wordt gegeven.